AN EXPERIMENTAL STUDY ON SETTLING BEHAVIOR OF TOE PROTECTION ELEMENTS OF RIVER BANK PROTECTION WORKS

K. M. AHTESHAM HOSSAIN RAJU

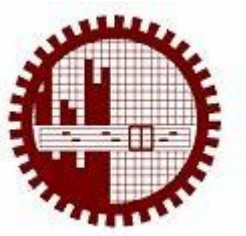

DEPARTMENT OF WATER RESOURCES ENGINEERING
BANGLADESH UNIVERSITY OF ENGINEERING AND TECHNOLOGY
DHAKA

DECEMBER, 2011

AN EXPERIMENTAL STUDY ON SETTLING BEHAVIOR OF TOE PROTECTION ELEMENTS OF RIVER BANK PROTECTION WORKS

K. M. AHTESHAM HOSSAIN RAJU

A thesis submitted to the Department of Water Resources Engineering
in partial fulfillment of the requirements for the Degree of
Master of Science in Water Resources Engineering

DEPARTMENT OF WATER RESOURCES ENGINEERING
BANGLADESH UNIVERSITY OF ENGINEERING AND TECHNOLOGY
DHAKA

DECEMBER, 2011

Bangladesh University of Engineering and Technology, Dhaka

Department of Water Resources Engineering

CERTIFICATION OF THESIS

The thesis titled **"An Experimental Study on Settling Behavior of Toe Protection Elements of River Bank Protection Works"**, submitted by K. M. Ahtesham Hossain Raju, Roll No. 0409162015P, Session April 2009, to the Department of Water Resources Engineering, Bangladesh University of Engineering and Technology, has been accepted as satisfactory in partial fulfillment of the requirements for the degree of Master of Science in Water Resources Engineering and approved as to its style and content. Examination held on 20th December, 2011.

_____

Dr. Md. Abdul Matin — **Chairman (Supervisor)**
Professor
Department of Water Resources Engineering
BUET, Dhaka-1000, Bangladesh

_____

Dr. Umme Kulsum Navera — **Member (Ex-Officio)**
Professor and Head
Department of Water Resources Engineering,
BUET, Dhaka-1000, Bangladesh

_____

Dr. Md. Ataur Rahman — **Member**
Associate Professor
Department of Water Resources Engineering,
BUET, Dhaka-1000, Bangladesh

_____

Dr. M. R. Kabir — **Member (External)**
Professor and Pro-Vice-Chancellor,
University of Asia Pacific, Dhaka, Bangladesh

20 DECEMBER, 2011

DECLARATION

This is to certify that this thesis work has been done by me and neither this thesis nor any part thereof has been submitted elsewhere for the award of any degree or diploma.

Dr. Md. Abdul Matin	**K. M. Ahtesham Hossain Raju**
Countersigned by the Supervisor	Signature of the Candidate

CHAPTER TWO

REVIEW OF LITERATURE

2.1 Introduction

Sustainability of river bank protection works had been the subject of research for a long time. There are several approaches available in literature for the design of bank protection works. The effectiveness of design of protection works mainly depends on its constructional aspects. The appropriate method of construction again depends on mechanism of settling behavior and incipient condition of protection element. In this chapter these hydraulic aspects of bank protection elements involved in the process are briefly reviewed.

2.2 River Bank Protection Works

River bank protection works are essentially important parts of river training works. The viewpoint of bank protection structure is to design and construct structures to guide the water course at desired level allowing certain degree of damages which may be taken care of through monitoring and repair during occurrence of the extreme events. The purpose of these structures is to prevent bank erosion to provide a stable river bank. Some other functions of bank protection works are-

(a) Safe and expeditious passage of flood flow.

(b) Efficient transportation of suspended and bed loads.

(c) Stable river course with minimum bank.

(d) Sufficient depth and good course for navigation.

(e) Direction of flow through a certain defined stretch of the river, (Przedwojski et al., 1995).

The various kinds of protective works can be broadly classified into two groups, this being-

(i) Direct protection

(ii) Indirect protection

Direct protection works are done directly on the banks such as-

- Slope protection of embankment and upper bank, and
- Toe protection of lower bank

As such works continuously cover a certain length of banks; they are also called ‘Continuous Protection’. Commonly seen direct protection works are banks protected against erosion by revetments or by a series of hard-points. Such bank protection is normally required to maintain the existing bank line for economic or other human interests.

Indirect protection works are not constructed directly on the banks but in front of them in order to reduce the erosive force of the current either by-

- Repelling Groynes- deflects the current from banks, or
- Sedimentation or Permeable Groynes- allows water to pass but not sediment. (These groynes have openings- so area is increased and the velocity of water is reduced. Therefore the water can no longer carry the sediment load and so the sediment is deposited.)

Examples of typical bank protection structures are:

- groynes,
- longitudinal dikes
- bank protection by means of revetments,
- cross dikes tying in longitudinal structures to the bank to divide the closed-off channel spaces,
- sills to stabilize the bottom of the regularized river according to a corresponding longitudinal slope,
- closures to cut off secondary channels,
- bed load traps: structures to trap and stabilize bed-load and causing its elevation (Przedwojski et al., 1995).

Indirect protection works are not used now-a-days in Bangladesh as they failed to protect the river bank. Therefore, direct protection works are usually followed to fulfill this purpose.

2.3 Revetment and Riprap Structures

Revetment is artificially roughening of the bank slope with erosion-resistant materials. A revetment mainly consists of a cover layer, and a filter layer. Toe

protection is provided as an integral part at the foot of the bank to prevent undercutting caused by scour. The protection can be divided as falling apron or launching apron, which can be constructed with different materials, e.g., CC blocks, rip-rap, and geobags. Figure 2.1 shows revetments and their different components.

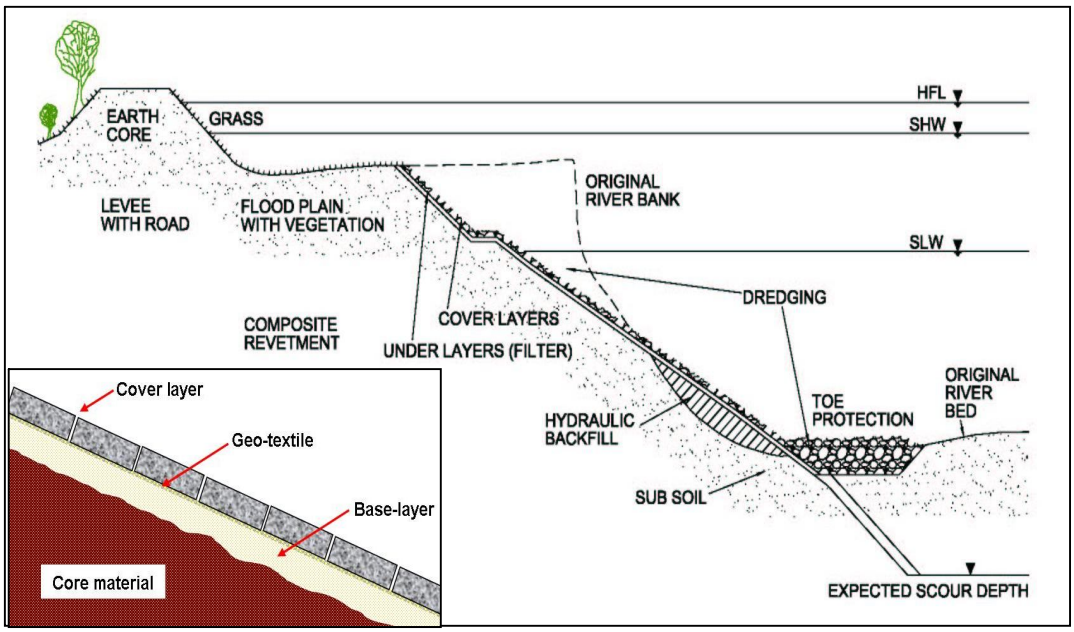

Figure 2.1: Components of a typical revetment on river bank (Source: BWDB, 2010)

Launching apron consists of interconnected elements that are placed horizontally on the floodplain and normally anchored at the toe of the embankment. The interconnected elements are not allowed to rearrange their positions freely during scouring but launch down the slope as a flexible unit. The falling apron, on the other hand, consists of loose elements (e.g., CC blocks, geobags, stones) placed at outer end of the structure. When scour hole approaches the apron, the elements can adjust their position freely and fall down the scouring slope to protect it.

Riprap is the term given to loose armour made up of randomly placed quarried rock. It is one of the most common types of cover layer used all over the world. Riprap structures are attractive because their outer slopes force storm waves to break and thereby dissipate their energy. They are also used extensively because:

- Rock can often be supplied from local quarries.

- Relative ease of placing (including under water sites).
- Flexibility and to some extent self-repairing.
- Durability
- High roughness to attenuate waves and currents.
- Even with limited equipment, resources and professional skills, structures can be built that perform successfully.
- There is only a gradual increase of damage once the design conditions are exceeded. Design or construction errors can mostly be corrected before complete destruction occurs.
- Low maintenance and repair works are relatively easy, and generally do not require mobilization of very specialized equipment.
- The structures are not very sensitive to differential settlements, due to their flexibility.
- Natural and environmentally acceptable appearance.

Riprap is made up of durable, angular stones ranging typically from 10 to 50 cm depending on the hydraulic loads. Its stability depends on the size and mass of the stones, their shape and gradation. The angular and cubical riprap stones show the best performance. Riprap mixture should form a smooth grading curve without a large spread between median and maximum sizes. It is normally placed in one, two or three layers, and a sub layer is often incorporated.

2.3.1 Choice of revetment

The type of material to be used for revetment depends upon the cost of materials, durability, safety and appearance. In many circumstances, attention is concentrated in Bangladesh on revetment because of its following advantages:

- It is flexible and is not impaired by slight movement of the embankment resulting from settlement.
- Local damage can be repaired easily.
- No special equipment or construction practices are necessary.
- Appearance is natural.
- Vegetation will often grow through the rocks.
- Additional thickness can be provided at the toe to offset possible scour.

2.3.2 Previous studies on geosynthetic products for revetment works

Liu (1981) performed experimental analysis to determine impact force of waves on a sausage (tube) for 1:15 slope under various water depths and breaking waves. From the 74 tests, 24 cases of complete impact forces striking on the test model occurred which implied that breaking waves were reproduced before they just hit the model. An equation to describe the equilibrium shape of sand sausage is also presented. Kobayashi and Jacobs (1985) conducted model tests in a wave flume to examine the effects of berm type slopes on the stability of armour units and wave run-up, compared to those of uniform slopes. A simple analysis procedure based on the proposed method is developed, using the 'Equivalent Uniform Slope', for a preliminary design of a berm configuration. Klusman (1998) conducted an analysis of the circumferential tension of geosynthetic tubes. Pilarczyk (2000) reviewed the existing geosynthetic systems, their design methods and their application for coastal and shoreline protection structures. However, Pilarczyk (1995, 2000) mentioned that a number of concepts discussed there still need further elaboration to achieve the level of design quality comparable with more conventional solutions and systems. In general, the previous studies are quite limited, since they are largely related to typical aspects in terms of design and construction. In spite of growing applications of geobags or geocontainers, relevant studies are still lacking (Zhu et al., 2004).

2.3.3 Toe scour estimation and protection

Riprap protection for open channels is subjected to hydrodynamic drag and lift forces that tend to erode the revetment and reduce its stability. Undermining by scour beyond the limits of protection is also a common cause of failure. The drag and lift forces are created by flow velocities adjacent to the stone. Forces resisting motion are the submerged weight of the stone and any downward and lateral force components caused by contact with other stones in the revetment.

Lack of protection of the toe of the revetment against undermining is a frequent cause of failure of revetment. Therefore, protection of the toe of revetment by suitable method is a must. This is true not only for riprap, but also for a wide variety

of protection techniques. The scour is the result of several factors including the factors mentioned below:

1. Change in cross-section in meandering channel after a bank is protected*:* after a bank is protected, the thalweg can move towards the outer bank and/or a channel with highly erodible bed and bank can experience significant scour along the toe of the new revetment.
2. Scour at high flows in meandering channel*:* Bed observed at low flows is not the same as that exists in high flows.
3. Braided Channels*:* Scour in a braided channel can reach a maximum at intermediate discharges where the flow in the channel braids concentrates along the protective work or attacks the banks at a sharp angle (USACE, 1994).

2.3.4 Toe protection methods of revetment

Toe protection of revetments may be provided by following methods:

(i) Extension to maximum scour depth: Lower extremity of revetment placed below expected scour depth or founded on non-erodible bed materials. Theses are preferred method, but can be difficult and expensive when underwater excavation is required.

(ii) Placing launchable stone: Launchable stone is defined as stone that is placed along expected erosion areas at an elevation above the zone of attack. As the attack and the resulting erosion occur below the stone, the stone is undermined and rolls/slides down the slopes, forming a surface cover layer reducing the erosion. In general, the design implies that the scouring and undermining process of the developing scour hole in front of the structure initiates the deformation process of the toe protection. At the estimated maximum scour depth, the launching apron is assumed to cover and stabilize the bank-sided river profile, reducing further erosion of the bank (USACE, 1994).

2.3.5 Dimension of falling apron

Among the various methods, launching apron or falling apron has been considered to be the most economic and common method of toe protection of revetment. Falling aprons are generally laid on river bed at the foot of the revetment with graded protection elements forming multilayer, so that when scour occurs, the material will launch and will cover the surface of the scour hole in a natural slope. Historically, starting from the limited understanding of Spring (1903) and Gales (1938), the launched quantity was computed assuming a launched apron thickness similar to the thickness of pitching work above water. The quantities were calculated as geometrical area depending on launched thickness, depth of scour, and slope of the launching apron. This approach was further substantiated by the results of the systematic model tests published by Ingles in 1949 and follow on model tests conducted in Bangladesh during the Flood Action Plan in the early 1990s.

Spring (1903) recommended a minimum thickness of apron equal to 1.25 times the thickness of stone riprap of the slope revetment. He recommended further that the thickness of apron at the junction of apron and slope should be same as that laid on the slope but should be increased in the shape of a wedge towards the river bed, where intensity of current attack is severe and hence probability of loss of stone is greater.

Since apron stone shall have to be laid mostly under water and cannot be hand placed, thickness of apron at junction of toe and apron according to Rao (1946, after Varma, Saxena and Rao, 1989) should be 1.5 times the thickness of riprap in slope. Thickness at river end of apron in such case shall be 2.25 times the thickness of riprap in slope.

The slope of the launched apron was suggested by Spring and Gales as 1:2 and according to Joglekar (1971) it should not be steeper, but also not flatter than 1:3. Different shapes and dimensions were suggested by the above mentioned authors for the apron to be placed in the river bed expecting/estimating a thickness of the launched apron as about 1.25 times the thickness of the slope cover layer. The face

slope of the launching apron may be taken as 2:1 for loose stone as suggested by Spring (1903) and Gales (1938). A schematic diagram of an apron is shown in Figure 2.2. Table 2.1 presents a summary of these dimensions.

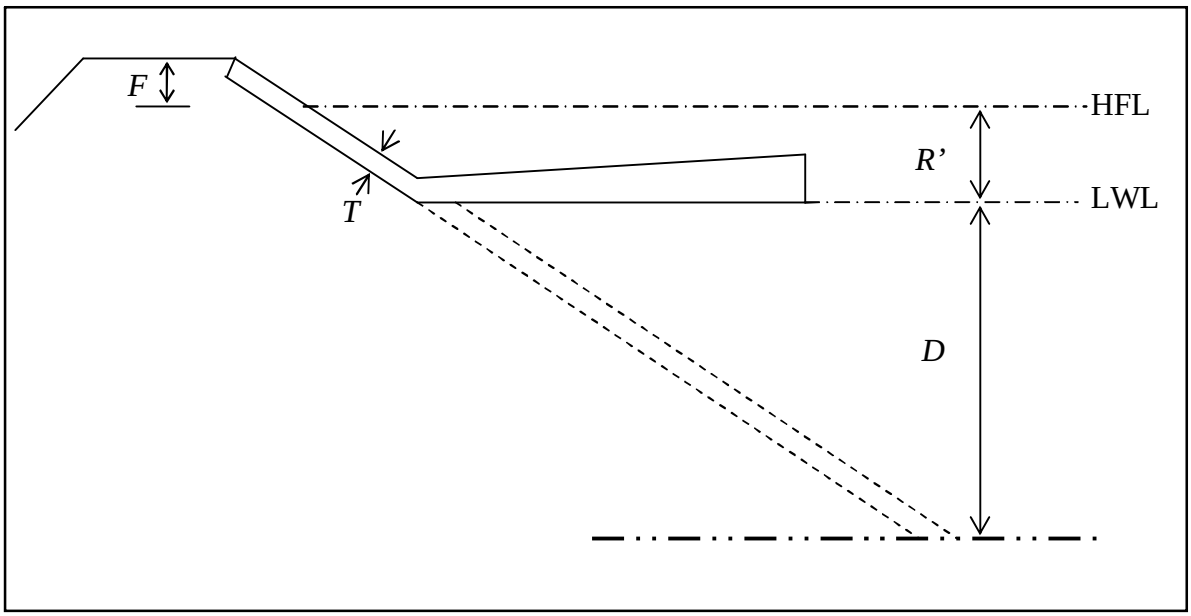

Figure 2.2: Schematic diagram of an apron

Table 2.1: Dimension of apron

Parameter	Spring (1903)	Gales (1938)	Rao (1946)
Area of slope stone	2.25 T(R'+F)	2.24 T(R'+F)	2.25 T(R'+F)
Area of apron stone	2.82 DT	2.24 DT_1	2.82 DT
Width of apron	1.50 D	1.50 D	1.50 D
Mean thickness of apron	1.88 T	1.5 T_1	1.88 T
Inside thickness of apron	T	1.5 T_1	1.5 T
Outside thickness of apron	2.76 T	1.5 T_1	2.25 T
Inclination of slope stone	1V:2H	1V:2H	1V:2H
Desired inclination of apron stone	1V:2H	1V:2H	1V:2H

Where F = freeboard, R' = rise of flood, D = deepest known scour, T = thickness of slope stone, T_1 = thickness of stone on prospective slope below bottom of apron.

Table 2.1 shows minor difference among these approaches. Gales (1938) shape of apron includes a berm and provides allowance for scour. Therefore, any approach can be followed for construction of an apron.

2.3.6 Underwater toe protection construction

During construction of toe, geobags and CC blocks are delivered directly from vessel for placement of protective elements at designated position in the settling fashion. This process is simple but their dumping behavior plays a significant role. However, in such a condition identification of placement of protective elements in underwater flowing situation is found to be more difficult. Presently such placement is roughly estimated without any strong basis as observed in field visits and information gathered from concerned officials. During the field visits at Sirajgonj Hard Point, the present practice of dumping geobags and CC blocks were observed and are shown in Photograph 2.1 and Photograph 2.2.

Photograph 2.1: Geobags are being dumped for toe protection at Sirajgonj Hard Point (Field visit on 21.07.2011)

Photograph 2.2: CC blocks are being dumped for toe protection at Sirajgonj Hard Point (Field visit on 21.07.2011)

2.4 Mechanism of a Falling Particle

When a particle falls through a fluid, the velocity at which the drag and gravity forces acting on the particle are in balance is defined as its fall velocity (w). For single particles, the fall velocity can be predicted from the equilibrium between the gravity and drag forces. In addition to the gravitational force on the particle, particle motion depends on the magnitude of forces caused by local flow patterns that develop around a freely falling particle. These patterns are as follows:

1. Separation: When the Reynolds number increases, the pattern of flow separation changes. Flow separation affects the shear and pressure distribution on the surface. If the separation point is well forward on the body there is a reduction in shear, an increase in pressure, and an increase in drag. The reverse effects are observed if the separation point is well downstream from the point of stagnation.

2. Vortex formation: As the separation zone develops, vortices are formed at the trailing edge of the particle, and they create fluctuations in pressure and alternating transverse thrust and torque on the particle.
3. Circulation is defined as the line integral of the tangential velocity component about any closed contour in the flow field. If a submerged particle rotates, the additional motion gives rise to circulation that causes a lift force acting on the particle perpendicular to the motion of the particle (Alger and Simons, 1968 and Mehta et al., 1980).

Because of the fluctuating forces, the fall of a particle in a liquid may be subjected to three classes of motion: sliding, tipping, and rotation. These forms of motion may occur separately or in combination.

2.4.1 Fall velocity equations

In 1851, Stokes obtained the solution for the drag resistance of flow past a sphere by expressing the simplified Navier-Stokes equation together with the continuity equation in polar coordinates. Using his solution, the following expression for settling velocity of spherical particles can be derived as:

$$R^* = \frac{\Delta g d^3}{18\nu^2} \tag{2.1}$$

$$or, R^* = \frac{A}{18} \tag{2.2}$$

Where $\Delta = (\rho_s - \rho)/\rho$; ρ_s and ρ = density of the particle and the density of the fluid, respectively; g = acceleration due to gravity; d = characteristics diameter of the particle; ν = kinematic viscosity of water; $A = \Delta g d^3 / \nu^2$ = Archimedes buoyancy index. Equation (2.1) is only valid for $R^* < 1$.

Rubey (1933) developed a simple equation to predict fall velocity based on equating the buoyant weight of a particle to the sum of viscous and turbulent flow resistance. Rubey's (1933) equation is:

$$R^* = \sqrt{\left\{36 + \frac{2g(\rho_s - \rho)d^3}{3\rho\,\nu^2}\right\}} - 6 \tag{2.3}$$

Hallermeier (1981) made an extensive study on settling velocity of particles over a wide range of Reynolds number. For turbulent flow the equation is:

$$R^* = 1.05\sqrt{A} \tag{2.4}$$

Van Rijn (1993) proposed a very simple equation to predict fall velocity as:

$$w = 1.1\sqrt{\Delta g d} \quad for \quad d > 0.1\ cm \tag{2.5}$$

Cheng (1997) shows two general relationships for drag coefficients for sediment particles falling in a fluid; they may be written as:

$$C_D = \frac{4\Delta g d}{3w^2} \tag{2.6}$$

and

$$C_D = \left\{(a / R^*)^{1/c} + b^{1/c}\right\}^c \tag{2.7}$$

where C_D = drag coefficient. Coefficients *a*, *b*, and *c* are dimensionless numbers which have approximately the following role: coefficient *a* is important at low Reynolds numbers, laminar flow; coefficient *b* is important at high Reynolds numbers, turbulent flow; and coefficient *c* was determined by fitting to data, with Reynolds numbers in the range $1<R^*<1000$. Cheng (1997) gives the following values for these constants: a = 32, b = 1.0, and c = 1.5, that are appropriate for his data set. Combining Equations (2.6) and (2.7) and solving for the positive root of the quadratic equation gives Cheng's (1997) fall velocity equation as:

$$R^* = \left(\sqrt{25 + 1.2{d_*}^2} - 5\right)^{1.5} \tag{2.8}$$

Where $d_* = d\left(\frac{\Delta g}{\nu^2}\right)^{1/3}$ is the dimensionless particle diameter.

Chang and Liou (2001) suggested a formula for computation of fall velocity in a fractional form as:

$$R^* = \frac{aA^n}{18\left(1 + aA^{n-1}\right)} \tag{2.9}$$

When the value of *A* is small and the value of n is less than one, (2.9) turns out to be $R^*=A/18$, because the value of aA^{n-1} is much larger than one. When the value of *A* is

large, (2.9) is converted into $R^*=aA^n/18$, because the value of aA^{n-1} is smaller than one. Chang and Liou (2001) suggested the following values for the coefficients a = 30.22 and n = 0.463.

Göğüş et al. (2001) developed an iterative technique in order to find fall velocity of regularly shaped angular particles. This technique consists of the following equations:

$$\Psi = \left(\frac{a_1 + b_1}{c_1}\right)\left(\frac{a_1 + b_1 + c_1}{\forall}\right) \tag{2.10}$$

$$R_* = w\rho\sqrt{(a_1 + b_1)} / \mu \tag{2.11}$$

$$C_D{}^* = \alpha(R_*)^{\beta} / \Psi \tag{2.12}$$

Where Ψ = shape factor; a_1, b_1 and c_1 = maximum, intermediate and minimum dimension of a particle respectively; $\forall$ = volume of original particle; R_* = modified Reynolds number; w = fall velocity of the particle; ρ = density of the fluid; μ = dynamic viscosity of the fluid; C^*_D = modified drag coefficient; α, β = empirical constants related with shape factor, Ψ.

Table 2.2: α and β values for shape factor

Shape	$\boldsymbol{\Psi}$	$\boldsymbol{\alpha}$	$\boldsymbol{\beta}$
Cube	2.83	3.396	0.0360
Box shaped prism	4-6	1.2533/ Ψ	0.2148
Box shaped prism	6-8	3.2507/ Ψ	0.1488
Box shaped prism	8-12	26.612/ Ψ	0.0123
Box shaped prism	12-16	25.148/ Ψ	-0.0039
Box shaped prism	16-21	94.164/ Ψ	-0.1262

The technique can be used with the following steps:

1. For a given particle, find a_1, b_1 and c_1 and calculate the shape factor using equation (2.10).
2. Find the relevant values for α and β with the calculated Ψ from table 2.2.

3. Assume a fall velocity, *w*, and calculate R^* then C^*_D from equation (2.11) and (2.12), respectively.
4. Find new value of *w* from the drag coefficient C^*_D, calculated in Step 3.
5. Compare assumed and calculated values of fall velocity; if the difference is reasonably negligible then it can be accepted that the assumed value is the fall velocity of the given particle. Otherwise, using the calculated value of w in Step 4, repeat the procedure from Step 3.

2.5 Placement of Protection Elements

Placement of protection elements is mainly governed by its settling behavior and incipient condition under various hydraulic conditions. Hydrodynamic characteristics, especially the settling behavior of geobags and blocks, are of practical significance particularly for the construction of toe of a revetment and submerged groins or dikes. Study related to these hydrodynamic characteristics is very scarce in literature.

2.5.1 Settling distance formula

Zhu et al. (2004) developed a formula for predicting the longitudinal settling distance of sandbags based on experimental observations as:

$$\frac{S}{h} = K \frac{V}{\sqrt{\Delta g d_t}} \tag{2.13}$$

Where S = settling distance; h = depth of flow; V = depth-averaged flow velocity; d_t = thickness of sand container; K = empirical constant of value 1.3. But equation (2.13) is limited for large sized geocontainers.

2.6 Threshold Condition of Protection Element

When the hydrodynamic force acting on a particle has reached a value that, if increased even slightly will put the particle into motion, critical or threshold condition are said to have been reached. When critical conditions obtain values of such quantities as the mean velocity, bed shear stress or the stage of a stream are said to have their critical or threshold values.

The driving forces are strongly related to the local near bed velocities. In turbulent flow conditions the velocities are fluctuating in space and time which make together with the randomness of both the particle size, shape and position that initiation of motion is not merely a deterministic phenomenon but a stochastic process as well.

2.6.1 Incipient condition based on critical shear stress

The forces acting on a particle over which a fluid is flowing are the gravity forces of weight and buoyancy, hydrodynamic lift normal to the bed, and hydrodynamic drag parallel to the bed. The lift is often neglected without proper justification because both analytical and experimental studies have established its presence. Most treatments of forces on a particle on a bed consider only drag; lift does not appear explicitly. But, because the constants in the resulting theoretical equations are determined experimentally and because lift depends on the same variable as drag, the effect of lift regardless of its importance is automatically considered (Vanoni, 1975).

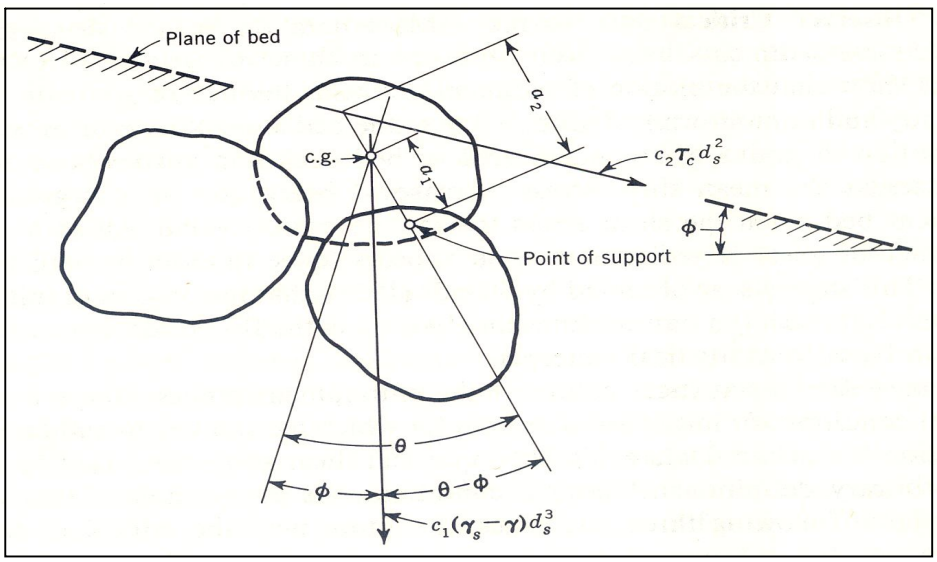

Figure 2.3: Forces on particle in flowing stream (Source: Vanoni, 1975)

The forces on a particle on the bed is depicted in Figure 2.3, in which ϕ = the slope angle of the bed; and θ = the angle of repose of the particle submerged in the fluid, and intergranular forces are ignored. The particle will be moved or entrained if the hydrodynamic forces overcome the resistance. When motion is impending, the bed shear stress attains the critical or competent value, τ_c, which is also termed the

critical tractive force. Under critical conditions, also, the particle is about to move by rolling about its point of support. The gravity or weight force is given by

$$W = c_1(\gamma_s - \gamma)d_s^{\,3} \tag{2.14}$$

in which $c_1 d_s^3$ = the volume of the particle where c_1 is a constant; d_s = its size, usually taken as its mean sieve size; and γ and γ_s = specific weights of fluid and sediment, respectively. The critical drag force is

$$F_D = c_2 \tau_c d_s^{\,2} \tag{2.15}$$

in which $c_2 d_s^2$ = the effective surface area of the particle exposed to the critical shear stress, τ_c where c_2 is a constant. Equating moments of the gravity and drag forces about the support yields:

$$W a_1 \sin(\theta - \phi) = F_D a_2 \cos\theta$$

$$c_1(\gamma_s - \gamma)d_s^{\,3} a_1 \sin(\theta - \phi) = c_2 \tau_c d_s^{\,2} a_2 \cos\theta$$

$$or, \tau_c = \frac{c_1 a_1}{c_2 a_2}(\gamma_s - \gamma)d_s \cos\phi(\tan\theta - \tan\phi) \tag{2.16}$$

For a horizontal bed, $\phi = 0$, and Equation (2.16) becomes:

$$\tau_c = \frac{c_1 a_1}{c_2 a_2}(\gamma_s - \gamma)d_s \tan\theta \tag{2.17}$$

When a_1 and a_2 are equal the forces on the particle act through its center of gravity and the fluid forces are caused predominantly by pressure. Also, when a_1 and a_2 are equal it will be seen that the ratio of the forces on the particle parallel to the bed i.e. hydrodynamic force, to those acting normal to the bed i.e. immersed weight, is equal to $\tan\theta$, resulting Equation (2.17) as:

$$\frac{\tau_c}{(\gamma_s - \gamma)d_s} = c\tan\theta \tag{2.18}$$

The left-hand side of equation (2.18) represents the ratio of two opposing forces: hydrodynamic force and immersed weight, which governs the initiation of motion.

Major variables that affect the incipient motion include τ_c, d_s, γ_s-γ, ρ and v. From dimensional analysis they may be grouped into the following dimensionless parameters

$$F\left[\frac{\tau_c}{(\gamma_s-\gamma)d},\frac{(\tau_c/\rho)^{1/2}d}{\nu}\right]=0 \tag{2.19}$$

$$or,\ \frac{\tau_c}{(\gamma_s-\gamma)d}=F\left(\frac{U_{*c}d}{\nu}\right) \tag{2.20}$$

Where $U_{*c}=\sqrt{(\tau_c/\rho)}$ is the critical friction velocity. The left-hand side of this equation is the dimensionless critical Shields stress, τ_{*c}. The right-hand side is called the critical boundary Reynolds number and is denoted by R_{*c}. Figure 2.4 shows the functional relationship of equation (2.20) established based on experimental data, obtained by Shields (1936) and other investigators, on flumes with a flat bed. It is generally referred to as the Shields diagram. Each data point corresponds to the condition of incipient motion.

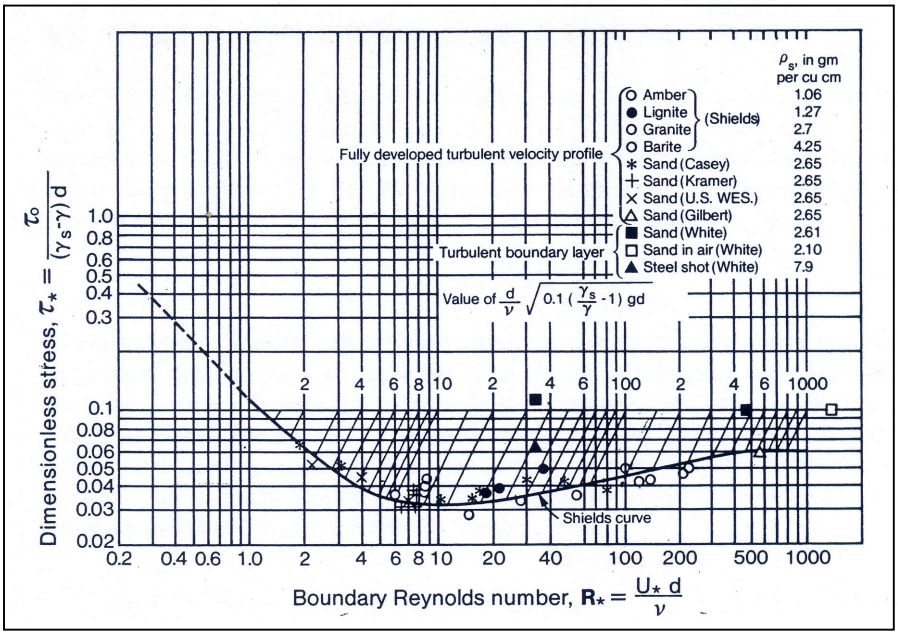

Figure 2.4: Shield's diagram for incipient motion (Source: Chang, 1992)

2.6.2 Incipient condition based on critical depth averaged velocity

The earliest studies were related to critical velocities of stones (Brahms, 1753 and Sternberg, 1875). They studied the critical near bed velocity and found that it was related to the particle diameter, as follows:

$$u_{oc}{}^2 \sim d_s$$

in which u_{oc} is the fluid velocity near the bed under critical conditions. Taking

$$\tau_c \sim u_{oc}{}^2$$

and substituting this in Equation (2.18) also gives:

$$u_{oc}{}^2 \sim d_s$$

Cubing both sides of the relation gives:

$$d_s{}^3 \sim u_{oc}{}^6$$

which is the well known sixth power law. Because the volume or weight of a particle is proportional to d_s^3, the law states that the weight of largest particle that a flow will move is proportional to the sixth power of the velocity in the neighborhood of the particle. Rubey (1948) found that this law applied only when d_s is large compared with the thickness of the laminar sub layer and the flow about the grain is turbulent.

The near bed velocity is, however, not very well defined and it is preferable to use the critical depth averaged velocity $\left(\overline{u_c}\right)$ as the characteristic parameter. It can be derived from the critical bed shear stress using the Chezy equation. Assuming hydraulic rough flow conditions $\left(\frac{u_* k_s}{\nu} > 70\right)$, the critical depth averaged flow velocity for a plane bed can be expressed as:

$$\overline{u_c} = 5.75 u_{*,c} \log\left(\frac{12h}{k_s}\right) \tag{2.21}$$

Where $\overline{u_c}$ = critical depth averaged flow velocity; h = water depth; $k_s = \alpha d_{90}$ = effective bed roughness of a flat bed; α = coefficient (α = 1 for stones $d_{50} \geq 0.1$ m and α = 3 for sand and gravel material); $u_{*c} = \left(\tau_{*c}\right)^{0.5}\left(\Delta g d_{50}\right)^{0.5}$ = critical bed shear velocity; and τ_{*c} = critical Shields parameter. Equation (2.21) can be expressed as:

$$\overline{u_c} = 5.75\left(\Delta g d_{50}\right)^{0.5}\left(\tau_{*c}\right)^{0.5} \log\left(\frac{12h}{k_s}\right) \tag{2.22}$$

Using Equation (2.19), $k_s = 3d_{90}$ and $d_{90} = 2d_{50}$ and the Shields curve, the critical depth averaged velocity can be expressed as:

$$\overline{u_c} = 0.19\left(d_{50}\right)^{0.1} \log\left(\frac{12h}{3d_{90}}\right) \quad \textit{for } 0.0001 \leq d_{50} \leq 0.0005 \text{ m} \tag{2.23}$$

$$\overline{u_c} = 8.50\left(d_{50}\right)^{0.6} \log\left(\frac{12h}{3d_{90}}\right) \quad \text{for } 0.0005 \le d_{50} \le 0.002 \text{ m} \tag{2.24}$$

Where d_{50} = median particle diameter; d_{90} = *90 %* particle diameter.

Inglis (1921) proposed a relationship for incipient motion of a single layer of stones on a flat bed on the basis of small scale experiments as:

$$\frac{d_{50}}{h} = 0.34\left[\left(\frac{\gamma}{\gamma_s - \gamma}\right)^{0.5} \frac{V}{\sqrt{gh}}\right]^{2.6} \tag{2.25}$$

Where d_{50} = median size of stone ;V = depth averaged flow velocity; g = gravitational acceleration; and h = depth of flow.

On the basis of experiments with natural gravels, glass spheres and low density spheres, Neil (1967) proposed a relationship designed to just maintain stability on a flat bed, which can be arranged in the form:

$$\frac{d_{50}}{h} = 0.32\left[\left(\frac{\gamma}{\gamma_s - \gamma}\right)^{0.5} \frac{V}{\sqrt{gh}}\right]^{2.5} \tag{2.26}$$

Maynored (1989) presented a relationship on the basis of more extensive experiments at larger scales, for incipient movement of riprap as:

$$\frac{d_{30}}{h} = 0.30\left[\left(\frac{\gamma}{\gamma_s - \gamma}\right)^{0.5} \frac{V}{\sqrt{gh}}\right]^{2.5} \tag{2.27}$$

Where d_{30} = riprap size for which 30% is finer by weight.

USACE (1991) modified the Maynord equation, replacing the primary coefficient 0.30 by a set of four multiplying coefficients and inserting a side slope correction factor, to obtain a relationship that can be arranged as follows:

$$\frac{d_{30}}{h} = S_f C_s C_v C_T \left[\left(\frac{\gamma}{\gamma_s - \gamma}\right)^{0.5} \frac{V}{\sqrt{K_1 gh}}\right]^{2.5} \tag{2.28}$$

Where V = depth averaged velocity; S_f = safety factor, minimum recommended value for riprap design = 1.1; C_s = stability coefficient for incipient failure having a value

of 0.30 for angular rock and 0.36 for rounded; C_V = coefficient for vertical velocity distribution, range 1.0 to 1.28 for straight channels to abrupt bends; C_T = coefficient for riprap layer thickness; K_1= side slope correction factor.

The dimensional analysis approach

According to the dimensional analyses presented by Neill (1967), the pertinent variables applicable to the stability of coarse particles can be arranged as:

$$f\,(h, d, \rho_w, V, \gamma'_s, , v) = 0 \tag{2.29}$$

Where h = depth of flow; d = characteristic particle size; ρ = water density; V = characteristic velocity; γ'_s = submerged specific weight of particle; and v = kinematic viscosity. For rough turbulent flow, the viscosity effects are eliminated and the dimensionless ratios are found to relate in the following functional form:

$$\frac{V^2}{\left(\frac{\gamma_s - \gamma_w}{\gamma_w}\right)gh} = f\left(\frac{d}{h}\right) \tag{2.30}$$

2.7 Remarks

Appropriate construction method is one of the main factors for the sustainability of bank protection works, particularly for the toe protection construction. Such method requires the combined knowledge of mechanism of settling behavior as well as threshold condition of protection element. However, not many studies related to the settling behavior of protective elements for the construction of toe in under water condition is available in literature.

In practice toe protection elements of bank protection works are dumped into the flowing water from the vessel and then it settled somewhere on the river bed to form a falling apron. The understanding of falling mechanism of protection elements is required so that an appropriate knowledge on placement of the toe protection element can be achieved. Since the settling behavior of geobags and blocks are of practical importance, particularly for the construction of toe of a revetment and submerged

groins or dikes, more attention related to this phenomenon is necessary. In this study an attempt has been made to carry out experimental investigation to get an understanding of the aforesaid objectives.

CHAPTER THREE

THEORETICAL ANALYSIS AND METHODOLOGY

3.1 Introduction

In previous chapter literature review on settling behavior and threshold condition has been discussed. Theoretical background of the specific objective and methodology of the present study is highlighted in this chapter. The theoretical knowledge gained from the analysis of various parameters will be investigated in laboratory experiment. The parameters discussed are mainly the fall velocity, settling distance and threshold condition of laboratory scale protection elements.

3.2 Analysis of Fall Velocity

To estimate the fall velocity of particles, two different approaches can be followed: (1) an idealized one in which the particle is assumed to be a sphere; and (2) a more realistic one in which the natural shape is considered. In general, the first approach is used extensively (for instance, sediment grain size is calculated by assuming it to be spherical), although some methods take into account the sediment shape.

For single particles, the fall velocity can be predicted from the equilibrium between the gravity and drag forces, the drag coefficient C_D being the main unknown. Stokes (1851) found that C_D is inversely proportional to the particle Reynolds number R^* ($R^* = wd/\nu$ where d = diameter of the particle and ν = kinematic viscosity of water) when $R^*<1$. On the other hand, under the condition of high Reynolds number ($R^*>10^5$), the drag coefficient was found to be a constant (Dallavalle, 1948 and Schlichting, 1979).

The settling or fall velocity of a sphere in water can be estimated by solving the balance between the gravitational force or submerged weight force and the drag resistance:

$$\text{Gravitational force, } F_g = (\rho_s - \rho) g \frac{\pi}{6} d_n^{\,3} \tag{3.1}$$

Where d_n is the nominal diameter of the particle defined as the diameter of a sphere

having the same volume and mass as the measured particle. It can be calculated as:

$$d_n = \left(\frac{6V}{\pi}\right)^{\frac{1}{3}} = \left(d_l d_w d_t\right)^{\frac{1}{3}} \tag{3.2}$$

where V = original volume of the particle; d_l, d_w, and d_t are the respective length, width and thickness of the particle.

$$\text{Drag force, } F_D = C_D \frac{\pi}{4} d_n{}^2 \frac{\rho w^2}{2} \tag{3.3}$$

where C_D = drag coefficient and w = fall velocity.

At terminal velocity, the drag force on the particle is equal to the particle's submerged weight. From equation (3.1) and (3.3), drag coefficient can be expressed as:

$$C_D = \frac{4\Delta g d_n}{3w^2} \tag{3.4}$$

Using the dimensionless particle diameter d_* defined as

$$d_* = d_n \left(\frac{\Delta g}{\nu^2}\right)^{\frac{1}{3}} \tag{3.5}$$

From equation (3.4) and (3.5) another relationship for C_D is found

$$C_D = \frac{4 d_*{}^3}{3 R^{*2}} \tag{3.6}$$

Fall velocity of an angular particle through a fluid can be expressed as a function of relevant variables as follows:

$$w = f\left(W', \rho, L, \mu, D, \Psi\right) \tag{3.7}$$

where W' = submerged weight of the particle; L = characteristics length of the particle; μ = dynamic viscosity of water; D = diameter of the settling column; and Ψ = nondimensional factor describing the shape of the particle.

In nondimensional form equation (3.7) can be written as:

$$f\left(\frac{W'\rho}{\mu^2}, \frac{wL\rho}{\mu}, \frac{D}{L}, \Psi\right) = 0 \tag{3.8}$$

The submerged weight, W' can be replaced by $g\left(\rho_s - \rho\right)L^3$. The characteristics

length of the particle is selected as the nominal diameter (d_n) defined by equation (3.2). Following this assumption the characteristics length, L, used in the expressions of the first, second and third nondimensional term of (3.8), is replaced by d_n. After all these changes, (3.8) become:

$$f\left(\left(\frac{\Delta g}{\nu^2}\right)^{\frac{1}{3}} d_n, \frac{w d_n}{\nu}, \frac{D}{d_n}, \Psi\right) = 0 \tag{3.9}$$

The first and second nondimensional term of equation (3.9) can be replaced by dimensionless particle diameter (d_*) defined in equation (3.5), and R^* respectively. Inserting d_* and R^* into equation (3.9) results in:

$$f\left(d_*, R^*, \frac{D}{d_n}, \Psi\right) = 0 \tag{3.10}$$

The effect of the settling column wall on the fall velocity predictions is considered in the term D/d_n of equation (3.10). However, the ratio of settling column diameter to maximum dimension of the particle used in the experiments showed that this effect is negligible in this study (McNown et al., 1948; McNown and Newlin, 1951). The shape of the particle influences its fall velocity. For the present study the shape of the particles was fixed, only box-shaped prism. Moreover, the C_D value decreases rapidly outside the Stokes region ($R^*<1$) and becomes nearly constant for $10^3 < R^* < 10^5$ (Van Rijn, 1993). When the particle fall velocity of a box-shaped prism increases ($R^*>10^4$), then the effect of shape on the drag decreases continuously (Göğüş et al., 2001). Therefore, Ψ may be assumed to be constant in this study. Thus, equation (3.10) can be reduced to:

$$R^* = f(d_*) \tag{3.11}$$

3.3 Analysis of Settling Distance

While a toe protection element settling in water, its settling distance is subjected to (i) its submerged weight, W which is a component of gravitational force, F_g; (ii) flow resistance or drag force, F_D; (iii) depth averaged velocity of flowing water, V which has immense influence on the horizontal velocity of elements, U; and (iv) the depth of flow, h.

It is known that settling velocity of a particle encompasses both of its gravitational and drag forces. Assuming that the settling velocity of an element is the same as its terminal settling velocity, *w*, then

$$\frac{dy}{dt} = w \tag{3.12}$$

The horizontal velocity of an element, *u*, is given by:

$$\frac{dx}{dt} = u \tag{3.13}$$

which decreases towards the channel bed. Here *x* is directed downstream and *y* is measured downwardly from the flow surface, as shown in Figure 3.1.

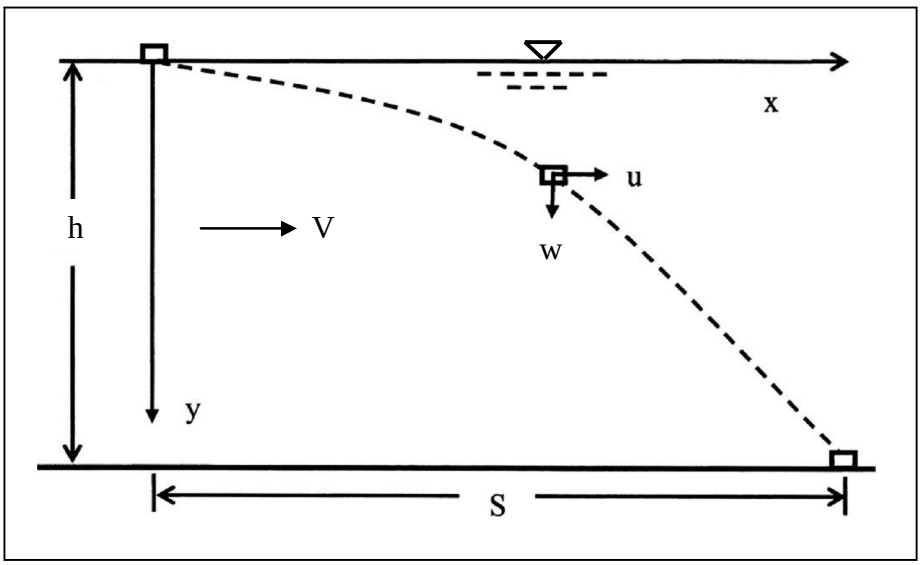

Figure 3.1: Schematic diagram showing features of horizontal settling distance

Combining equations (3.12) and (3.13) yields:

$$dx = \frac{u}{w} dy \tag{3.14a}$$

Integration of equation (3.14a) gives:

$$x = \frac{u}{w} y + \text{Constant} \tag{3.14b}$$

Constant of integration is zero when $x = 0$ and $y = 0$. For $x = S$ and $y = h$, u becomes U (horizontal depth averaged velocity of the elements). Therefore, from the free surface ($y = 0$) to the channel bed ($y = h$) the settling distance, S, is given by:

$$S = \frac{U}{w} h \tag{3.15}$$

where U is a function of fall velocity of an element and the depth averaged flow velocity. Furthermore, it is assumed that U may be expressed as a power function considering nonuniformity of flow behavior:

$$U = \frac{kV^m}{w^{m-1}} \tag{3.16}$$

where k = empirical coefficient and m = empirical exponent. Substituting this in equation (3.15) gives:

$$\frac{S}{h} = k\left(\frac{V}{w}\right)^m \tag{3.17}$$

3.4 Analysis of Incipient Motion

Shear stress is frequently used in river bank protection works (USACE, 1994; Stevens and Simons, 1971; Maynord et al., 1989) because it describes the forces that occur in the channel boundaries. Several investigations (Meyer-Peter and Muller, 1948; Blench, 1966; Neil, 1967; Bogardi, 1978; Bettess, 1984) have shown that the Shields coefficient (also called the dimensionless shear stress) is not constant as used in many design procedures but varies directly with relative roughness (particle size/depth).

Neil and Hey (1982) have noted that many engineers prefer design procedures based on velocity. The appropriate velocity for use in the riprap design procedure must be determined. The velocity used must be representative of flow conditions at the riprap and must be able to be determined by the designer by relatively simple methods. Local bottom velocity is the most representative velocity but is difficult for the designer to predict. Local average velocity, also called depth-averaged velocity is representative of flow conditions at the point of interest and can be estimated by the designer (Maynord et al., 1989).

The dimensional analysis follows the analyses previously presented by Neill (1967). The pertinent variables applicable to the stability of coarse particles are

$$f(h, d, \rho_w, V, \gamma'_s, , v) = 0 \tag{3.18}$$

where h = depth of flow; d = characteristic particle size; ρ_w = water density; V = characteristic velocity; γ'_s = submerged specific weight of particle; and v = kinematic viscosity. By requiring rough turbulent flow, the viscosity effects are eliminated and the dimensionless ratios are found to relate in the following form:

$$\frac{d}{h} = f\left[\left(\frac{\gamma_s - \gamma_w}{\gamma_w}\right)^{0.5} \frac{V}{\sqrt{gh}}\right] \tag{3.19}$$

where γ_s = specific weight of particle = $g\rho_s$. In this study, the pertinent variables are as shown in equation (3.18) with the repeating variables of V, d, and γ'_s.

Equation (3.19) is presented in the same form in Bogardi (1978). The right side of equation (3.19) contains a local Froude number. Almost all riprap problems concern subcritical flow and that reduces the significance of defining this as a Froude number.

3.5 Stepwise Methodology

The study has been carried out according to following steps of activities:

(i) Theoretical analysis of governing parameters
(ii) Design of experiments
(iii) Test scenarios and experimental run
(iv) Measurements and observations
(v) Analysis of data and development of equations
(vi) Predictive performance of proposed equation and comparison with others

The stepwise methodology can be better explained in a flow diagram as shown in Figure 3.2.

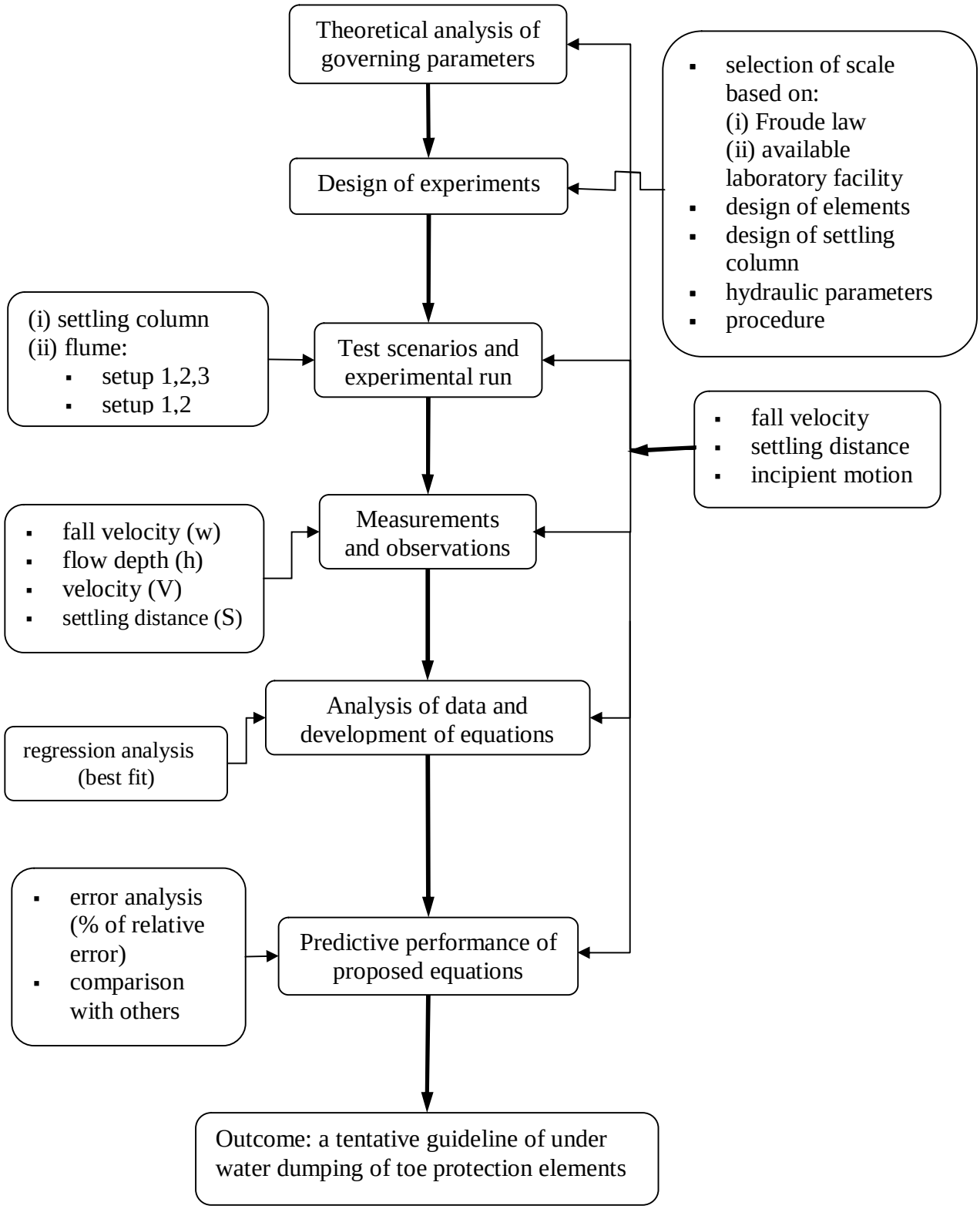

Figure 3.2: Flow diagram of methodology of the study

3.6 Remarks

The theoretical basis of governing parameters of settling behavior has been analyzed in this chapter. Detail of the experimentation, measurements and observations is reported in chapter four. Measured data from experiments will be used to obtain empirical relationships using equations (3.11), (3.17) and (3.19) for fall velocity, settling distance and threshold condition, respectively. Also the predictive performance of the proposed equation will be evaluated by error analysis and comparison with other equations. These are explained in chapter five.

CHAPTER FOUR

EXPERIMENTATION AND OBSERVATION

4.1 Introduction

Present study deals with the investigation of the settling phenomena and threshold condition for movement of toe protection elements in bank protection structures in the context of conventional underwater construction procedure followed in Bangladesh. A brief description of the experimental design, procedure and observation is depicted here.

4.2 Experimental Setup

The experiments are conducted in a settling column and in the large tilting flume of the Hydraulics and River Engineering Laboratory of Water Resources Engineering Department, Bangladesh University of Engineering and Technology (BUET), Dhaka. Schematic diagram of the flume setup is shown in Figure 4.1. In addition a settling column has been fabricated to test the settling characteristics of the protection elements.

4.2.1 Fabrication of settling column

A square shaped Plexiglas settling column of 30 cm a side and 1.3 m height was constructed at the Hydraulics and River Engineering Laboratory. The confining effect of the size of settling column on the fall velocity may be evaluated on the basis of the work of McNown et al. (1948) who related d/D with W_d/W_i , for a range of particle Reynolds number in which d = diameter of a falling sphere; D = diameter of the column; W_d = measured fall velocity of the sphere; and W_i = fall velocity of the same sphere in a fluid of infinite extent. The longest dimension of the particles used in the experiment was 7.2 cm, so that d/D = 0.24, if the particle is replaced by a sphere of 7.2 cm diameter. For this ratio and R^* in the range of $9\text{x}10^3$ to $4\text{x}10^4$ corresponding to the range of test data, W_d/W_i = 0.95, which indicates a 5% measurement error caused by the column. The settling column is shown in Photograph 4.1.

Photograph 4.1: Plexiglas settling column

4.2.2 Flume setup

The experiment has been carried out in a 21.34 m long, 0.762 m wide and 0.762 m deep rectangular tilting flume in the Hydraulics and River Engineering Laboratory. The side walls of the flume are vertical and made of clear glass. The bed is painted by water resistant color to avoid excess bed friction. A tail gate is provided at the end of the flume to control the depth of flow. Two pumps are there to supply water from the reservoir to the flume through a recirculating channel. A photograph of the flume is shown in Photograph 4.2. Point gauge is used to measure the depth of flow. The gauge is mounted on a trolley laid across the width of the flume. The whole structure of point gauge could be moved over the side rails. The point gauge can measure with 0.10 mm accuracy.

Photograph 4.2: Laboratory flume

4.2.3 Electromagnetic flow meter

Discharge measurements are taken from the electromagnetic flow meter. Of the two flow meters one is 200 mm and the other is 150 mm diameter. The flow through the pipe is controlled by the valve. Photograph 4.3 shows an electromagnetic flow meter.

Photograph 4.3: Electromagnetic flow meter.

4.2.4 Current meter

A small current meter is used for velocity measurement. It consists of three basic parts: 50 mm diameter propeller, 1 m long 9 mm diameter rod and signal counter set. Minimum depth of water for using the instrument is approximately 4 cm. It is capable of measuring velocity from 3.5 cm/s to 5 m/s. Time and impulse measurement accuracy is ±0.01 seconds and ±0.5 impulses, respectively. Photograph 4.4(a) shows the current meter and 4.4(b) shows measurement in the flume.

Photograph 4.4(a): Small current meter

Photograph 4.4(b): Velocity measurement using current meter

4.3 Experimental Size of Protection Elements

Following sections describe the process to determine the dimension of blocks and geobags.

4.3.1 Selection of scale for experimentation

A geometrically similar undistorted scale factor 20 has been selected to conduct the experiment. This selection of scale is based on (i) the available laboratory flume facilities and (ii) the Froude law criteria.

4.3.2 Design of various model parameters

From the above considerations, various scale ratios of model parameters are designed as shown in Table 4.1.

Table 4.1: Scale ratios of model parameters

Quantity	Dimension	Scale ratio
Length	L	1:20
Volume or weight	L^3	1:8000
Velocity	$L^{1/2}$	1:4.47
Discharge	$L^{5/2}$	1:1789

It is assumed that the material and porosity remain unchanged for the experiment and prototype. Therefore, protection elements used for the laboratory experiment should be the same as those designed for field construction except for the reduced dimension.

4.3.3 Design of size of sand cement block

Sand cement blocks of different sizes are prepared using iron mold. The cement-sand ratio is 1:4. After one day of preparation, curing of blocks is done for 48 hours. The blocks are cubical and box shaped prism. The cube shaped blocks are commonly used in Bangladesh context. Others are used to have a generalized and more precise correlation for fall velocity computation. Different blocks used for the present study is shown in Photograph 4.5. The dimensions of blocks are listed in Table 4.2.

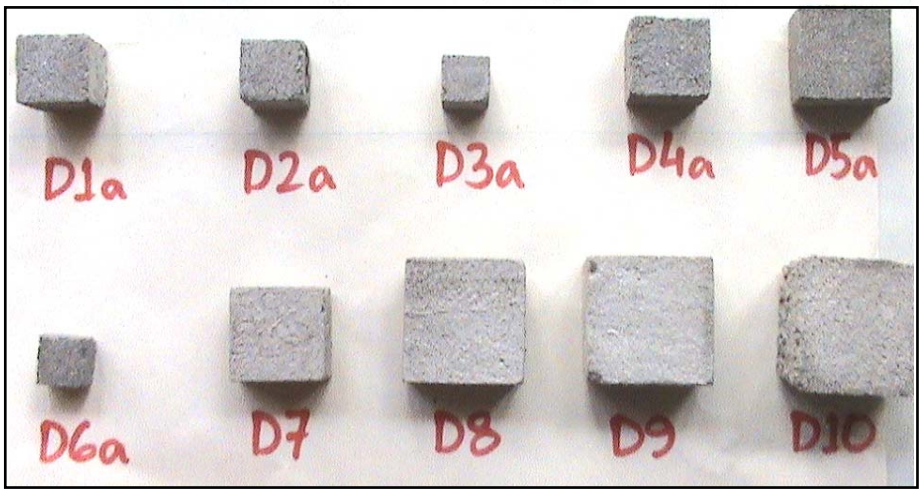

Photograph 4.5: Various sizes of CC blocks

Table 4.2: Dimension of CC blocks used in the experiment

Type of block	Length, d_l (mm)	Width, d_w (mm)	Thickness , d_t (mm)
D1a	22.90	23.16	24.10
D2a	20.98	20.72	20.48
D3a	15.96	15.98	16.02
D4a	30.08	31.30	16.26
D5a	25.70	26.10	19.20
D6a	16.24	16.12	13.00
D7	31.30	30.88	16.26
D8	40.10	40.72	16.56
D9	40.68	40.60	20.60
D10	40.98	41.28	26.66

Different methods regarding calculations of unit dimensions of revetment cover layers and toe protections (e.g. PIANC, 1987; Pilarczyk, 1989; FAP 21/22, 1993) show only marginal deviations within the range of application for the rivers of Bangladesh. Since the widely used Pilarczyk formula (Pilarczyk, 1989; Przedwojski et al., 1995) includes the turbulence intensity, velocity and shear stress, it is followed to determine the nominal thickness of a protection unit. The formula is:

$$D_n = \frac{\phi_c K_T K_h}{\Delta K_s} \frac{0.035}{\theta_c} \frac{\bar{u}^2}{2g} \tag{4.1}$$

The values of the parameters of the formula are considered according to Zaman and Oberhagemann (2006). Here, D_n = nominal thickness of protection unit, m; ϕ_c = stability factor = 0.75 for continuous protection of loose units; K_T = turbulence factor = 1.5 for nonuniform flow with increased turbulence; K_h=depth and velocity distribution factor= $\left(h/D_n+1\right)^{-0.2}$, h=water depth, m; Δ=relative density of protection unit= $\left(\rho_s-\rho\right)/\rho=1$; K_s = slope reduction factor = $\sqrt{\left(1-\sin^2\alpha/\sin^2\phi\right)}$

= 0.72, α = slope angle = 26.57^0 (for 1V:2H); ϕ = angle of repose = 40^0 (for blocks); θ_c = critical value of dimensionless shear stress = 0.035 for free blocks; ū = depth averaged flow velocity, m/s. Details calculation is shown in Appendix A.

4.3.4 Design of size of geobag

Geobags of six different sizes were prepared by expert technician. For a bag, the exact amount of sand is weighted first. Then it is put in the one side open bag made of cloth. After that it is sewed to get a complete one. The shape is rectangular and square. The length to width ratio ranges from 1.73 to 1.09. For some typical block sizes, the equivalent sizes of geobags are provided in FAP 21 (2001). Consequently block type D1a and D2a is equivalent to geobag type A1, A2 and B1, B2, respectively. The dimensions of the bags are listed in Table 4.3. Photograph 4.7 shows different bags used in the experiment.

Table 4.3: Dimension of geobags used in the experiment

Type of geobag	Length, d_l (mm)	Width, d_w (mm)	Thickness , d_t (mm)
A1	60.24	38.60	7.02
A2	51.94	47.70	7.02
B1	51.60	29.80	8.60
B2	42.90	38.00	9.04
C	42.06	26.20	8.14
E	71.20	40.90	10.9

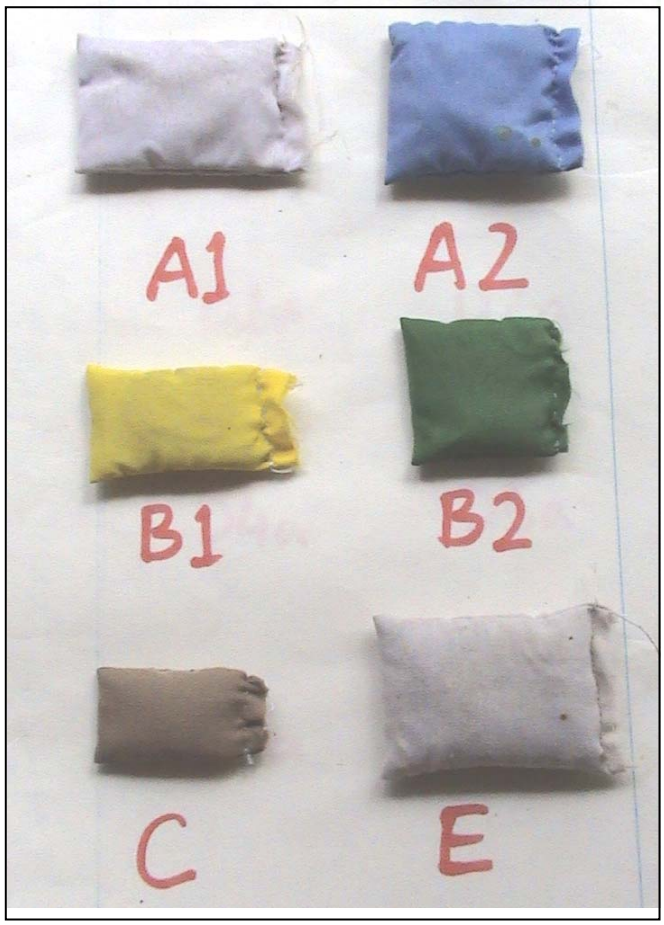

Photograph 4.6: Various sizes of geobags

Photograph 4.7: CC blocks and geobags used in experiments

4.3.5 Design of apron

Design scour depth can be estimated by Lacey's regime formula as it is widely used in this subcontinent in unconstricted alluvial rivers. This empirical regime formula is:

$$R = 0.47\left(\frac{Q}{f}\right)^{1/3} \tag{4.2}$$

With $D_s = XR\text{-}h$ (4.3)

Where D_s = Scour depth at design discharge, m; Q = Design discharge, m^3/s; h = Depth of flow, m; may be calculated as (HFL-LWL); f = Lacey's silt factor = $1.76\,(d_{50})^{1/2}$; d_{50} = Median diameter of sediment particle, mm; X = Multiplying factor for design scour depth.

Table 4.4: Hydraulic parameters of typical field condition

High Water Level, HWL	9.0 m PWD
Low Water Level, LWL	3.0 m PWD
Design discharge, Q	20,000 m^3/s
Median diameter of sediment particle, d_{50}	0.12 mm
Multiplying factor for design scour depth, X	1.25 for straight reach of channel

Considering a typical field condition presented in Table 4.4 and from equation 4.2 and 4.3, D_s = 9.75 m. Therefore,

Width of apron, $W_{apron} = 1.5\,D_s$ = 14.63 m.

Width of apron in the flume, W_{apron} = 14.63/20 = 73 cm.

Thickness of protection over scoured slope, $T = 1.25\,D_n$.

Shape of the apron for blocks is followed according to Rao, 1946, discussed previously and shown in Figure 4.2.

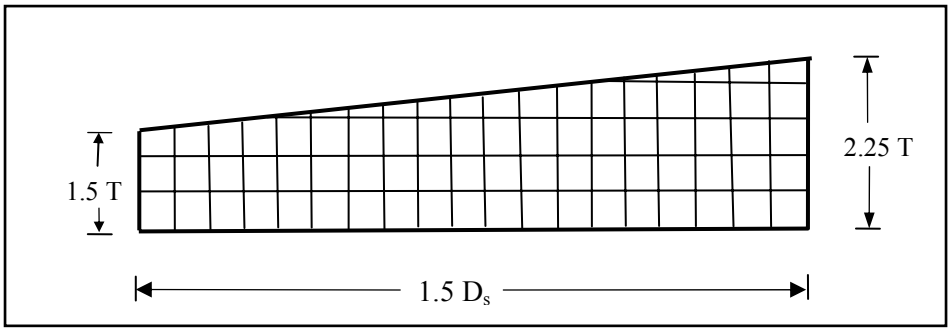

Figure 4.2: Schematic diagram for shape of apron for CC block

Quantity of block:

Inside thickness of apron = 1.5 T

Outside thickness of apron = 2.25 T

Quantity of block, $V_{block} = L\ (1.5T + 2.25T)/2$ m^3/m

Number of block per unit length = V_{block}/D_n^3

This amount of block is dumped so as to achieve the shape according to Figure 4.2, over the width of apron per unit length to investigate its threshold condition.

Quantity of geobag:

In mass dumping concept, a falling apron is developed from the water line by dumping a calculated quantity of geobags as a heap below LWL along the river section. The geobags are assumed to launch in a slope of 1V:2H, to cover the slope and future scour holes. According to Halcrow and Associates (2002), a protection thickness of 0.61 m on the scour surface for a scour depth up to 17 m is required. For a typical condition as mentioned above, the calculated scour depth is 9.75 m.

Therefore,

Volume of geobag, $V_{geobag} = (10^2+20^2)^{0.5}$ x 0.61 m^3/m

Number of geobag per unit length = V_{geobag}/D_n^3

This amount of geobag is dumped from the water surface over the width of apron per unit length in the flume to investigate its threshold condition.

4.3.6 Hydraulic parameters

Utility of an experimental investigation in field practice lies in the simulation of the field situations in the experimental setup. In order to simulate field conditions observed in different bank protection works already undertaken in Bangladesh, it is necessary to keep the velocity, water depth within a range. The flow depth is selected considering the High Water Level (HWL) and Low Water Level (LWL) in a typical field condition. This will facilitate the tasks of engineers and researchers to compare the test results with the field circumstances and to search for the option best suited for a given site condition for sustainable bank protection works. The hydraulic parameters are presented in Table 4.5.

Table 4.5: Hydraulic parameters regarding experiment of settling distance

Flume discharge, Q (m^3/h)	Experimental value		Corresponding field value	
	Depth of flow, h (m)	Velocity, V (m/s)	Depth of flow, h (m)	Velocity, V (m/s)
730	0.525	0.512	10.5	2.29
405	0.350	0.460	7	2.05
179	0.200	0.365	4	1.63

Total maximum discharge of the two pumps together is about 750 to 780 m^3/h. Discharge can be varied from 80 m^3/h to 760 m^3/h. Considering different hydraulic parameters like velocity, freeboard, water depth etc. a maximum discharge of 730 m^3/h is selected. Three discharges are taken into account to evaluate general behavior of settling phenomenon for different protection elements.

For incipient motion experiments the hydraulic parameter is set based on the typical field Low Water Level (LWL) condition and is given in Table 4.6.

Table 4.6: Initial hydraulic parameters regarding experiment of incipient condition

Type of element	Flume discharge, Q (m^3/h)	Experimental value		Corresponding field value	
		Depth of flow, h (m)	Velocity, V (m/s)	Depth of flow, h (m)	Velocity, V (m/s)
CC Block	186	0.20	0.35	4	1.56
CC Block	140	0.15	0.35	3	1.56
Geobag	150	0.20	0.29	4	1.33
Geobag	120	0.15	0.29	3	1.33

4.3.7 Test duration

Duration of a run for settling distance measurement is about 20 minutes for CC blocks and 40 minutes for geobags. After dumping the elements from water surface,

they are allowed to be stable on the bed and then the measurements are made. For incipient motion tests, the duration of a run is about 40 minutes to 70 minutes for geobags and 60 minutes to 90 minutes for CC blocks, depending on their sizes.

4.4 Test Scenarios

Experiments are conducted with ten types of CC block and six types of geobag with three different hydraulic conditions to investigate settling behavior as presented in Table 4.7. Also three types of block and five types of geobag are used for threshold condition experiments shown in Table 4.8.

Table 4.7: Test scenarios for settling distance

Run no.	Type of Protection Element	Depth of flow (m)	Velocity (m/s)	Discharge (m^3/h)
1-6	Geobag: A1 A2 B1 B2 C E	0.525	0.512	730
7-12		0.350	0.460	405
13-18		0.200	0.365	179
19-28	CC block: D1a D2a D3a D4a D5a D6a D7 D8 D9 D10	0.525	0.512	730
29-38		0.350	0.460	405
39-48		0.200	0.365	179

Table 4.8: Test scenarios for incipient motion

Run no.	Type of Protection Element	Depth of flow (m)	Velocity (m/s)	Discharge (m^3/h)
49-53	Geobag: A1 A2 B1 B2 E	0.20	0.29	150
54-58		0.15	0.29	120
59-61	CC block: D1a D2a D3a	0.20	0.35	186
62-64		0.15	0.35	140

4.5 Test Procedure

The course of actions followed during all the experiments are stated below chronologically. Firstly, the fall velocity of protection element is determined. Secondly, the settling behavior, specially the horizontal settling distance of dumped element is investigated. Finally, incipient condition for element dumped in flowing water is studied.

4.5.1 Procedure for fall velocity measurement

Following stepwise procedure have been followed for fall velocity measurement in laboratory:

i) At first five numbers of elements is randomly taken from each type to measure its physical properties. They are immersed in water for one day before taking wet weight. After oven drying dry weight is measured. Also the dimension is measured with a slide calipers.

ii) The settling column has been fabricated in the laboratory by plexiglas, glue, formalin and iron flat bars. The flat bars are used horizontally to resist the hoop tension resulted due to water pressure. Clear, fresh water is

poured in the column and waited for about five hours to attain uniform temperature and zero velocity. Trial test is done before final test to observe the performance of the column with water.

iii) Elements are immersed in water for one day before conducting the experiment.

iv) The particles are released with the help of a tweezer and observed them crossing the initial line of measurement. The time between the initial line and final line has been recorded with a stop watch.

v) Elements were released in the water with zero departure velocity and without any rotation. The initial orientations of geobags and prism shaped blocks are with their maximum surface areas and cubes with one of the surfaces normal to the motion of the particle.

vi) They were released 5 cm below the maximum water level with the help of tweezer. Their required time of fall over 90 cm vertical distances was timed by a stopwatch, which had 0.01 second accuracy.

vii) The fall velocities of particles were low enough that there was no need to use photographic or any other sophisticated method of measurement; therefore the particles could be timed using a stopwatch over the chosen distance of 90 cm. The test conducted for each particle was repeated three times under the same conditions to reduce the probable error of the average observed time interval. Therefore the ultimate fall velocity for each type of particle is obtained by averaging fifteen measurements.

viii) A thermometer was placed at the upper, middle and lower section of the column to measure the temperature of the water. The temperature gradient between the top and the bottom of the column was found negligible during all experiments. All particles were dropped in water at the temperatures ranging between 28 ^{0}C and 28.5 ^{0}C and the effect of viscosity on fall velocity is negligible.

ix) The behavior of element while falling is monitored and documented over the period of experiment by taking snaps and videos.

4.5.2 Procedure for settling distance measurement

i) For each run forty geobags and thirty blocks are dumped at a time from a platform to the flowing water. This number is determined from the observation of trial runs.

ii) Six types of bag and ten types of block are used. Three different combinations of hydraulic parameters are investigated. The elements are dumped from 4 cm above the water surface in all tests.

iii) For a particular set up, the discharge is controlled by the valve and the depth of flow is fixed by adjusting the tail gate. Depth averaged flow velocity is measured using a small current meter.

iv) The duration of a run is determined by monitoring the movement of bags and blocks on the bed. As the movement is over, run continues for more ten minutes and the flume is drained out.

v) Then the state of protection element is documented.

vi) The horizontal settling distance is measured from the initial dumping line to the center of each element.

4.5.3 Procedure followed for incipient motion experiment

i) The shape of apron and number of element required per unit length is determined as mentioned previously. This amount is dumped during the run.

ii) Five types of bag and three types of block are used. Two different combinations of hydraulic parameters are investigated. The elements are dumped from 4 cm above the water surface in all run.

iii) Red, yellow and blue colored blocks are used in first, second and third layers to observe their post dumping condition.

iv) For a particular set up, the discharge is set by the valve and the depth of flow is fixed by adjusting the tail gate. Depth averaged flow velocity is measured using a small current meter.

v) Then discharge is increased very slowly at a rate of 5 m^3/h and observed for five to eight minutes. After that if there is no movement in apron

material flow is increased again. This process continues till the incipient motion occurs.

vi) Incipient motion is considered as the displacement of an element from its initial position. When this condition is satisfied, the flow depth and depth averaged velocity of approach flow is measured.

vii) The significant feature of the test is that elements are dumped in the flowing water rather placed in a dry bed prior to flow of water. This procedure depicts the real field condition.

4.6 Observations

During the experiments, the following observations were made:

4.6.1 Observations during measurement of fall velocity

i) The cubic blocks, in general, did not follow the centerline of the column while they were falling, and in addition to tipping and sliding, they rotated all the time following a helical path.

ii) The box shaped blocks followed almost the centerline of the settling column having the largest surface area perpendicular to the motion of the particle. Oscillation about the shortest axis and little sliding was observed.

iii) As geobags have voids in it their travel trail is not fixed.

iv) The path followed by geobag was nonvertical and approximately helical with significant sliding.

v) Initial orientation of falling of a particle has no effect on fall velocity.

4.6.2 Observations during experiment of horizontal settling distance

i) Small cube shaped block spin while falling and rolled down 5 to 10 cm after touching the bed of the flume. Sometimes cluster consisting of about three blocks are formed.

ii) Few blocks at the front side stopped the rolling of others coming behind them.

iii) 2 to 3 cubical blocks moved few cm even after 16 minutes of dumping.

iv) Prism shaped block do not roll while falling and after touching the bed and settled on their large surface.

v) For the first set up about six bags and small blocks moved two to three meter from dumping line.

vi) During the second and third set up, there was no rolling, movement or cluster formation for both bags and blocks.

vii) Square shaped bags traveled more distance than rectangular bags.

viii) While falling a bag, the air bubbles are formed. As the bag sinks, bubble moves past them and reaches the water surface at a location down stream of the bag. This is due to the velocity of the flowing water. Therefore watching the air bubble at the water surface the location of a bag cannot be identified.

4.6.3 Observations during experiment of threshold condition

i) The water surface down stream of the test section was slightly lower.

ii) The velocity over the apron was higher than that of down stream and approach velocity was less than down stream velocity.

iii) As the velocity increases the toe elements starts vibrating.

iv) For geobags, group movement or sliding was observed while blocks moved individually.

Photographs 4.8 to 4.13 show the various experimentations in the laboratory.

Photograph 4.8: Measurement of settling distance for CC blocks

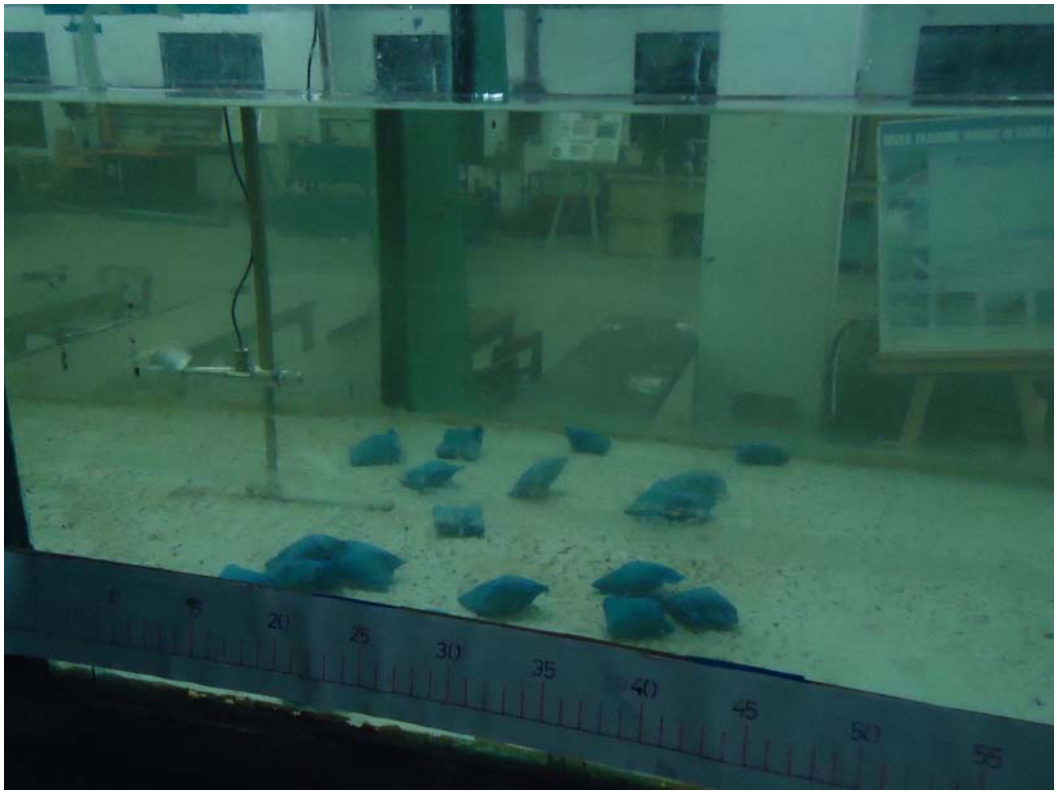

Photograph 4.9: Measurement of settling distance for geobags

Photograph 4.10(a): Fall velocity measurement

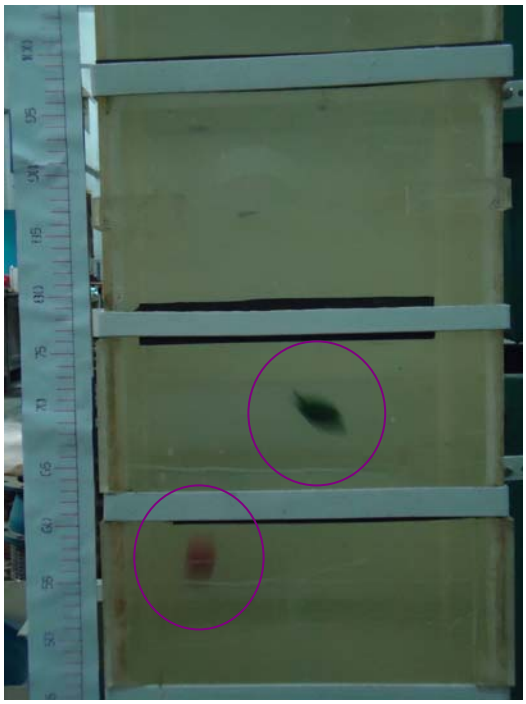

Photograph 4.10(b): CC block is falling faster than geobag

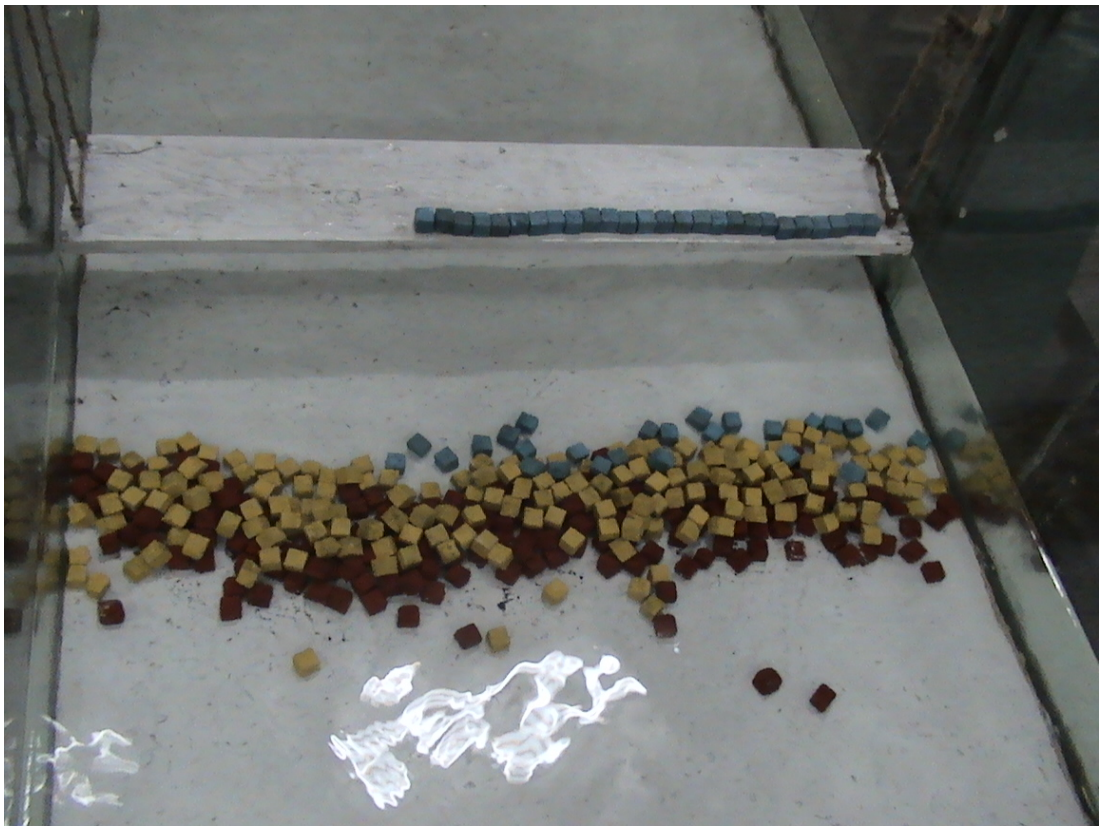

Photograph 4.11: Dumping of CC block to construct apron in the flume

Photograph 4.12: Investigation of threshold condition of block

Photograph 4.13: Investigation of threshold condition of geobag

CHAPTER FIVE

RESULTS AND DISCUSSIONS

5.1 Introduction

With the intention of investigating settling behavior of bank protection elements (e.g. CC blocks and geobags), foremost requirement is to assess the fall velocity of these particles. Therefore, fall velocity of CC blocks, geobag and a combined outcome of the experiments are described here. These results are then utilized to study the horizontal settling distance of the elements when they are dumped in the flowing water. The later parts of this chapter explain the incipient behavior of the blocks and geobags when they provide a protection layer over the channel bed.

5.2 Results of Fall Velocity of Block

The value of different parameters of fall velocity test for CC block is presented in Table 5.1. Parameters mentioned here are discussed previously in chapter 2.

Table 5.1: Parameters of fall velocity test for different CC block

Type of CC Block	Charact-eristics diameter, d (m)	Dimensionless particle diameter, d^*	Relative density, Δ	Kinem-atic viscosity, v, (m^2/s) x 10^{-7}	Archime-des buoyancy index, A x 10^{+8}	Fall veloc-ity, w (m/s)	Particle Reynolds no., R^*
D1a	0.023	589.86	1.074	8.10	2.1	0.732	21124
D2a	0.020	522.78	1.074	8.10	1.4	0.647	16547
D3a	0.016	403.49	1.074	8.10	6.6	0.595	11745
D4a	0.024	626.18	1.074	8.10	2.5	0.631	19330
D5a	0.023	591.12	1.074	8.10	2.1	0.738	21342
D6a	0.015	379.33	1.074	8.10	5.5	0.574	10652
D7	0.025	631.68	1.074	8.10	2.5	0.636	19655
D8	0.030	756.93	1.074	8.10	4.3	0.66	24440
D9	0.032	817.16	1.074	8.10	5.5	0.729	29144
D10	0.035	897.65	1.074	8.10	7.2	0.85	37328

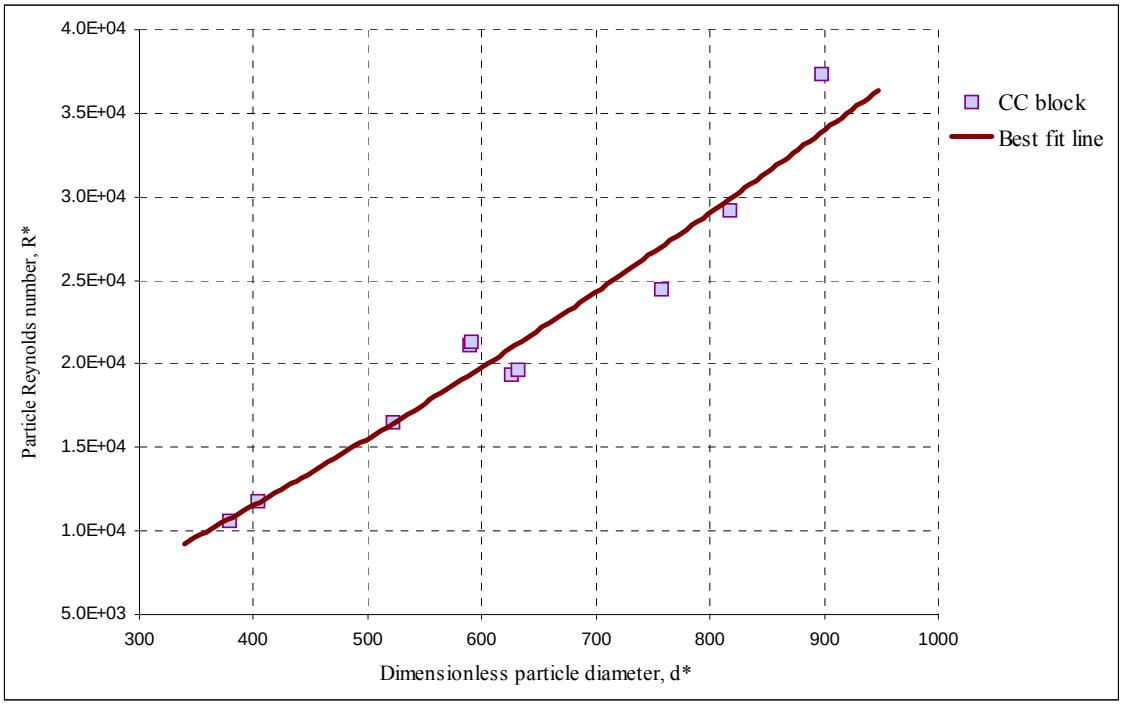

Figure 5.1: Particle Reynolds number versus dimensionless particle diameter for CC block

On the basis of expression of fall velocity shown in equation (3.11), a power regression analysis of the experimental data has been performed. The plot is shown in Figure 5.1. The coefficient of determination (R^2) is found to be 0.96 indicating a good correlation. It is seen that as the dimensionless particle diameter increases the particle Reynolds number also increases.

The final expression of fall velocity for block becomes

$$R^* = 3.965\, d_*^{1.33} \tag{5.1}$$

Equation (5.1) is valid within the experimental ranges of $10^4 < R^* < 4\text{x}10^4$ for particle Reynolds number and $380 < d^* < 900$ for dimensionless particle diameter.

5.2.1 Comparison of proposed empirical equations for block with others

The basic parameter used for the determination of accuracy of a formula is the average value of relative error where error is defined as

$$error = \frac{|predicted - observed|}{observed} \times 100 \tag{5.2}$$

A comparison here can be made by predicted values using the equation of different investigators and the measured values from the experiment.

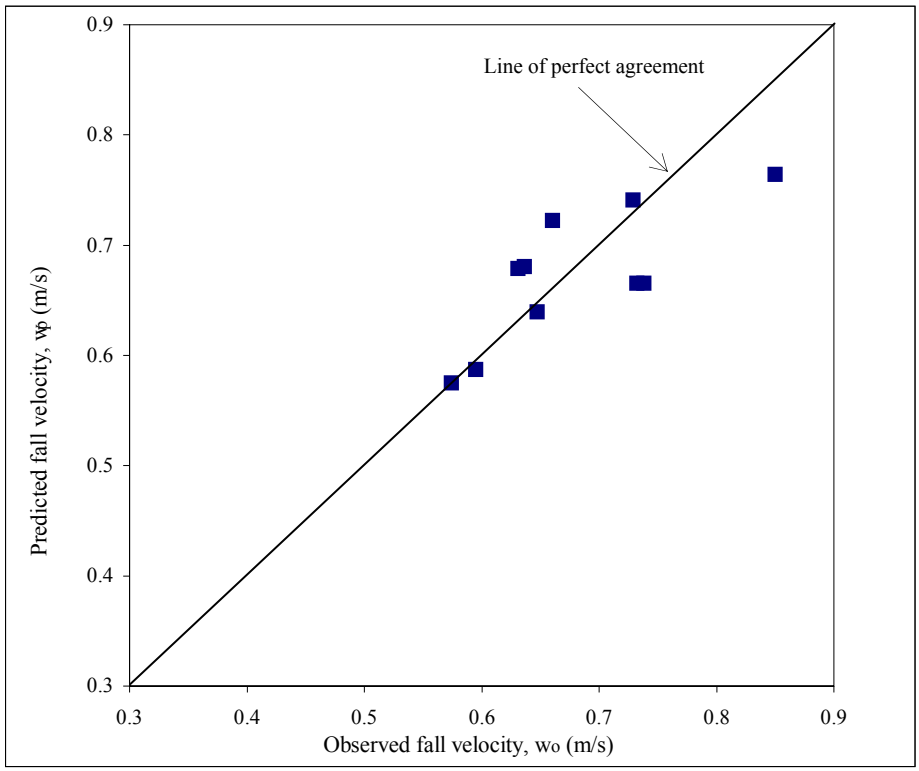

Figure 5.2: Comparison of observed and predicted fall velocity using equation (5.1) for CC block

Figure 5.2 represents the predicted fall velocity by proposed empirical equation (equation 5.1) versus measured in this study. Three points are below the line of perfect agreement indicating predicted value is less than measured one. Three points are above the perfect line indicating predicted value is greater than measured one. Four points lie on the line of perfect agreement. The average relative error is 3.91%.

Figure 5.3(a) represents the predicted fall velocity by proposed empirical equation (equation 5.1), Van Rijn (1989) and Cheng (1997) versus measured in this study. According to Van Rijn (1989) all data points are below the perfect line indicating predicted value is less than measured one. The average relative error is 12.97%. According to Cheng (1997) all data points except one are below the perfect line indicating predicted value is less than measured one. The average relative error is 10.95%.

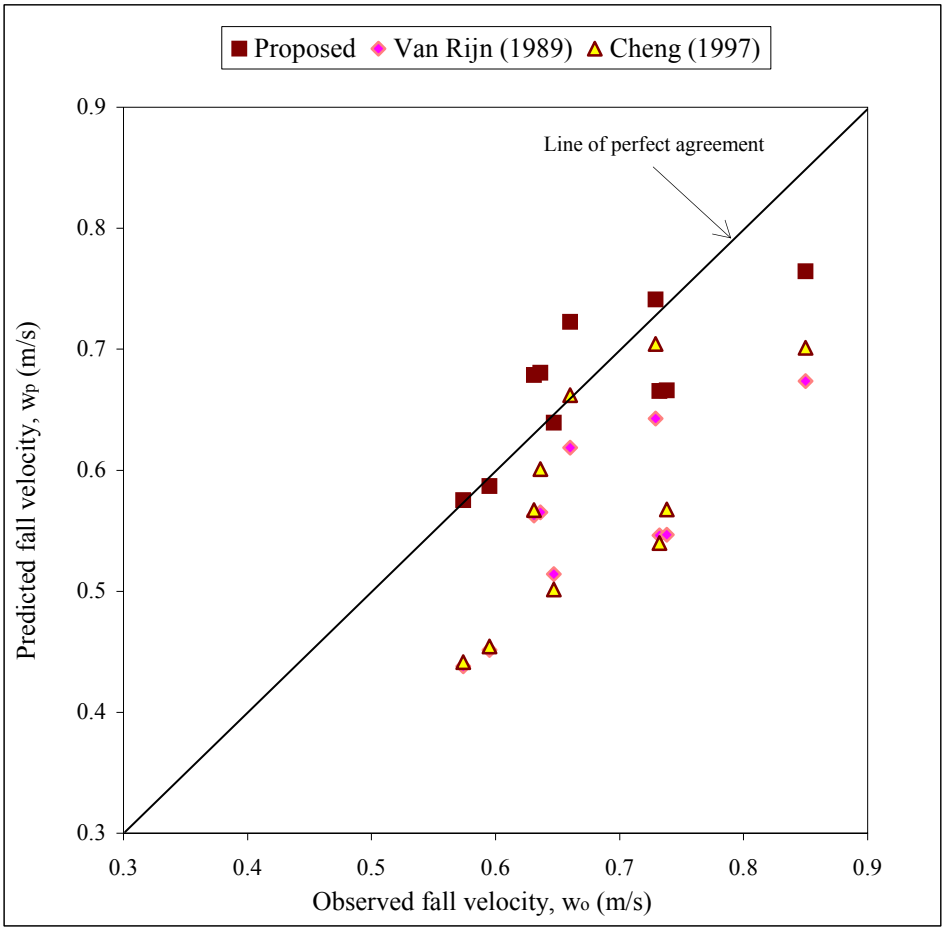

Figure 5.3(a): Comparison of observed and predicted fall velocity for CC block

Figure 5.3(b) represents the predicted fall velocity by proposed empirical equation (equation 5.1), Hallermeier (1981), Göğüş et al. (2001), Chang and Liou (2001) versus measured in this study. According to Hallermeier (1981) all data points are below the perfect line indicating predicted value is less than measured one. The average relative error is 21.78%. According to Göğüş et al. (2001) four points are below the perfect line indicating predicted value is less than measured one. Four points are above the perfect line indicating predicted value is greater than measured one. Two points lie on the line of perfect agreement. The average relative error is 23.25%.

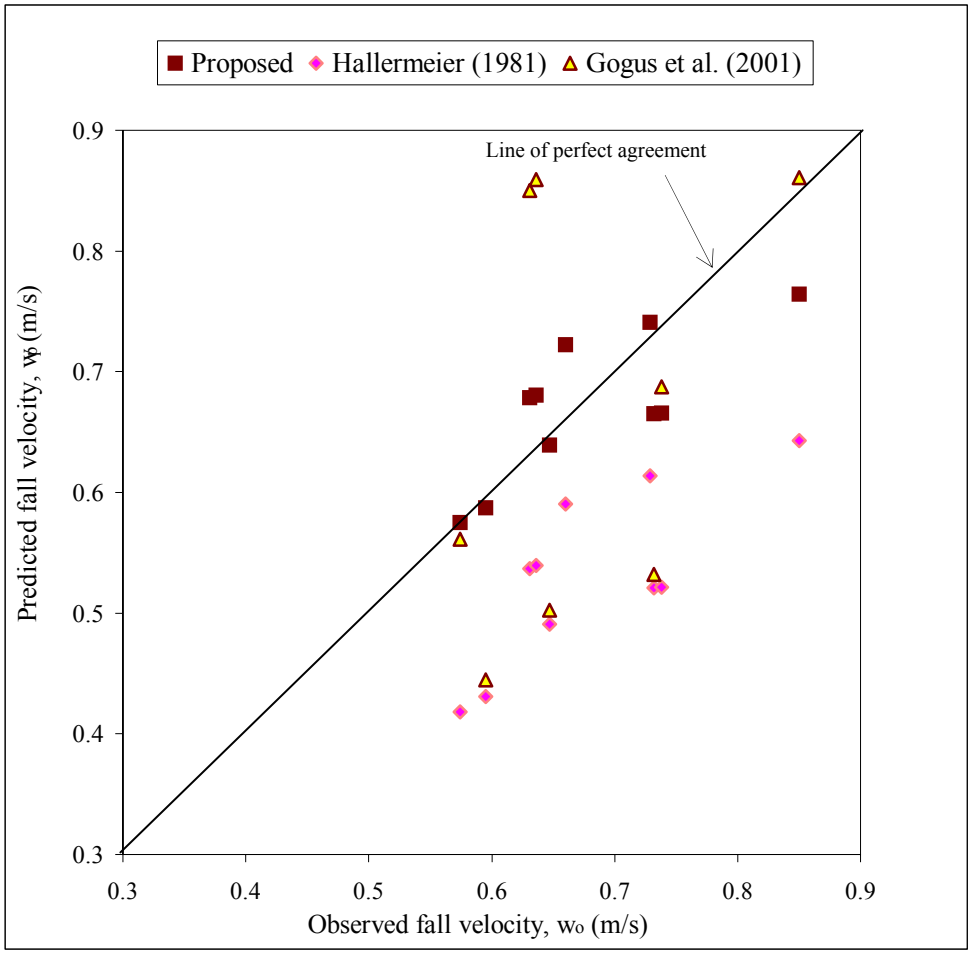

Figure 5.3(b): Comparison of observed and predicted fall velocity for CC block

5.3 Results of Fall Velocity of Geobag

The value of different parameters of fall velocity test for geobag is presented in Table 5.2. Parameters mentioned here are discussed previously in chapter 2. On the basis of expression of fall velocity shown in equation (3.11), a power regression analysis of the experimental data has been performed. The plot is shown in Figure 5.4. The coefficient of determination (R^2) is found to be 0.95 indicating a good correlation. It is seen that as the dimensionless particle diameter increases the particle Reynolds number also increases which is consistent with literature. The two data point beside the best fit line is for square shaped geobag.

Table 5.2: Parameters of fall velocity tests for different geobag

Type of Geobag	Charact-eristics diameter, d (m)	Dimensio-nless particle diameter, d^*	Relative density, Δ	Kinem-atic viscosity, v, (m^2/s) X 10^{-7}	Archime-des buoyancy index, A X 10^{+8}	Fall veloc-ity, w (m/s)	Particle Reynolds no., R^*
A1	0.02537	510.92	0.5349	8.01	1.3	0.373	11807
A2	0.02591	521.83	0.5349	8.01	1.4	0.357	11542
B1	0.02365	476.29	0.5349	8.01	1.1	0.367	10829
B2	0.02452	493.80	0.5349	8.01	1.2	0.397	12146
C	0.02078	418.48	0.5349	8.01	7.3	0.357	9256
E	0.03166	637.71	0.5349	8.01	2.6	0.396	15646

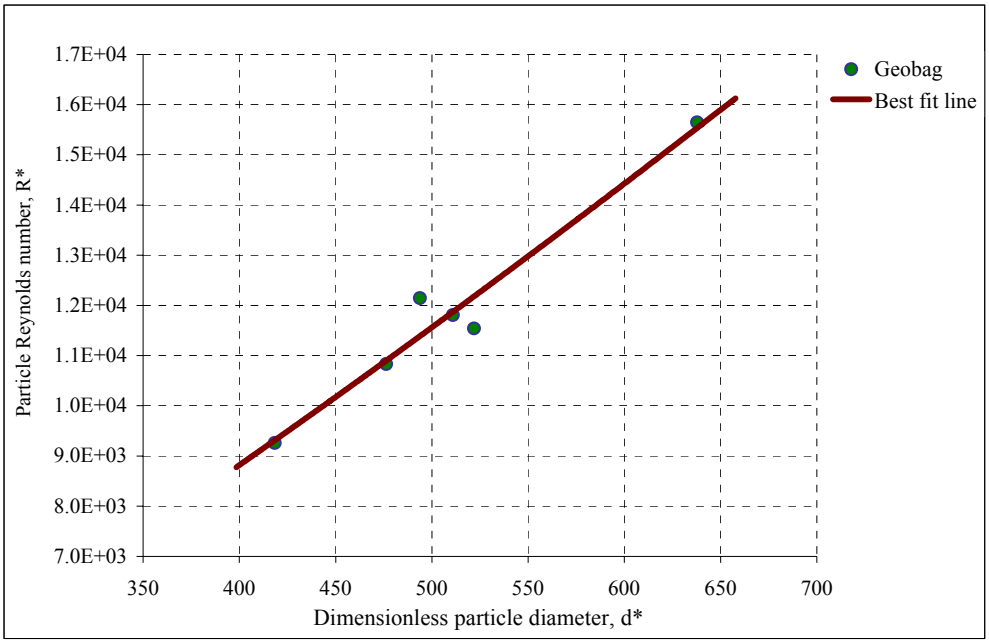

Figure 5.4: Plot of particle Reynolds number against dimensionless particle diameter for geobag

The final expression of fall velocity for geobag becomes

$$R^* = 6.124\, d_*^{1.21} \tag{5.3}$$

Equation (5.3) is valid within the experimental ranges of $9x10^3<R^*<16x10^3$ and $410<d^*<640$.

5.3.1 Performance of proposed empirical relationship for geobag

Figure 5.5 represents the predicted fall velocity by proposed empirical equation (equation 5.3) versus measured in this study. Four points lie on the line of perfect agreement. One point lie down in positive and one point on negative side. The average relative error is 2.38%; where error is obtained by equation (5.2).

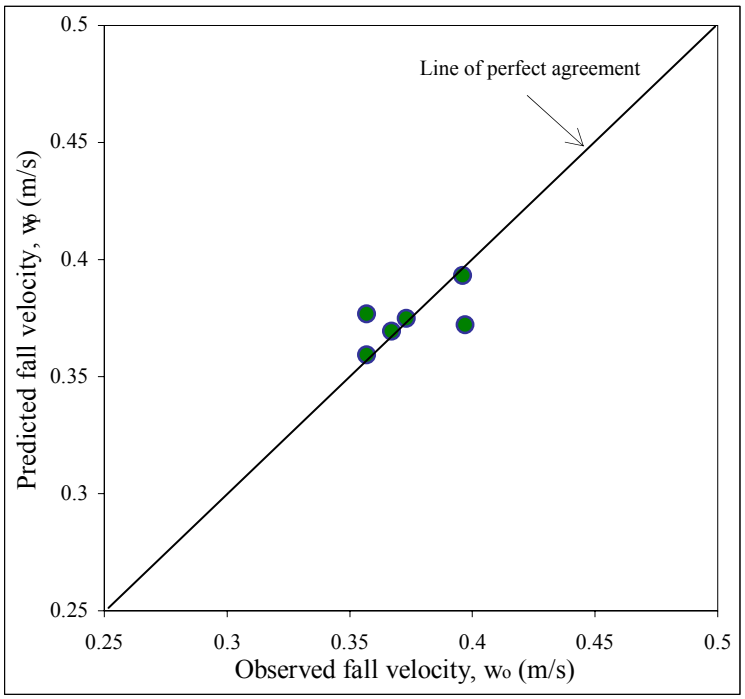

Figure 5.5: Comparison of observed and predicted fall velocity using equation (5.3) for geobag

Figure 5.6(a) represents the predicted fall velocity according to Van Rijn (1989) and Cheng (1997) versus measured in this study. According to Van Rijn (1989) two points lie on the line of perfect agreement. Four points are above the perfect line indicating predicted value is greater than measured value. The average relative error is 7.06%. According to Cheng (1997) no data point lie on the line of perfect agreement. Four points are above the perfect line indicating predicted value is greater than measured value. Two points are below the perfect line indicating predicted value is less than measured value. The average relative error is 9.87%.

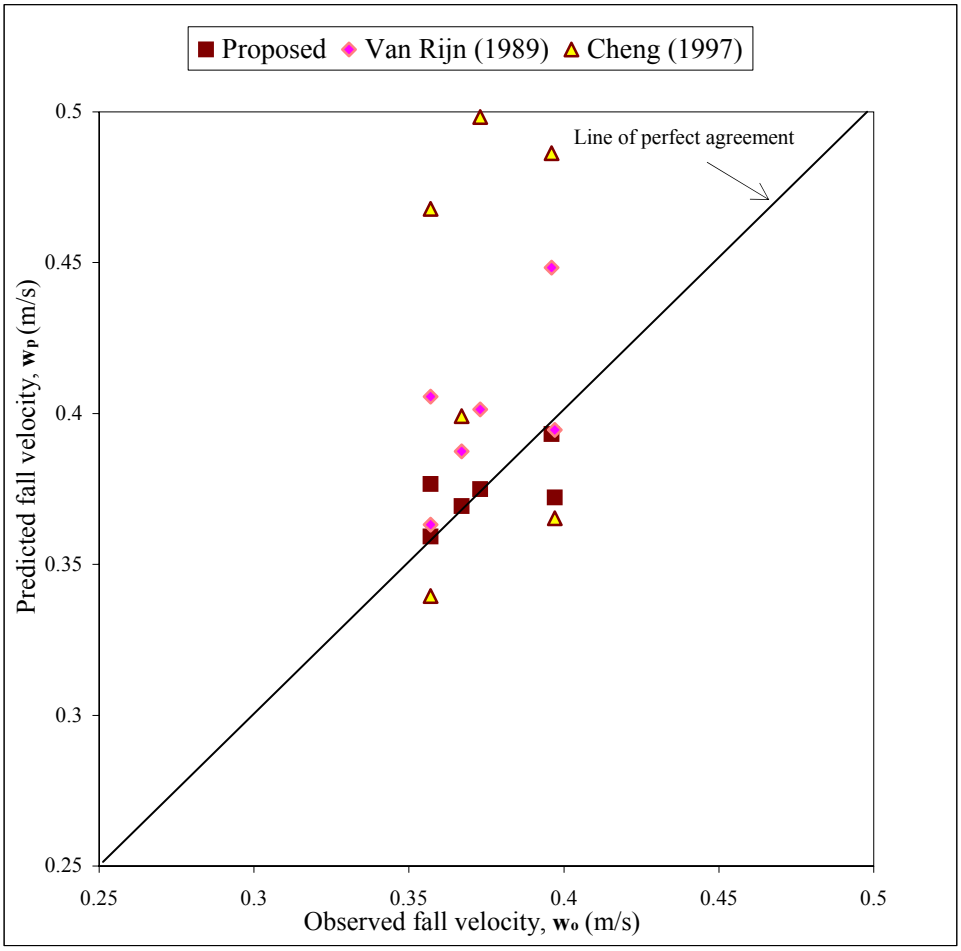

Figure 5.6(a): Comparison of observed and predicted fall velocity for geobag

Figure 5.6(b) represents the predicted fall velocity according to Hallermeier (1981) and Chang and Liou (2001) versus measured in this study. According to Hallermeier (1981), no data point except one, lie on the line of perfect agreement. Three points are above the perfect line indicating predicted value is greater than measured value. Two points are below the perfect line indicating predicted value is less than measured value. The average relative error is 4.67%. According to Chang and Liou (2001) no data point lie on the line of perfect agreement. All data points lie below the line of perfect agreement indicating predicted value is less than measured value. The average relative error is 15.67%.

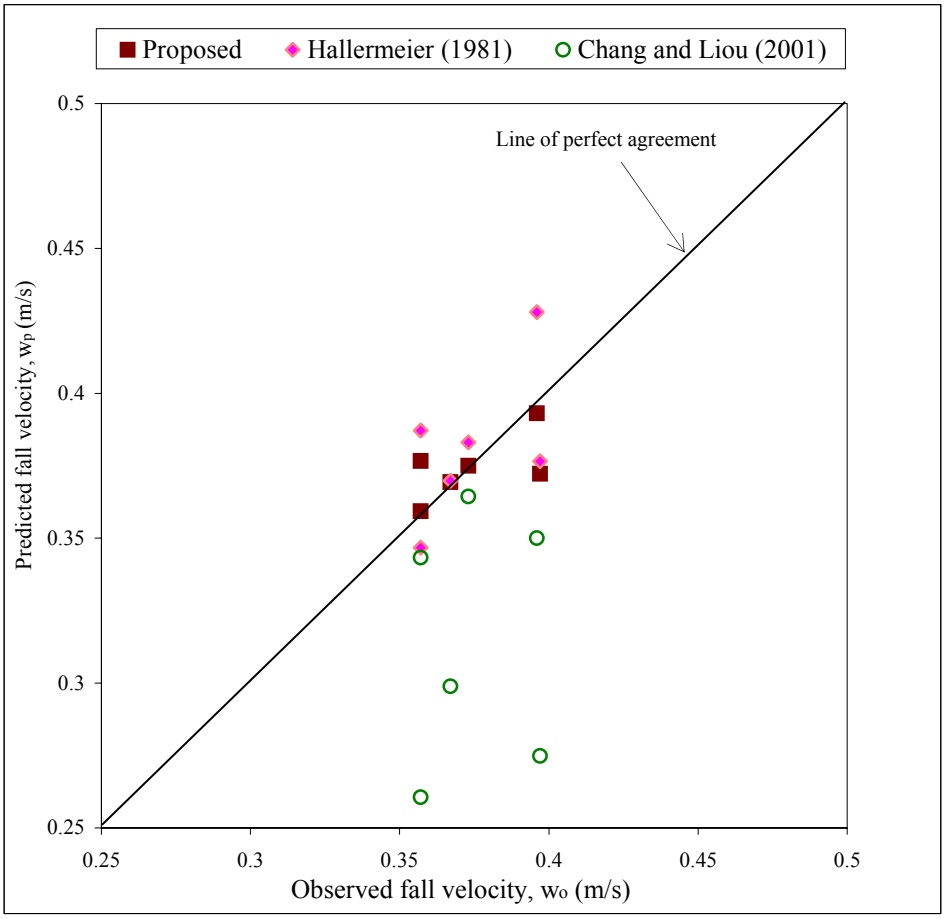

Figure 5.6(b): Comparison of observed and predicted fall velocity for geobag

5.4 Proposed Empirical Relationship of Settling Velocity

Figure 5.7(a) shows separate plot of particle Reynolds number against dimensionless particle diameter for CC block and geobag. Due to higher weight, data points of CC block is above the data points for geobag. The slope of the best fit line for CC block is steeper than that of geobag indicating a faster rate of increasing fall velocity and for this the two best fit lines show diverging trend at higher values and converging trend at lower values. On the basis of expression of fall velocity shown in equation (3.11), a power regression analysis of the experimental data has been performed. The plot is shown in Figure 5.7(b). The coefficient of determination (R^2) is found to be 0.86. It is seen that as the dimensionless particle diameter increases the particle Reynolds number also increases at an increasing rate.

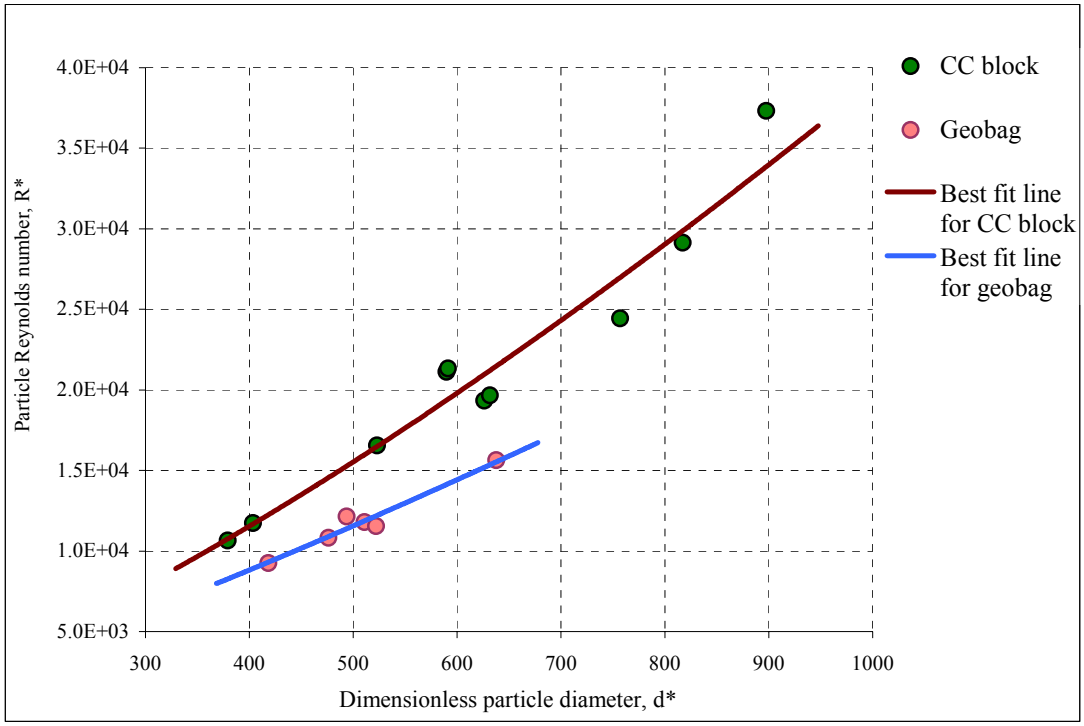

Figure 5.7(a): Separate plot of particle Reynolds number against dimensionless particle diameter

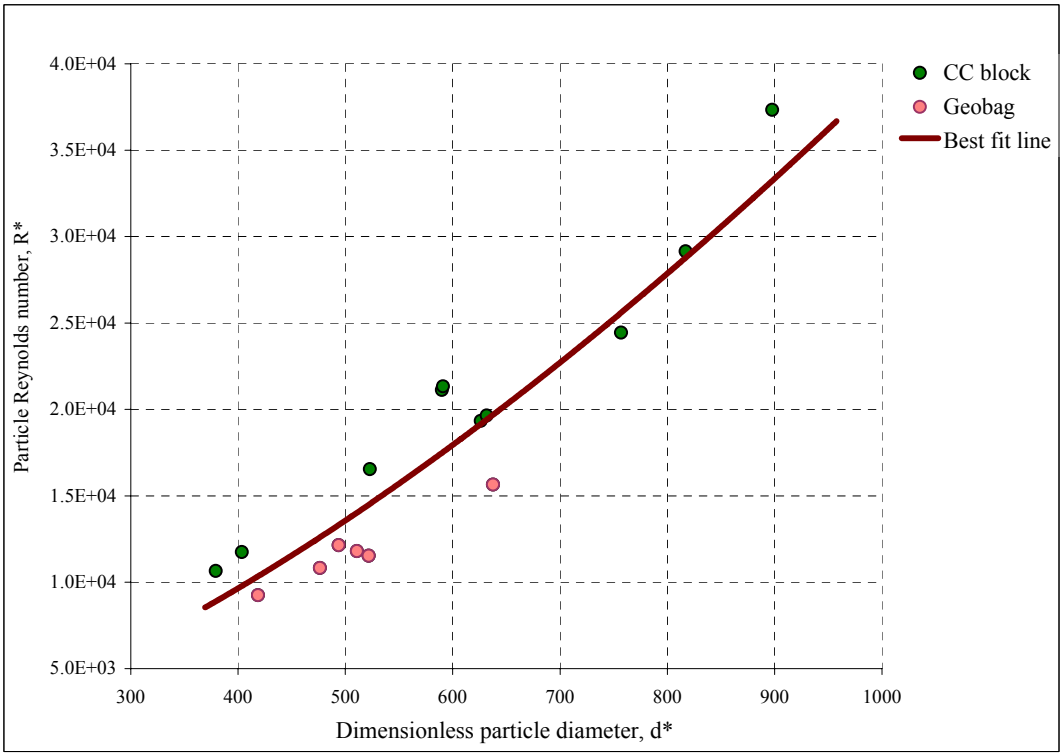

Figure 5.7(b): Combined plot of particle Reynolds number against dimensionless particle diameter for CC block and geobag

The final expression of fall velocity for both blocks and geobags becomes

$$R^* = 1.01 d_*^{1.53} \tag{5.4}$$

Equation (5.4) is valid within the experimental ranges of $9\text{x}10^3 < R^* < 4\text{x}10^4$ for particle Reynolds number and $310 < d^* < 900$ for dimensionless particle diameter. Figure 5.8 shows that with the increase in particle Reynolds number the Archimedes buoyancy index increases at a decreasing rate.

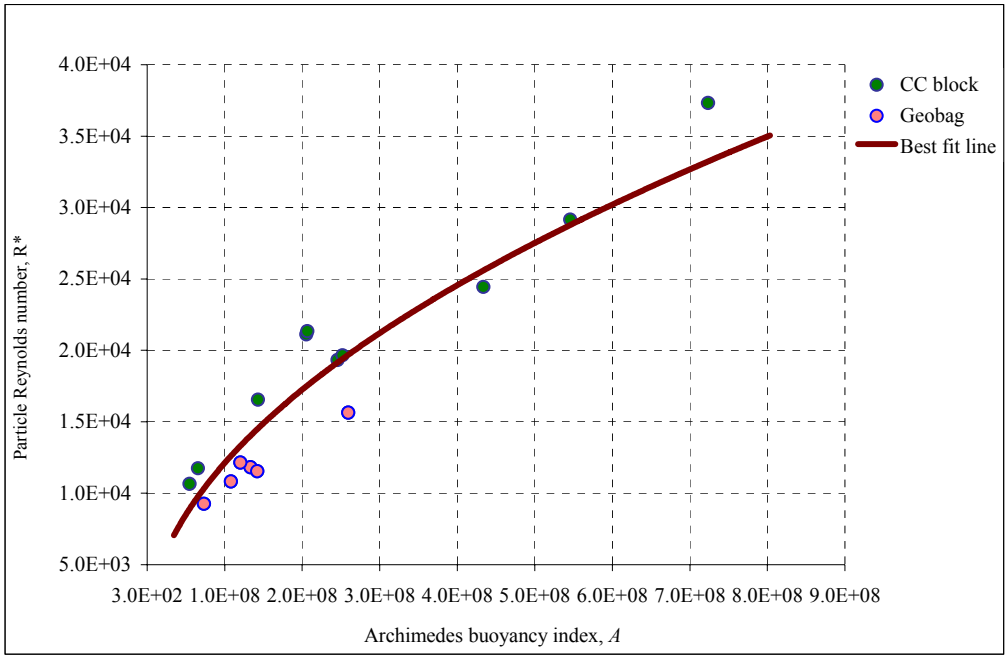

Figure 5.8: Plot of particle Reynolds number against Archimedes buoyancy index for both CC block and geobag

5.4.1 Comparison of proposed empirical relationship with other equations

Figure 5.9 represents the predicted fall velocity by proposed empirical equation (equation 5.4) versus measured in this study. It is seen that using equation (5.4) the predicted fall velocity of geobag is greater than observed and for block it is lower. The average relative error for this comparison is obtained as 12.97% which is the lowest of all prediction formulas mentioned previously.

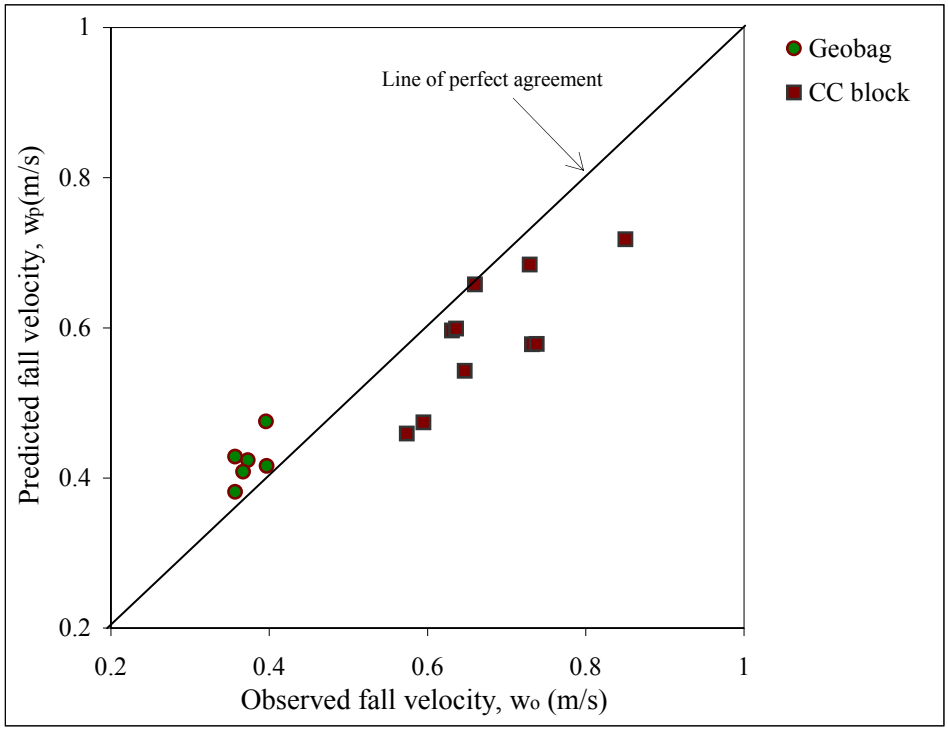

Figure 5.9: Comparison of observed and predicted fall velocity using equation (5.4) for both CC block and geobag

Figure 5.10(a) represents the predicted fall velocity by proposed empirical equation (equation 5.1), Van Rijn (1989), Cheng (1997), and Ruby (1933) versus measured in this study. Van Rijn (1989) shows the same trend as equation (5.4) but the error is third lowest. The average relative error for this comparison is obtained as 13.71%. Cheng (1997) shows the same trend as equation (5.4) but the error is second lowest. The average relative error for this comparison is obtained as 13.43%. According to Ruby (1933) the predicted fall velocity of both geobag and block is lower than the observed values. The average relative error for this comparison is obtained as 32.28%.

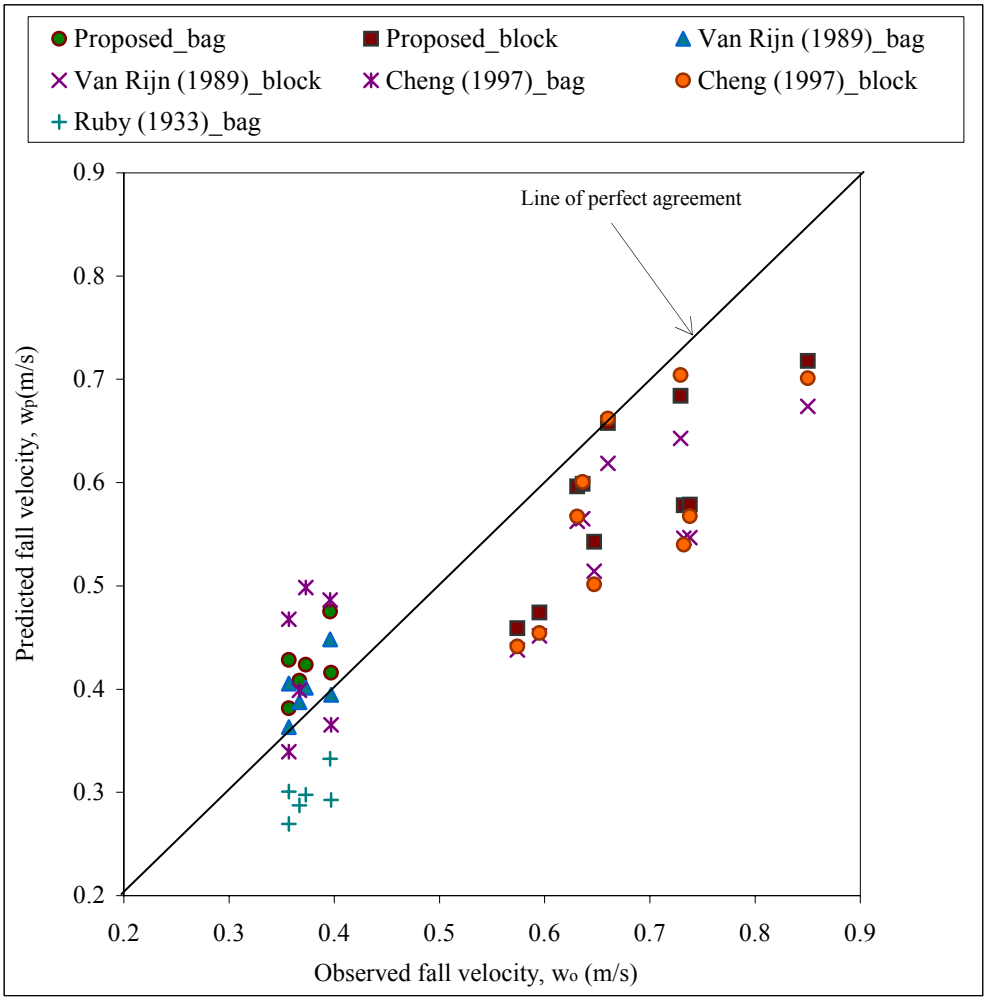

Figure 5.10(a): Comparison of observed and predicted fall velocity for both CC block and geobags

Figure 5.10(b) represents the predicted fall velocity according to Hallermeier (1981), Göğüş et al. (2001), Chang and Liou (2001), versus measured in this study. It is seen that according to Hallermeier (1981) the predicted fall velocity of block is lower than observed values. The average relative error for this comparison is obtained as 15.36%. According to Göğüş et al. (2001) the predicted fall velocity of geobag is extremely higher than the observed values. All block data points are scattered below and above the line of perfect agreement. The average relative error for this comparison is obtained as 69.05%. According to Chang and Liou (2001) the predicted fall velocity of both geobag and block is lower than the observed values. The average relative error for this comparison is obtained as 29.97%. It is seen that using equation (5.4) the predicted fall velocity of geobag is greater than observed and for block it is lower.

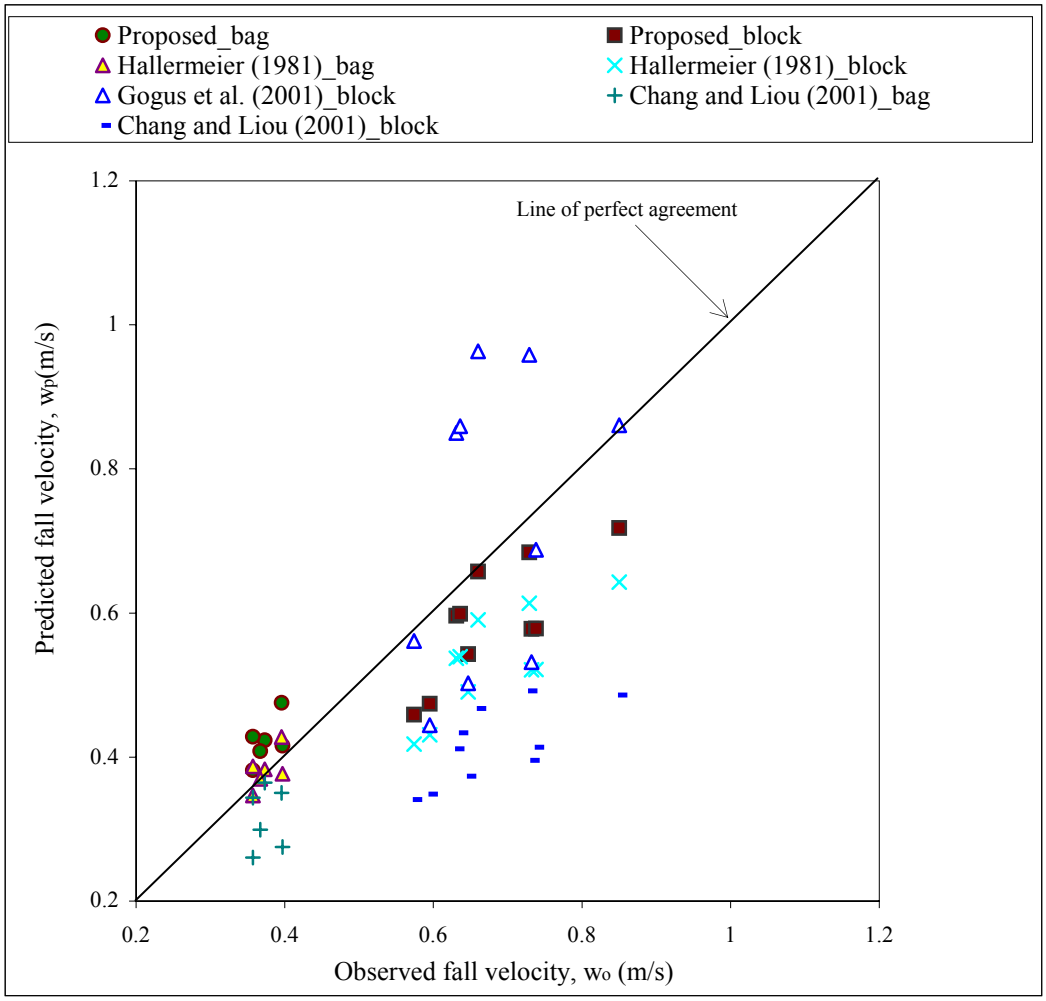

Figure 5.10(b): Comparison of observed and predicted fall velocity for both CC block and geobag

Summary of Comparison

Comparison among fall velocity formula mentioned previously is done on the basis of measured fall velocities of sixteen different sized particles. The summary of the comparison is presented in Table 5.3. From the table it is seen that the proposed empirical equations have the lowest average value of relative error for block, geobag and combination of them. Equation (5.1) has an average value of relative error 3.91% where Cheng (1997) is the next with 10.95% error. Equation (5.3) has an error of 2.38% where Hallermeier (1981) equation performs better than the rest with 4.67% error. When a combined formula is considered equation (5.4) has the minimum error of 12.97% where Cheng (1997) and Van Rijn (1989) are next with 13.43% and 13.71% error, respectively. However, it is needless to mention that equation (5.1) and

(5.3) is always a better predictor for block and geobag, respectively, than equation (5.7).

The errors in predicting fall velocity by the previously mentioned formulas is mainly due to the fact that the size of the elements used in this experiment is quite larger than those used in other studies. Most of the equations are proposed for natural sand particles (e. g. Ruby, 1933; Hallermeier, 1981; Cheng 1997; Chang and Liou, 2001). Cheng (1997) used the largest size of particle of 4.5 mm and Van Rijn (1989) formula is for particles larger than 1 mm. Gogus et al. (2001) conducted experiments using larger particles but the proposed characteristic dimensions of a particle is not capable to predict the fall velocity of the particles used in this experiment.

Table 5.3: Performance of various fall velocity prediction formulas

Fall Velocity Equation	**Error (%)**		
	Block	**Geobag**	**Combined**
Present study	3.91	2.38	12.97
Cheng (1997)	10.95	9.87	13.43
Van Rijn (1989)	12.97	7.06	13.71
Hallermeier (1981)	21.78	4.67	15.36
Chang and Liou (2001)	38.55	15.67	29.97
Ruby (1933)	30.27	14.01	32.28
Göğüş et al. (2001)	23.25	145	69.05

5.5 Results of Settling Distance

Three set up were investigated for both block and geobag during the experiment to obtain a correlation between dimensionless settling distance which is the ratio of settling distance and depth of flow with dimensionless flow parameter. On the basis of expression of settling distance shown in equation (3.17), a power regression analysis of the experimental data has been performed yielding the value of k = 1.49 and m = 1.06 with a coefficient of determination (R^2) of 0.69.

Finally equation (3.17) attains the form as:

$$\frac{S}{h} = 1.49\left(\frac{V}{w}\right)^{1.06} \tag{5.5}$$

In this equation fall velocity, w can be substituted using equation (5.1) or equation (5.3) to obtain settling distance of CC blocks or geobags, respectively yielding:

$$\frac{S}{h} = 1.49\left\{\frac{V}{\left(3.965\frac{\nu}{d}d_*^{1.33}\right)}\right\}^{1.06} \tag{5.6a}$$

and

$$\frac{S}{h} = 1.49\left\{\frac{V}{\left(6.124\frac{\nu}{d}d_*^{1.21}\right)}\right\}^{1.06} \tag{5.6b}$$

The depth averaged velocity of a protection element expressed previously in equation (3.16) becomes:

$$U = 1.49\,\frac{V^{1.06}}{w^{0.06}} \tag{5.7}$$

Equation (5.5) gives the relationship for predicting horizontal settling distance and equation (5.7) gives the depth averaged horizontal velocity of a protection element. It is seen that settling distance is proportional to flow velocity and depth and inversely proportional to fall velocity. Also the horizontal velocity of block or geobag is proportional to depth average flow velocity and inversely proportional to its fall velocity.

Figure 5.11 is a dimensionless plot of forty eight data points obtained from the same number of test run and presents identification of the type of element and set up. Set up 1 for geobag has the highest ratio due to their low density while set up 3 for block has the lowest ratio due to their high density as expected.

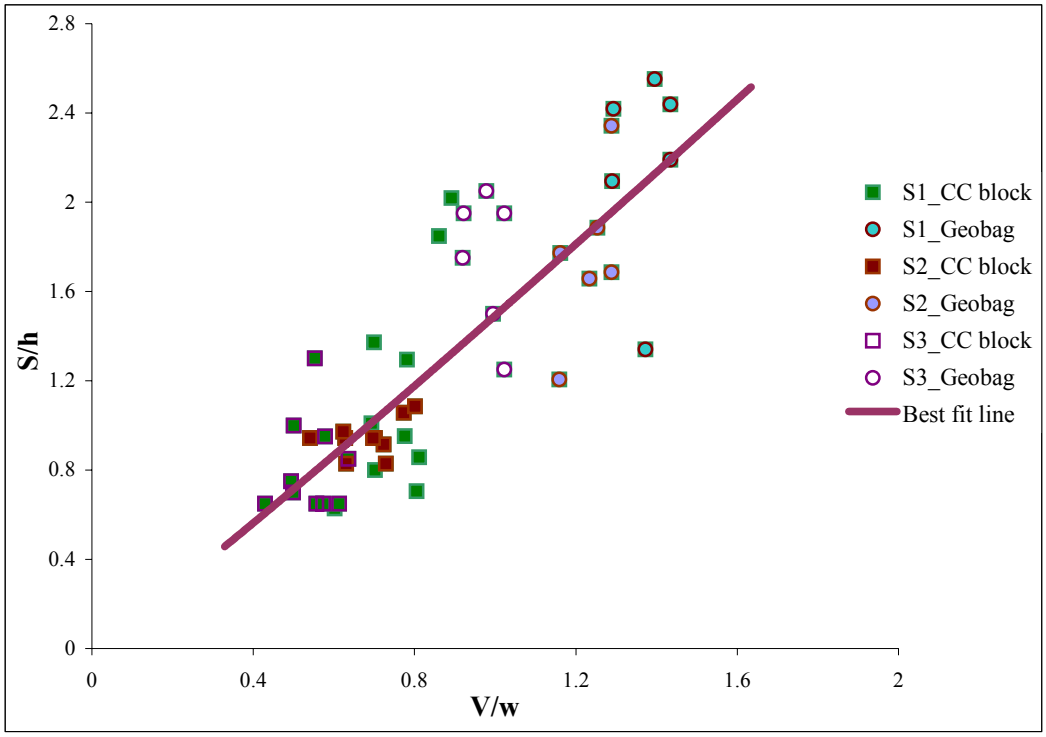

Figure 5.11: Plot of *S/h* against *V/w*

5.5.1 Performance of equations

In the literature dealing with settling distance only one empirical equation by Zhu et al. (2004) is found so far and the out come of the present study as equation (5.5) is compared with it. Figure 5.12 represents the predicted settling distance by proposed empirical equation (equation 5.5) versus measured in this study for block. Region above the line of perfect agreement indicates predicted value is less than measured one. Region below the line of perfect agreement indicates predicted value is greater than measured one. It is seen that using equation (5.5) the predicted settling distance is balanced in both sides of the line of perfect agreement. The average relative error for this comparison is obtained as 20.03%.

Figure 5.13 represents the predicted settling distance by Zhu et al. (2004) versus measured in this study for block. It is seen that almost all the predicted settling distance is above the line of perfect agreement indicating the predicted values are greater than observed values. The average relative error for this comparison is obtained as 46.68% which is two times greater than equation (5.5).

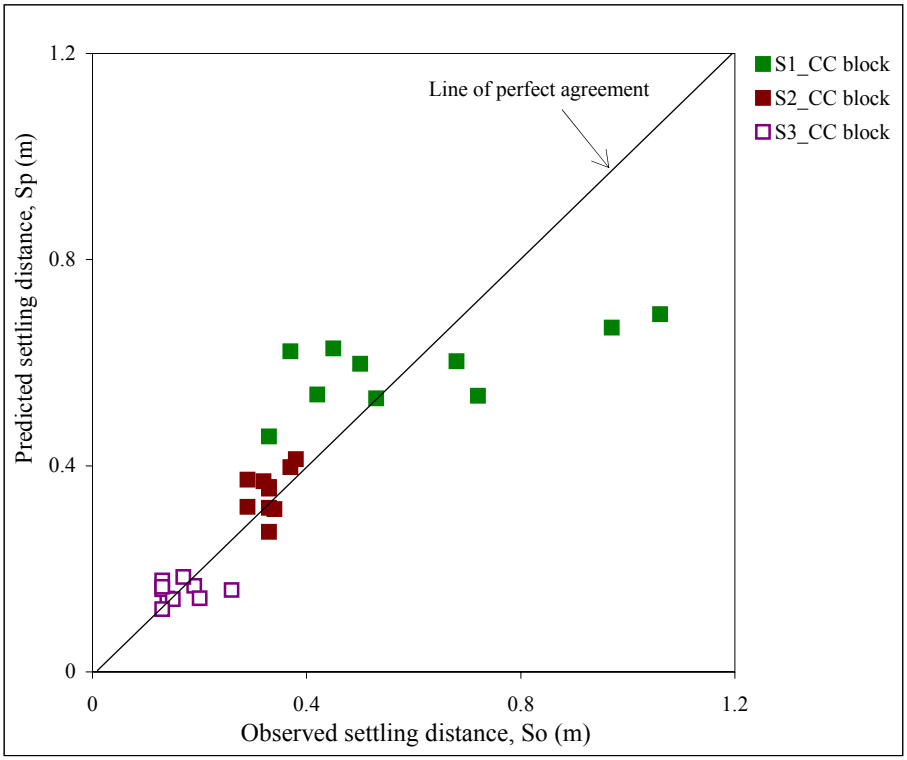

Figure 5.12: Comparison of observed and predicted settling distance using equation (5.5) for CC block

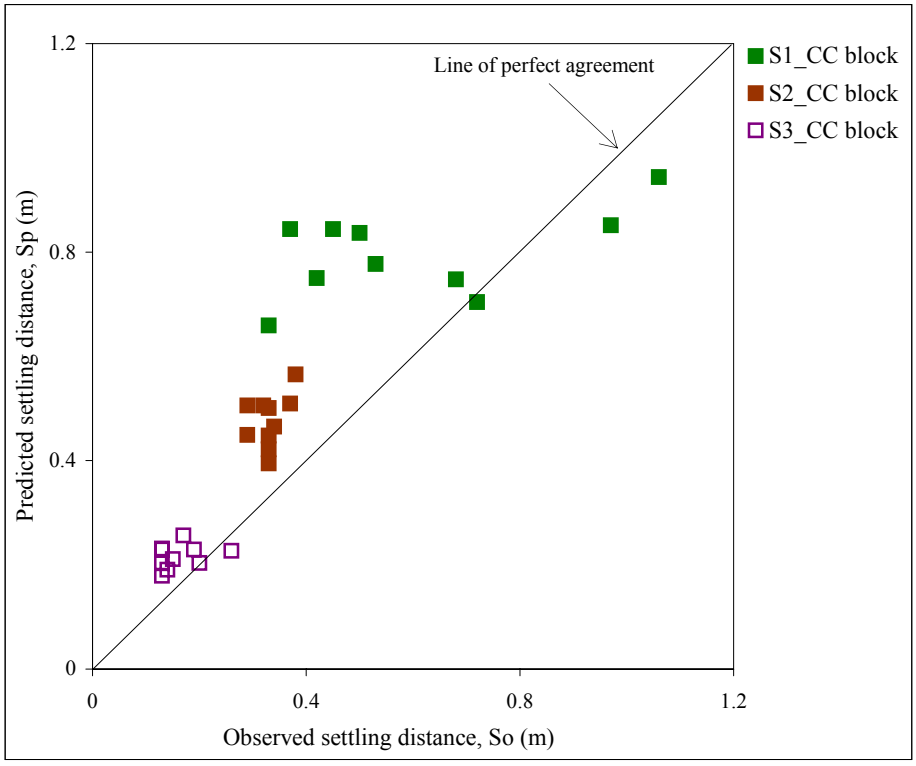

Figure 5.13: Comparison of observed and predicted settling distance according to Zhu et al. (2004) for CC block

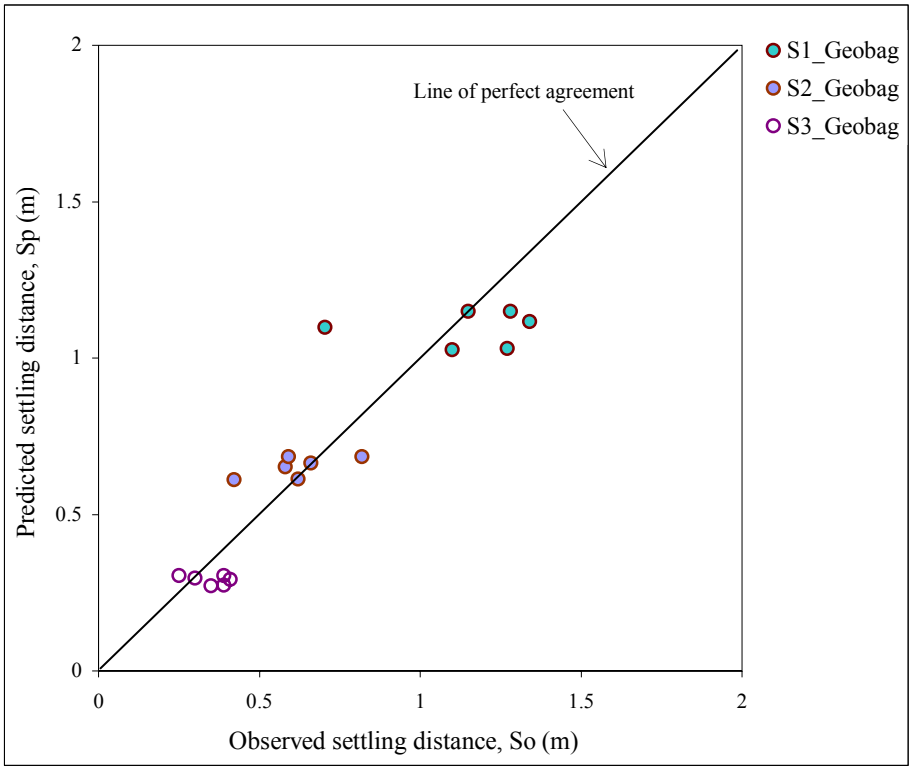

Figure 5.14: Comparison of observed and predicted settling distance using equation (5.5) for geobag

Figure 5.14 represents the predicted settling distance by proposed empirical equation (equation 5.5) versus measured in this study for geobag. It is seen that using equation (5.5) the predicted settling distance is balanced in both sides of the line of perfect agreement. The average relative error for this comparison is obtained as 18.09%.

Figure 5.15 represents the predicted settling distance by Zhu et al. (2004) versus measured in this study for geobag. Almost all the predicted settling distance is above the line of perfect agreement indicating the predicted values are greater than observed values. The average relative error for this comparison is obtained as 53.20% which is about three times greater than equation (5.5).

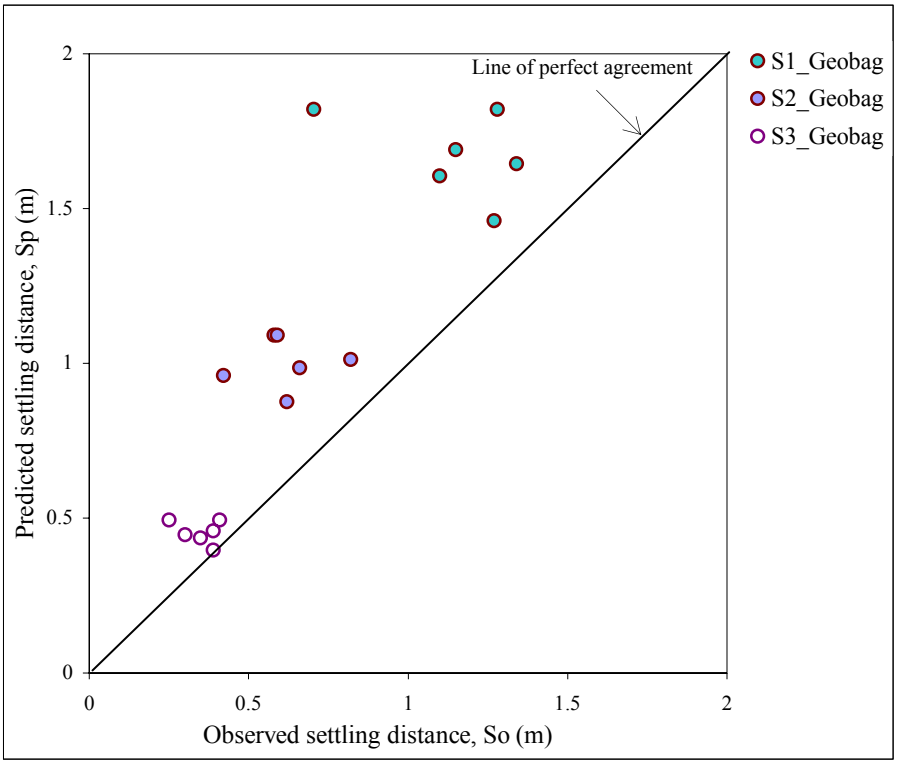

Figure 5.15: Comparison of observed and predicted settling distance according to Zhu et al. (2004) for geobag

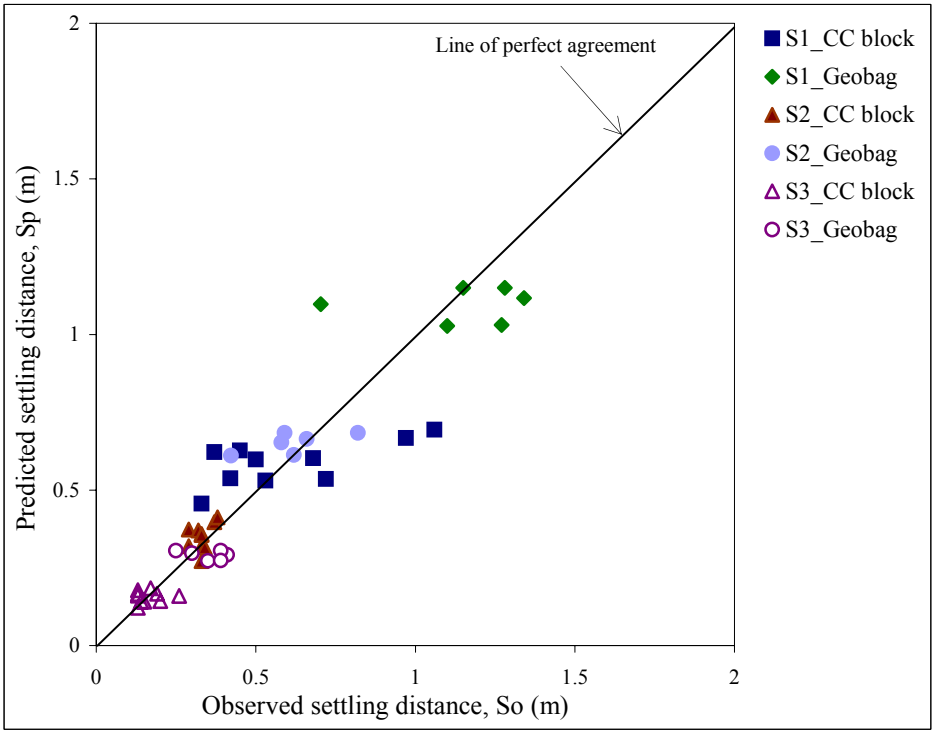

Figure 5.16: Comparison of observed and predicted settling distance using equation (5.5) for both CC block and geobag

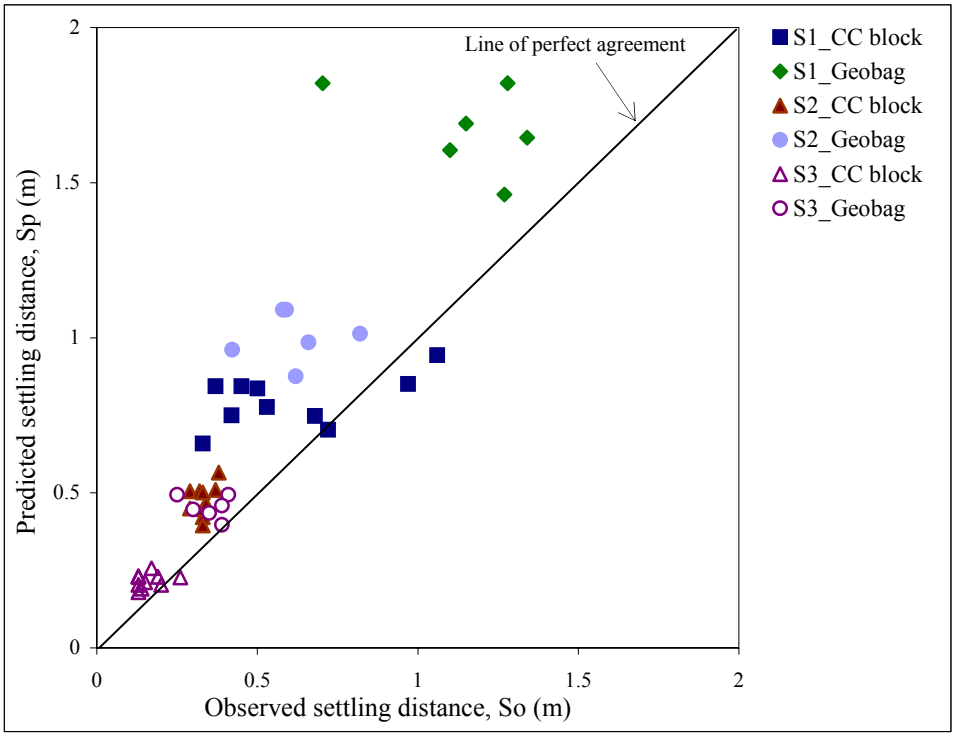

Figure 5.17: Comparison of observed and predicted settling distance according to Zhu et al. (2004) for both CC block and geobag

Figure 5.16 represents the predicted settling distance by proposed empirical equation (equation 5.5) versus measured in this study for block and geobag. It is seen that using equation (5.5) the predicted settling distance is balanced in both sides of the line of perfect agreement. Data points of setup 1 are the most scattered due to high flow velocity and depth than other setup. The average relative error for this comparison is obtained as 19.31% which is lower than Zhu et al. (2004).

Figure 5.17 represents the predicted settling distance by Zhu et al. (2004) versus measured in this study for block and geobag. The same as before almost all the predicted settling distance is above the line of perfect agreement indicating the predicted values are greater than observed values. The average relative error for this comparison is obtained as 47.13% which is more than two times greater than values obtained from proposed equation.

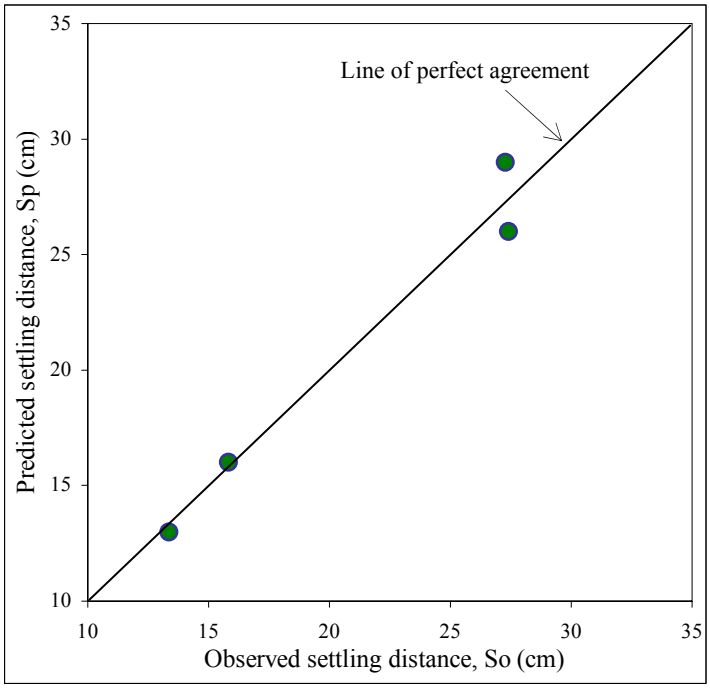

Figure 5.18: Verification of proposed settling distance relationships

To assess the performance of proposed relationship, verification is carried out in the laboratory for a new setup with 34.5 cm flow depth and depth averaged velocity of 0.183 m/s. Figure 5.18 shows a comparison of the predicted and observed settling distances for four types of element and the agreement is found to be satisfactory with a relative average error of 3.80%.

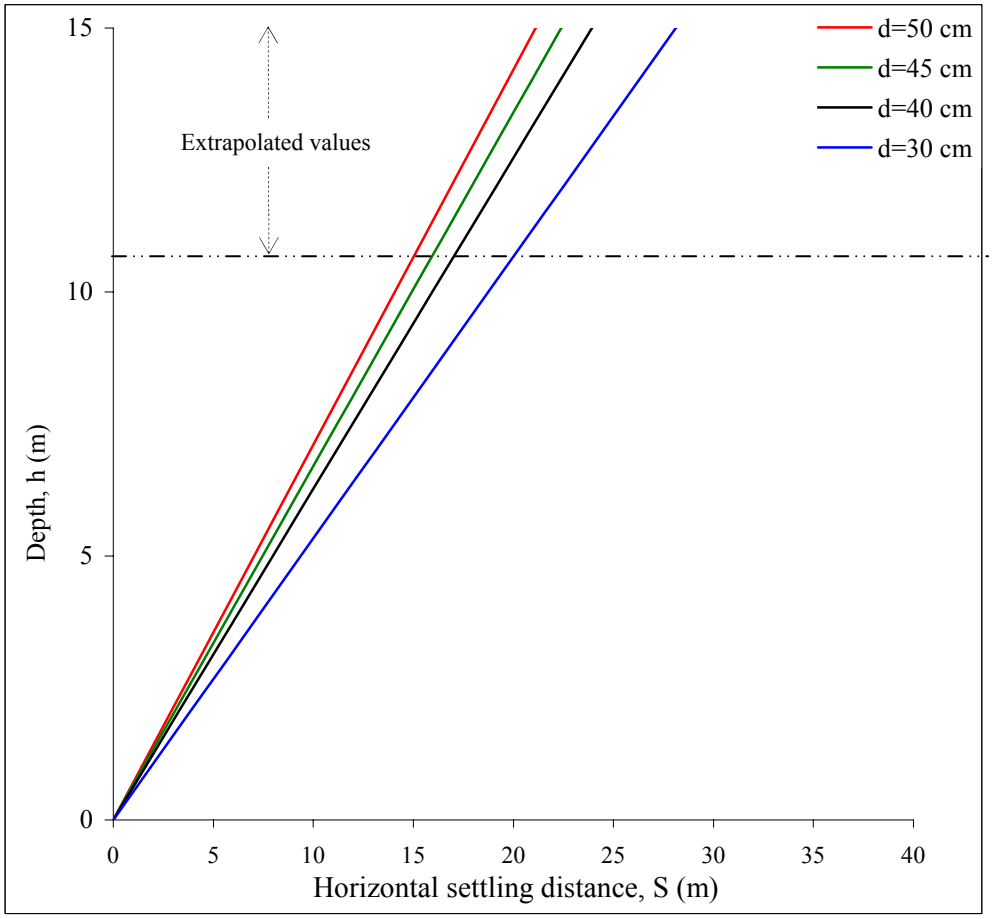

Figure 5.19: Plot of depth versus horizontal settling distance for prototype condition

Equation (5.5) is used to generate values that are shown in Figure 5.19, which is applicable to a protection unit weighing 2500 kg/m^3 with a characteristic diameter of 30, 40, 45 and 50 cm. The depth averaged velocity is 3.5 m/s. It is seen that the trend of the curves are linear. This nomograph implies that for a given protection unit, local velocity and depth of flow, it can predict the distance by which the unit will be displaced from its dumping location. Similar graphs can be developed for protection element of different unit weight and different velocity.

Summary

Table 5.4 shows the average value of the relative errors where error is computed by equation (5.2). The overall error of the proposed relationship is 19.31% and for Zhu et al. (2004) formula it is 47.13%. The discrepancy may be due to the variation in the elements used in laboratory experiments. Zhu et al. (2004) equation might be valid

for a particular condition where he considered large sized sand filled geocontainers but not for the size of protection element used in Bangladesh. The overall performance of the proposed equation is better than other formula. For first setup the errors are more as the depth of flow was higher resulting more difference in settling distance.

Table 5.4: Average value of relative error of prediction formulas

Set up	Type of element	Error (%)	
		Proposed equation	**Zhu et al. (2004)**
S1	Block	29.65	54.34
	Bag	18.06	55.29
	Both	25.31	54.70
S2	Block	11.53	44.57
	Bag	15.28	69.09
	Both	12.94	53.77
S3	Block	18.92	41.13
	Bag	20.94	35.22
	Both	19.68	37.33
Total		**19.31**	**47.13**

5.6 Results of Incipient Motion

Incipient motion test is conducted as per the construction method applied in real life condition. Two set up were investigated for both block and geobag during the experiment and on the basis of expression of incipient motion as shown in equation (3.19). A power regression analysis of the experimental data has been performed and the value of coefficient of determination (R^2) is found to be 0.905. In the following sections the results of experiments for block and geobag are presented.

Table 5.5: Results of incipient motion experiments for CC block

Setup	Size of Block, d (m)	Depth of flow, h (m)	Velocity, V (m/s)	d/h	V/√(Δgh)
S1	0.023	0.212	0.604	0.108	0.42
	0.021	0.196	0.56	0.107	0.41
	0.016	0.194	0.54	0.082	0.38
S2	0.023	0.257	0.604	0.094	0.38
	0.021	0.25	0.578	0.084	0.37
	0.016	0.24	0.53	0.067	0.34

Table 5.5 shows the parameter values of the tests for CC block. Two setups for three types of block are conducted. On the basis of expression of incipient motion as shown in equation (3.19), a power regression analysis of the experimental data has been performed resulting:

$$\frac{d}{h} = 0.86\left(\frac{V}{\sqrt{\Delta gh}}\right)^{2.38} \tag{5.8}$$

Equation (5.8) can be used to determine the CC block size to be used in toe protection when other parameters are known. Figure 5.20 shows the plot of equation (5.8). The coefficient of determination (R^2) for this equation is 0.95 which may be considered satisfactory.

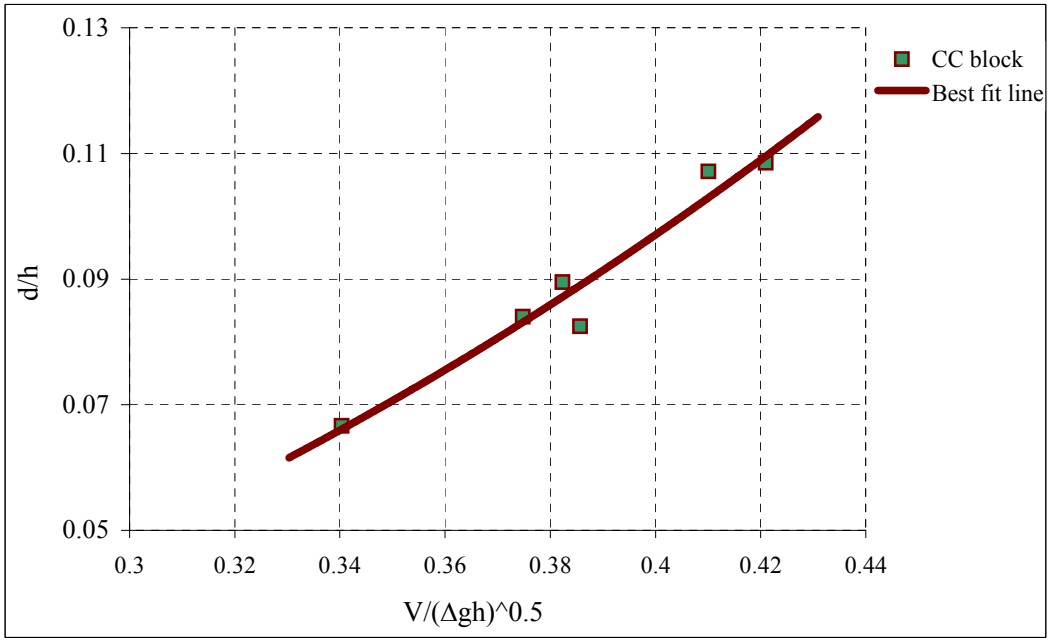

Figure 5.20: Plot of *d/h* against *V/√(Δgh)* for CC block

Table 5.6: Results of incipient motion experiments for geobag

Setup	Size of bag, d (m)	Depth of flow, h (m)	Velocity, V (m/s)	d/h	$V/\sqrt{(\Delta gh)}$
S1	0.0253	0.190	0.451	0.134	0.451
	0.0259	0.193	0.438	0.134	0.435
	0.0236	0.189	0.425	0.125	0.427
	0.0245	0.182	0.413	0.135	0.422
	0.0316	0.194	0.502	0.163	0.497
S2	0.0253	0.246	0.464	0.103	0.408
	0.0259	0.247	0.464	0.105	0.407
	0.0236	0.243	0.425	0.097	0.377
	0.0245	0.246	0.438	0.099	0.386
	0.0316	0.260	0.514	0.122	0.441

Table 5.6 shows the parameters of the tests for geobag. Two setups for five types of geobag are conducted. On the basis of expression of incipient motion as shown in equation (3.19), a power regression analysis of the experimental data has been performed resulting:

$$\frac{d}{h} = 0.64\left(\frac{V}{\sqrt{\Delta gh}}\right)^{1.95} \tag{5.9}$$

Equation (5.9) can be used to determine the size of geobag to be used in toe protection when other parameters are known. Figure 5.21 shows the plot of equation (5.9). The coefficient of determination (R^2) for this equation is 0.87 which may be considered satisfactory.

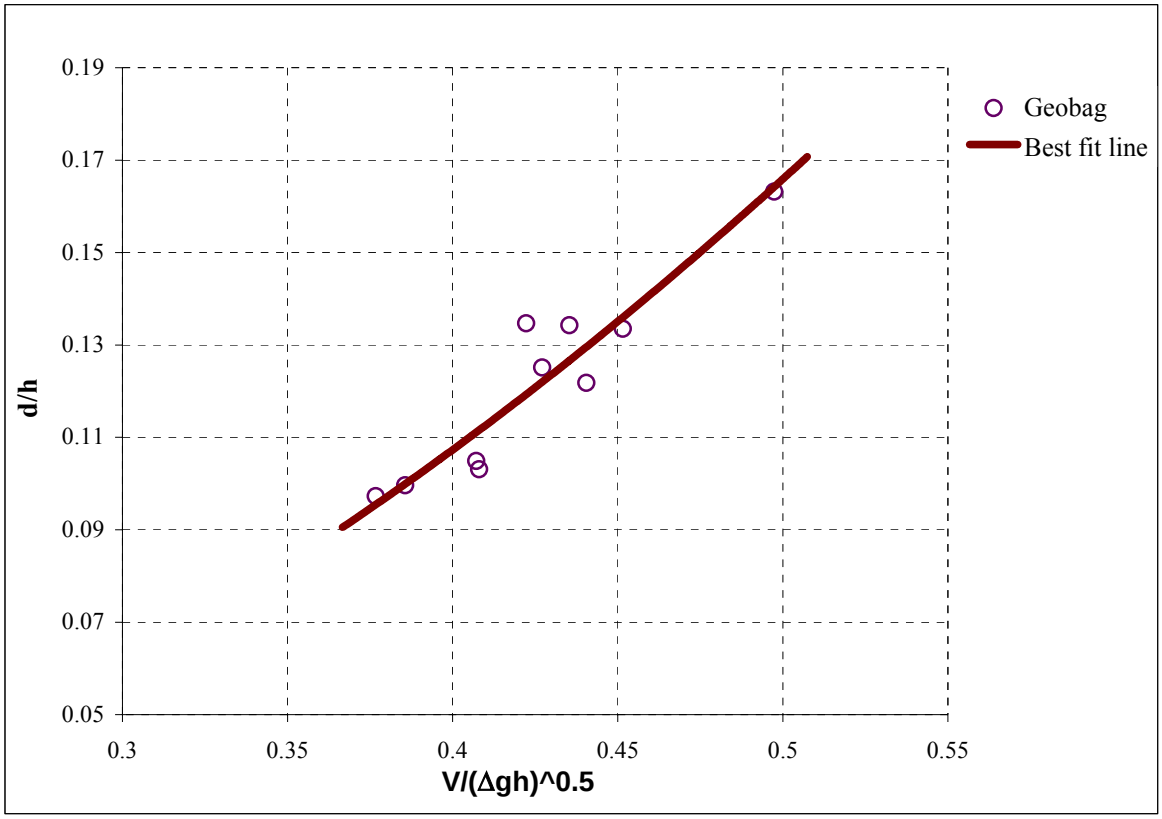

Figure 5.21: Plot of *d/h* against $V/\sqrt{(\Delta gh)}$ for geobag

On the basis of expression of incipient motion as shown in equation (3.19) a power regression analysis using both (CC block and geobag) experimental data has been performed resulting:

$$\frac{d}{h} = 0.92\left(\frac{V}{\sqrt{\Delta gh}}\right)^{2.4} \tag{5.10}$$

Equation (5.10) can be used to determine the size of block and geobag to be used in toe protection when other parameters are known. Figure 5.22 shows the plot of equation (5.10). The coefficient of determination (R^2) for this equation is 0.91 which may be considered as satisfactory. However, it is needless to mention that equation (5.8) and (5.9) is better for CC block and geobag, respectively.

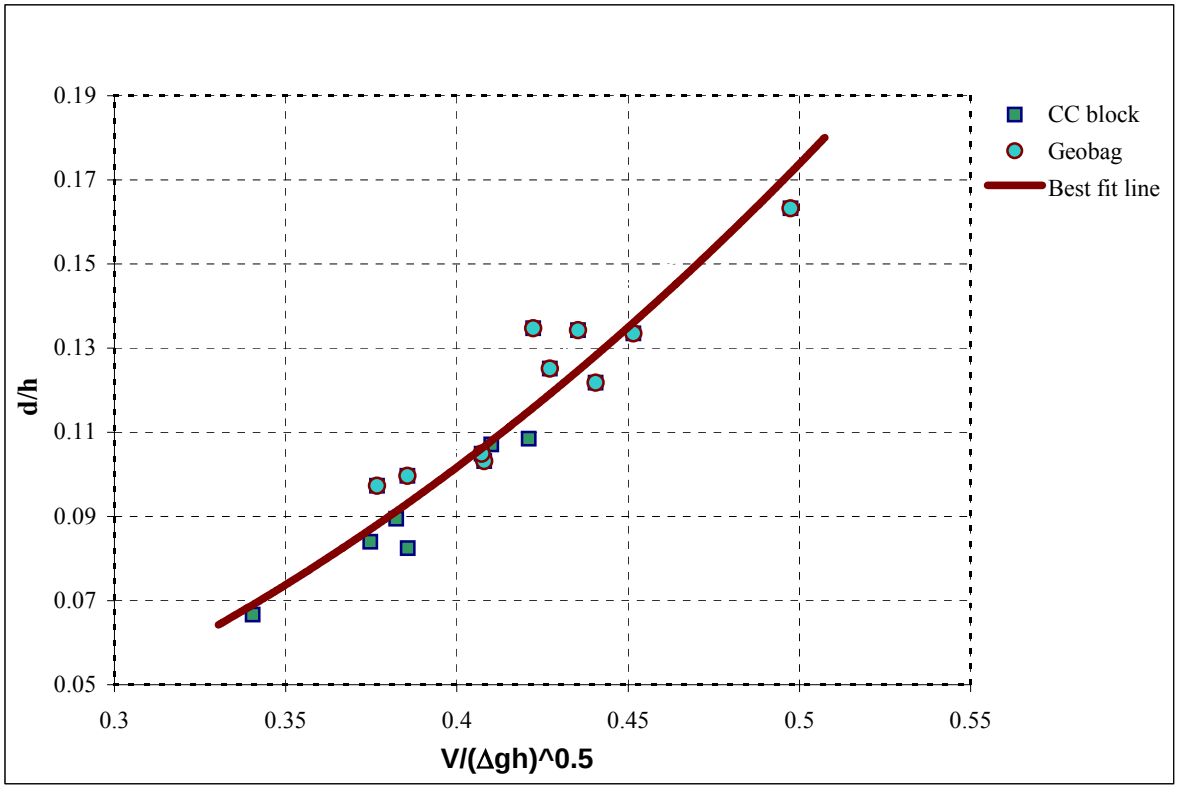

Figure 5.22: Plot of *d/h* against $V/\sqrt{(\Delta gh)}$ for both CC block and geobag

The data measured for the experiment on incipient condition have been compared with that of Shields diagram (Figure 2.4). Dimensionless shear stress, τ_{*c} obtained from the experiments are found to be in the range between 0.007 and 0.014, which demonstrates that the protection elements studied are in 'no motion' condition.

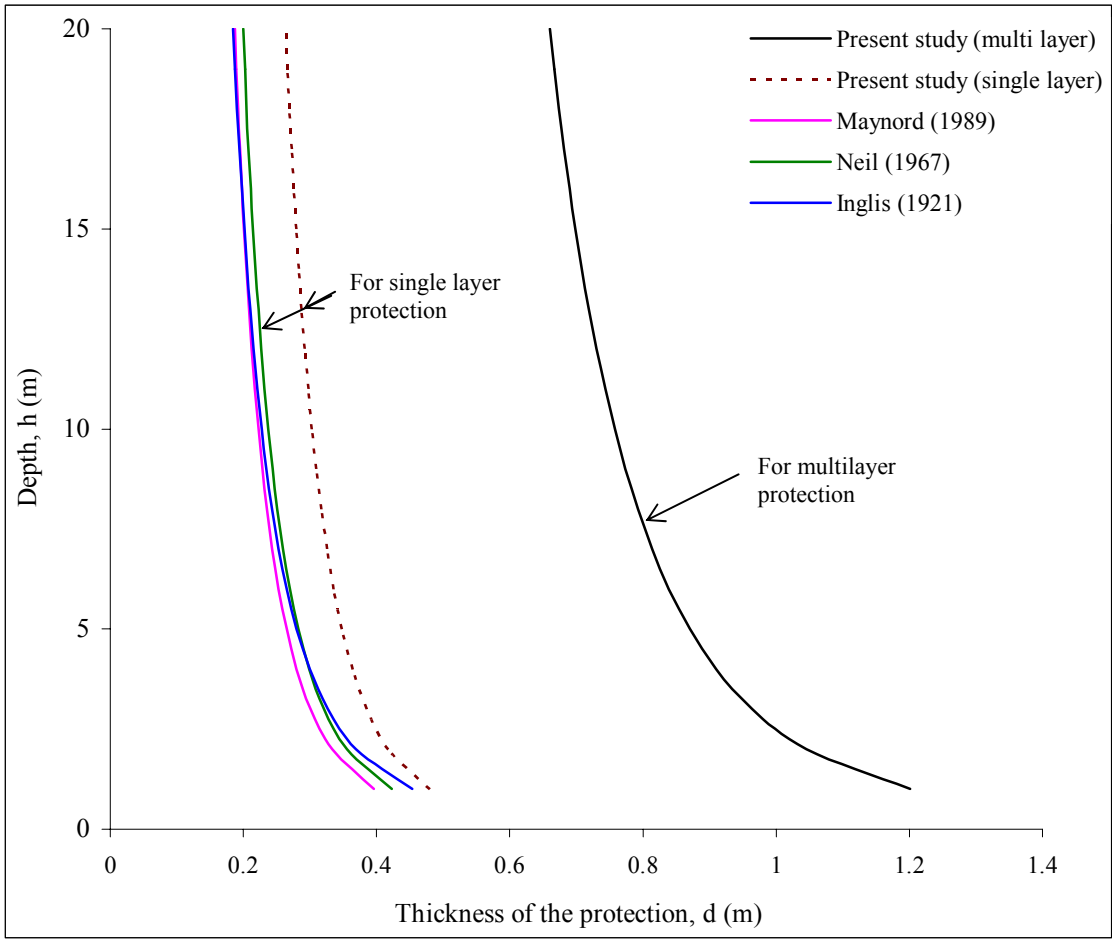

Figure 5.23: Depth versus thickness of protection for prototype condition according to different equation

Figure 5.23 shows a comparison among the obtained relationship and equations given by Maynord (1989), Neil (1967) and Inglis (1921). Here ρ_s = 2000 kg/m^3, ρ_w = 1000 kg/m^3 and V = 3.5 m/s. The present study finds that requirement of protection thickness is more than other equations. For multilayer protection, the thickness changes at a higher rate than that for single layer, especially at low depths.

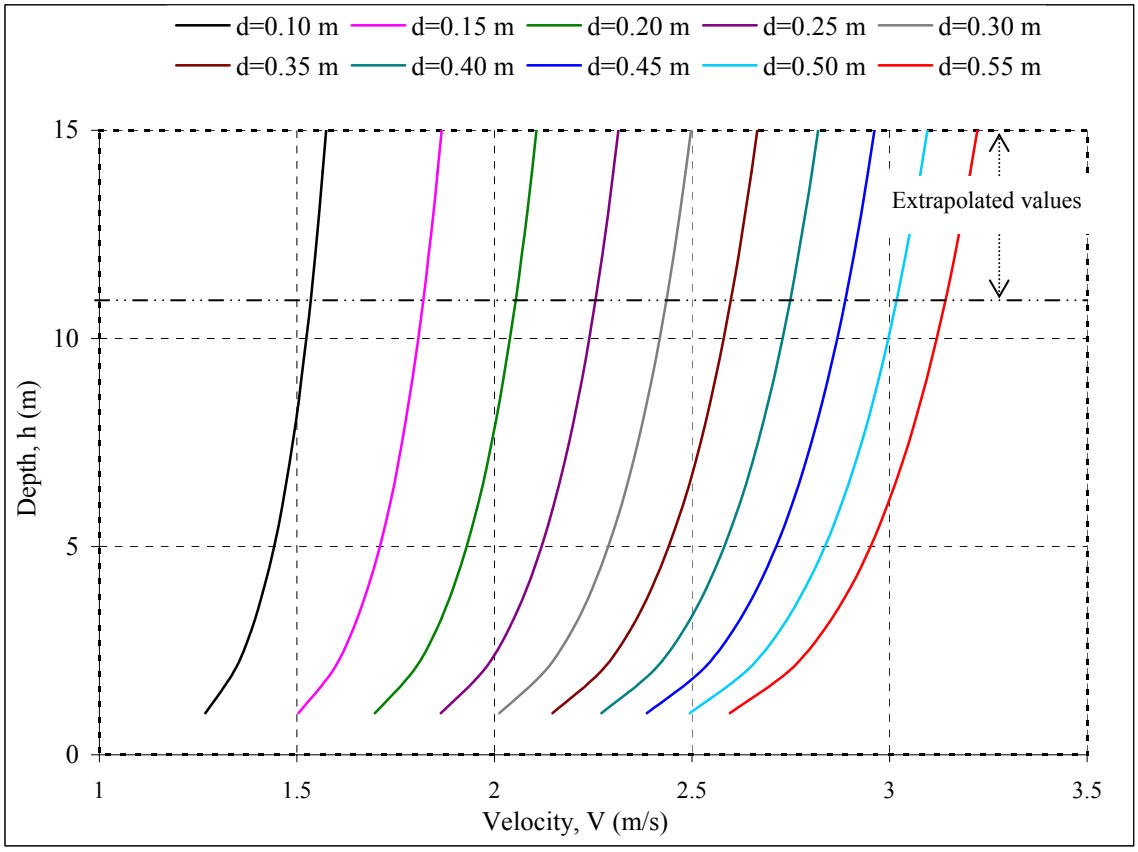

Figure 5.24: Plot of depth versus depth averaged velocity for CC block

Equation (5.8) is used to develop the nomograph shown in Figure 5.24, which is applicable to a cc block weighing 2000 kg/m^3. It is seen that the trend of the curves at higher depth are towards right. This implies that for a given block size it can withstand a high velocity at higher depth. For given flow depth and depth averaged velocity, the required thickness of protection using CC block can be selected from this graph.

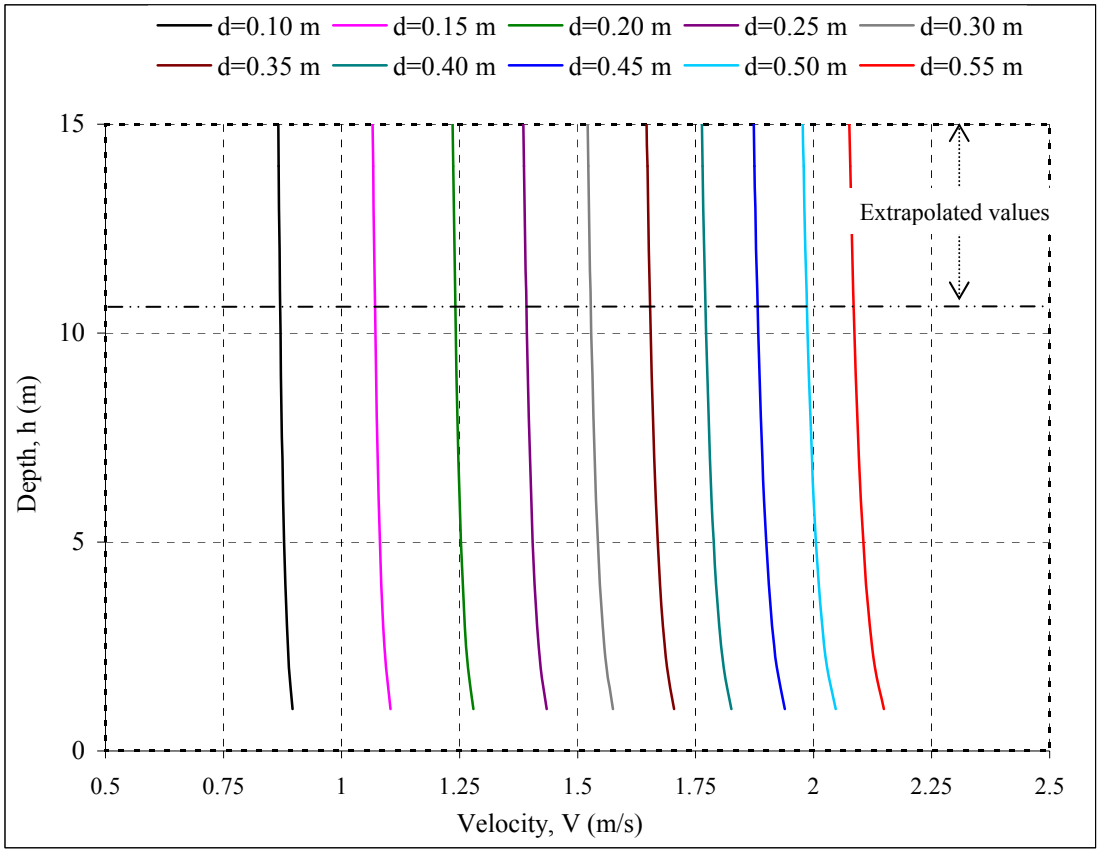

Figure 5.25: Plot of depth versus depth averaged velocity for geobag

Equation (5.8) is used to develop the nomograph shown in Figure 5.25, which is applicable to a geobag weighing 1550 kg/m^3. It is seen that the curves are almost vertical at higher depths while the trend of the curves at lower depth is towards right whereas that of the block is towards left. This implies that for a given geobag size it can withstand a high velocity at lower depth which is a reverse behavior than block. This discrepancy may be due to the fact that the geobags are relatively flat and less dense so that their under water functional behavior in a group become more composite. For given flow depth and depth averaged velocity, the required thickness of protection using geobag can be selected from this graph.

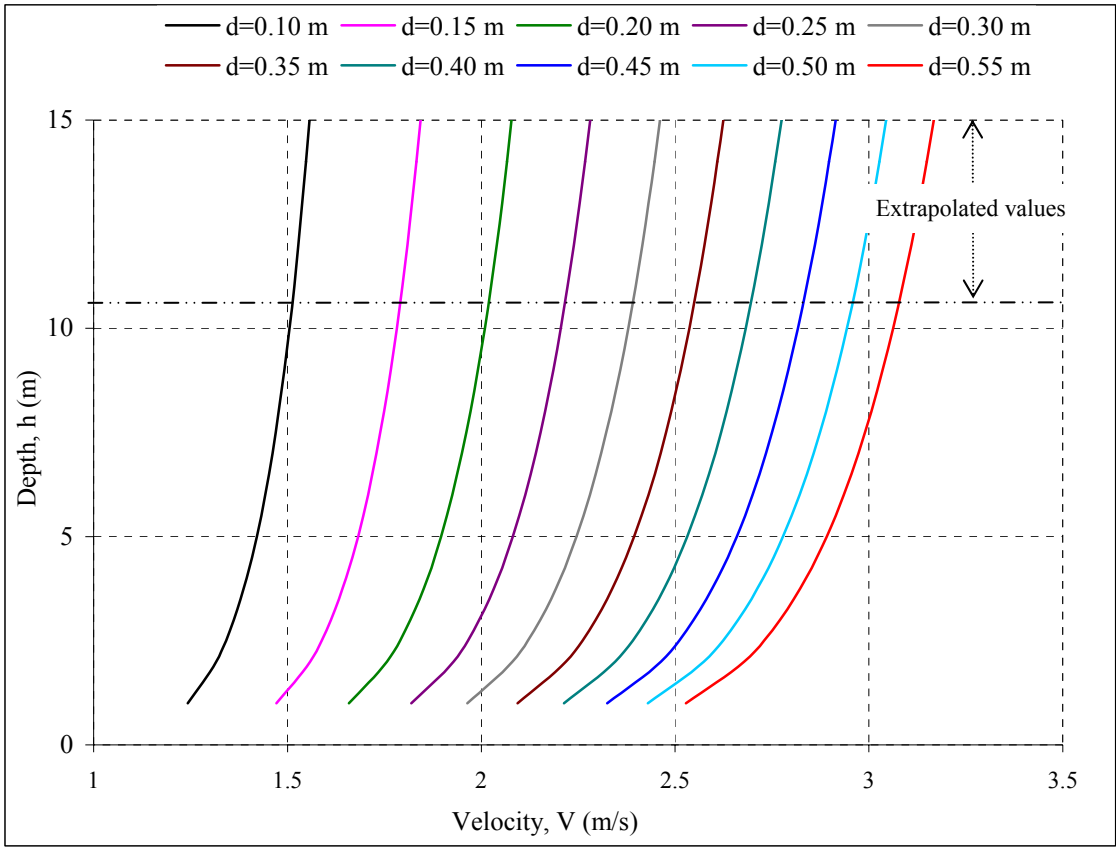

Figure 5.26: Plot of depth versus local averaged velocity for both CC block and geobag

Equation (5.10) is used to develop the nomograph shown in Figure 5.26, which is applicable to a protection unit weighing 2000 kg/m^3. For a given depth of flow and local depth averaged velocity the required size of multilayer protection using CC block or geobag can be selected from this graph.

However, it is needless to mention that Figure 5.24 and Figure 5.25 are better for the determination of CC block and geobag sizes, respectively, than Figure 5.26.

CHAPTER SIX

CONCLUSIONS AND RECOMMENDATIONS

6.1 Introduction

Most of the river bank toe protection structures are usually constructed in under water condition. In such condition, the placement of toe protection elements at designated location is a difficult task. During field visits and information gathered from concerned BWDB officials, it reveals that such placement of protection elements is carried out roughly based on experience and judgment where no prior estimation is made before under water dumping. In this study an attempt has been made to suggest a procedure so that position of the toe protection elements after dumping can be estimated beforehand.

6.2 Conclusions

Based on detailed theoretical analysis, experimental investigations and results obtained from this study the following conclusions are made:

i) Relationships for governing parameters of the settling behavior of toe protection elements such as the fall velocity, settling distance and threshold condition have been theoretically analyzed. These relationships are then calibrated using laboratory data.

ii) A total of sixteen types of elements consisting of six different sizes of geobags ranging from 4.2 cm X 2.6 cm X 0.08 cm to 7.1 cm X 4.1 cm X 1.1 cm and ten types of CC blocks ranging from 1.6 cm X 1.6 cm X 1.3 cm to 4.1 cm X 4.1 cm X 2.7 cm have been used to conduct experiments.

iii) For measurement of fall velocity a square shaped settling column of 30 cm X 30 cm X 130 cm has been fabricated. In this settling column fall velocity was measured for each of the element. Using the fall velocity data empirical equation 5.1 for CC block and equation 5.3 for geobag are obtained.

iv) Predictive performances of the proposed relationships between particle Reynolds number and dimensionless particle diameter have been compared with other available equations. It is found that the predictive

capacity of proposed relationships show satisfactory performance (3.91% and 2.38% error for equation 5.1 and equation 5.3, respectively).

v) Forty eight experimental runs with all types of elements have been conducted for investigating settling distance for discharges range from 0.05 m^3/s to 0.203 m^3/s. An empirical relationship (equation 5.6 and equation 5.6b) is developed to estimate horizontal settling distance of a toe protective element after dumping. Verification of the proposed relationship using independent set of laboratory data has been done and shows satisfactory agreement with an error of 3.80%.

vi) For given hydraulic conditions, generated values of settling distance to determine the location of toe protective element are shown graphically (Figure 5.19). These values can be used to estimate settling distance. Settling distance of geobag is found longer than that of CC block due to its thin shape and low density.

vii) Sixteen experimental runs with eight types of elements have been conducted for investigating incipient condition for discharges range from 0.033 m^3/s to 0.052 m^3/s. An empirical relationship (equation 5.10) to determine the size of toe protection element based on incipient condition is developed. Equation 5.10 is used to generate values of the size of toe protection elements as shown in Figure 5.26.

viii) For given hydraulic condition, CC blocks can withstand at higher velocity at higher depths but geobags show slightly the reverse trend (Figure 5.24 and Figure 5.25). This discrepancy may be due to the fact that the geobags are relatively flat and less dense, and thus their under water functional behavior become more composite as a group.

ix) Finally, it is expected that the outcome of the present study can be taken as a tentative guideline for under water construction of river bank toe protection works.

6.3 Recommendations for Future Study

Following recommendations can be suggested for further study, these are as follows:

i) Similar experimental study for predicting the settling distance can be conducted in a large sand bed channel.

ii) The proposed equation to determine settling distance of protective element has been verified based on laboratory data and in future it may be verified in field condition.

iii) Future research may be undertaken to investigate hydraulic behavior around an apron of transverse type river training structures.

iv) Morphological impact of the river bed due to irregular placement of toe protection element during construction can be investigated.

v) Similar study may be undertaken in physical modeling facility considering a prototype condition.

REFERENCES

Ahrens, P. A. (2000). “A fall velocity equation”. J. Waterway, Port, Coastal, and Ocean Eng., ASCE, 126 (2), 99-102.

Ahrens, P. A. (2003). “Simple equations to calculate fall velocity and sediment scale parameter”. J. Waterway, Port, Coastal, Ocean Eng., ASCE, 129 (3), 146-150.

Alger, G. R., and Simons, D. B. (1968) “Fall velocity of irregular shaped particles”. J. Hydraulic Div., ASCE, 94 (HY3), 721-737.

Beheshti, A. A., and Ashtiani, B. A. (2008). “Analysis of threshold and incipient conditions for sediment movement”. J. Coastal Eng., Elsevier, 55 (2008), 423-430.

Bettess, R. (1984). “Initiation of sediment transport in gravel streams.” Proceedings of the Institution of Civil Engineers, Technical Note 407, Part 2.

Blench, T. (1966). Discussion of “Sediment transport mechanics: initiation of motion.” J. Hydraulics Div., ASCE, 92(HY5), 287-288.

Bogardi, J. L. (1978). “Sediment transport in alluvial streams.” Akademiai Kiado, Budapest.

Brahms, A. (1753). Anfangsgründe der deich-und. Wasserbaukunst, Aurich (Source: Van Rijn, 1993).

BWDB, (2010). “Guidelines for river bank protection”, prepared for Bangladesh Water Development Board under Jamuna-Meghna River Erosion Mitigation Project, Government of the People’s Republic of Bangladesh.

Buffington, J. M., and Montgomery, D. R. (1997). “A systematic analysis of eight decades of incipient motion studies, with special reference to gravel bedded rivers”. Journal of Water Resources Research, Vol. 33, No. 8

Camenen, B. (2007). “Simple and general formula for the settling velocity of particles.” J. Hydraul. Eng., ASCE, 133 (2), 229-233.

Chang, H. H. (1992). “Fluvial processes in river engineering”, Krieger Publishing Co., Malabar, Florida

Chang, H. –K., and Liou, J. –C. (2001). “Discussion of a free-velocity equation, by John P. Ahrens”. J. Waterway, Port, Coastal, Ocean Eng., ASCE, 127 (4), 250-251.

Cheng, N. -S. (1997). “Simplified settling velocity formula for sediment particle”. J. Hydraul. Eng., ASCE, 123 (2), 149-152.

Dallavalle, J. (1948). “Micrometrics: the technology of fine particles.” Pitman, London. (Source: Camenen, 2007).

FAP 21/22 (1993). Main Report on Bank Protection; FAP 21; Volume 1A: Bank Protection and River Training (AFPM); Pilot Project; FAP 21/22; Final Report, Planning Study; Consulting Consortium, RHEIN-RUHR ING. GES. MBH, Dortmund, Germany.

FAP 21 (2001). “Guidelines and design manual for standardized bank protection structures”, Flood Action Plan, Bank Protection Pilot Project, prepared for Water Resources Planning Organization.

Gales, R. (1938). “The principles of river training for railway bridges and their application to the case of the Hardinge Bridge over the lower Ganges of Sara”. Journal of the Institution of Civil Engineers, December 1938. Paper No, 5167, India.

Göğüş, M., İpekçi, O. N., and Köpinar, A. (2001). “Effect of particle shape on fall velocity of angular particles”. J. Hydraul. Eng., ASCE, 127 (10), 860-869.

Göğüş, M., and Defne, Z. (2005). “Effect of shape on incipient motion of large solitary particles”. J. Hydraul. Eng. Div, ASCE, 131 (1), 38-45.

Halcrow and Associates, (2002). “Feasibility Study - Final Report”, Jamuna-Meghna River Erosion Mitigation Project, Volume 1 (Phase II), main report prepared for Bangladesh Water Development Board, Government of the People’s Republic of Bangladesh, and Asian Development Bank.

Haque, M. E. (2010). “An experimental study on flow behavior around launching apron”. M.Sc. Thesis, Department of Water Resources Engineering, BUET, Dhaka.

Inglis, C. C. (1949). “The behavior and control of rivers and canals (with the aid of models)”, Part II. Central Waterpower Irrigation and Navigation Research Station, Poona, India.

Jiménez, J. A., and Madsen, O. S. (2003). “A simple formula to estimate settling velocity of natural sediments”. J. Waterw., Port, Coastal, Ocean Eng.,ASCE, 129 (2),

70-78.

Klusman,C.R. (1998). ‘‘Two-dimensional analysis of stacked geosynthetic tubes.’’ Masterthesis, Virginia Polytechnic Institute and State Univ., Blackburn,Va. (Source: Zhu et al., 2004)

Kobayashi, N., and Jacobs, B. K. (1985).‘‘Experimental study on sandbag stability and runup.’’ Proc., Coastal Zone’85, O.T. Magoonetal., eds., ASCE, NewYork. (Source: Pilarczyk, 2000)

Lick, W., Jin, L., and Gailani, J. (2004). “Initiation of movement of quartz particles”. J. Hydraul. Eng., ASCE, 130 (8), 755-761.

Ling, C. H., (1995). “Criteria for incipient motion of spherical sediment particles”. J. Hydraul. Eng., ASCE, 121 (6), 472-478.

Liu, G. S. (1981). ‘‘Design criteria of sand sausages for beach defense.’’ Proc., 19th Congress of the Int. Association for Hydraulic Research, 3, 123–131. (Source: Pilarczyk, 2000)

Marsh, N. A., Western, A. W., and Grayson, R. B. (2004). “Comparison of methods for predicting incipient motion for sand beds”. J. Hydraul. Eng., ASCE, 130 (7), 616-621.

Maynord, S. T., Ruff, J. F. and Abt, S. R. (1989). “Riprap Design”. J. Hydraul. Eng., ASCE, 115 (7), 937-949.

McNown, J. S. and Newlin, J. T. (1951). “Drag of spheres within cylindrical boundaries”. Proc. 1st Congr. Of Appl. Mech., ASME, New York, 801-806.

Mehta, A. J., Lee, J. and Christensen, B. A. (1981). “Fall velocity of shells as coastal sediment”. J. Hydraul. Div., ASCE, 106 (HY11), 1727-1744.

Meyer-Peter, E., and Muller, R. (1948). “Formulas for bed load transport.” International Association for Hydraulic Structures Research, Second Meeting, Stockholm, Appendix 2, 39-64.

Neill, C. R. (1967). “Mean velocity criterion for scour of coarse uniform bed material”. Proceedings 12th Congress, International Association for Hydraulic Research, Vol. 3.

nhc, (2006). Northwest Hydraulic Consultants: Physical Model Study (Vancouver Canada), Final Report. Prepared for Jamuna-Meghna River Erosion Mitigation Project. Bangladesh Water Development Board.

PIANC, (1987). “Guidelines for the design and construction of flexible revetments incorporating geotextiles for inland waterways”, Report of Working group 4, Supplement to Bulletin No.57, Belgium.

Pilarczyk, K. W. (1995). “Novel systems in coastal engineering; geotextile systems and other methods, an over view.” Rijkswaterstaat, Delft, the Netherlands.

Pilarczyk, K. W. (2000). “Geosynthetics and geosystems in hydraulic and coastal engineering”, Balkema, Rotterdam, The Netherlands.

Przedwojski, B., Błażejewski, R. and Pilarczyk, K. W. (1995). “River training techniques: fundamentals, design and applications”. A. A. Balkema, Rotterdam, The Netherlands.

Rao, T. S. N. (1946). “History of the Hardinge Bridge upto 1941,” Railway Board, Government of India, New Deldi, Technical paper no. 318.

Reico, J., and Oumeraci, H. (2009). “Process based stability formulae for coastal structures made of geotextile sand containers” J. Coastal Eng., Elsevier, 56 (2009), 632-658.

Restall, S. J., Jackson, L. A., Heerten, G., and Hornsey, W. P. (2002). “Case studies showing the growth and development of geotextile sand containers: an Australian perspective”. J. Geotextiles and Geomembranes, Elsevier, 20 (2002), 321-342.

RRI (2010). River Research Institute. “Additional test to carryout investigation regarding performance of falling apron, drop test for dumping of geobag and outflanking problem by physical model to address bank erosion of Bangladesh”. Prepared for Bangladesh Water Development Board.

Ruby, W. W. (1933). “Settling velocities of gravel, sand and silt particles.” Am. J. Sci.,25(148), 325-338. (Source: Ahrens, 2003).

Schlichting, H. (1979). “Boundary layer theory.” McGraw-Hill, New York. (Source: Camenen, 2007).

Smith, D. A., and Cheung, K. F. (2004). “Initiation of motion of calcareous sand”. J. Hydraul. Eng., ASCE, 130 (5), 467-472.

Sping, F. J. (1903). “River training and control on the guide bank system”, Railway Board Technical Paper No. 153, New Delhi.

Sternberg, H. (1875). “Untersuchungen über das Längen und querprofil geschiebeführender”. Flüse Zeitschrift Bauwesen, vol. 25 (Source: Van Rijn, 1993).

Stevens, M. A., and Oberhagemann, K. (2006). SpecialReport 17: “Geobag revetments.” Prepared for Jamuna-Meghna River Erosion Mitigation Project. Bangladesh Water Development Board.

Stevens, M. A., and Simons, D. B. (1971). “ Stability analysis for coarse granular material on slopes”. River Mechanics, H. W. Shen, Ed., Fort Collins, Colo., 1, 17-1-17-27.

Swamee, P. K., and Ojha, C. S. P. (1991). “Drag coefficient and fall velocity of nonspherical particles”. J. Hydraul. Eng., ASCE, 117 (5), 660-667.

Ünal, N. E., and Bayazit, M. (1998). “Incipient motion of coarse particles on a slope by regular or irregular waves”. J. Waterw., Port, Coastal, Ocean Eng.,ASCE, 124 (1), 32-35.

USACE, (1994). “Hydraulic design of flood control channels”. U. S. Army Corps of Engineers, Manual EM 1110-2-1601.

Van Rijn, L.C. (1993). “Principles of Sediment Transport in Rivers, Estuaries and Coastal Seas”. Amsterdam, Aqua Publications.

Vanoni, V. A., ed. (1975). Sedimentation Engineering, Manual no. 54, ASCE.

Zaman, M. U., and Oberhagemann, K. (2006). SpecialReport 23: “Design brief for river bank protection implemented under JMREMP.” Prepared for Jamuna-Meghna River Erosion Mitigation Project. Bangladesh Water Development Board.

APPENDIX - A

- **Sample Calculation to Determine Experimental Size of CC Block**

(i) Let,

ū = 3.3 m/s

h = 10 m and

D_n = 0.4 m.

Then, $K_h = \left(h / D_n + 1\right)^{-0.2}$

= 0.52

Now from equation (4.1) and other values mentioned above results in

D_n = 451 mm ≈ 460 mm.

For present study, D_n = 460/20 = 23 mm that is block type ‘D1a’ of Table 4.2.

(ii) Let,

ū = 3.1 m/s

h = 9 m and

D_n = 0.4 m.

Then, $K_h = \left(h / D_n + 1\right)^{-0.2}$

= 0.53

Now from equation (4.1) and other values mentioned above results in

D_n = 405 mm ≈ 420 mm.

For present study, D_n = 420/20 = 21 mm that is block type ‘D2a’ of Table 4.2.

(iii) Let,

ū = 2.8 m/s

h = 8 m and

D_n = 0.3 m.

Then, $K_h = \left(h / D_n + 1\right)^{-0.2}$

= 0.51

Now from equation (4.1) and other values mentioned above results in

D_n = 318 mm ≈ 320 mm.

For present study, D_n = 320/20 = 16 mm that is block type ‘D3a’ of Table 4.2.

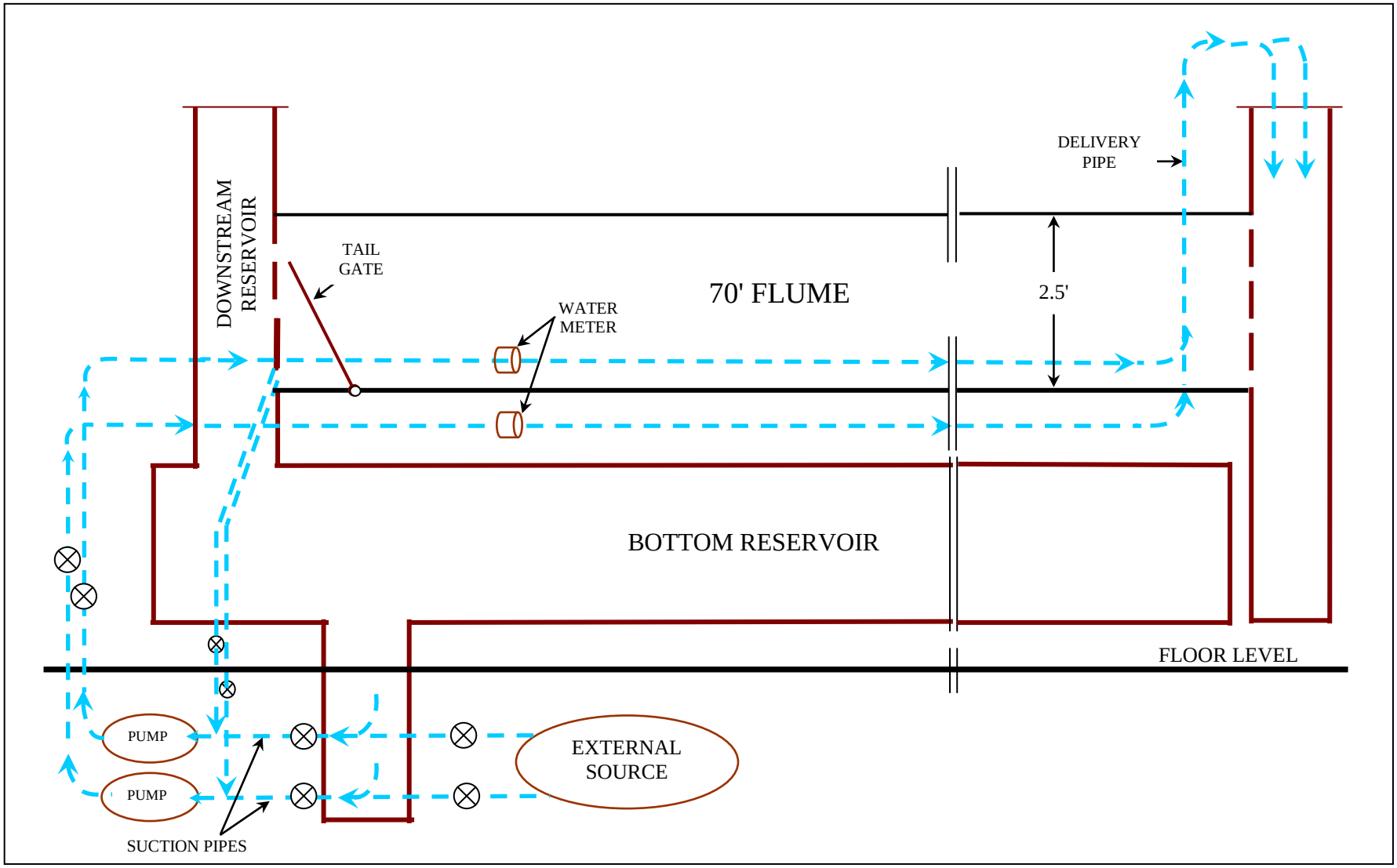

Figure 4.1: Schematic diagram of the flume set-up

TABLE OF CONTENTS

LIST OF FIGURES

LIST OF TABLES

LIST OF PHOTOGRAPHS

LIST OF NOTATIONS

A	Archimedes buoyancy index
a, b, c	Dimensionless numbers
a_1, b_1, c_1	Maximum, intermediate and short dimension of a particle, respectively
c_2	Constant
C_D	Drag coefficient
C^*_D	Modified drag coefficient
C_T	Stability coefficient for incipient failure
C_T	Coefficient for riprap layer thickness
C_V	Coefficient for vertical velocity distribution
D	Depth of scour
D_n	Nominal thickness of protection unit
d	Characteristics diameter
d_n	Nominal diameter
d_l	Length of a particle
d_s	Mean sieve size of a particle
d_t	Thickness of a particle
d_w	Width of a particle
d_*	Dimensionless particle diameter
d_{30}	Particle size for which 30% by weight is finer
d_{50}	Median particle diameter for which 50% by weight is finer
d_{90}	Particle size for which 90% by weight is finer
F	Free board
F_D	Drag force
g	Gravitational acceleration
h	Depth of flow
K	Empirical constant
k	Empirical coefficient
K_1	Side slope correction factor

k_s	Effective bed roughness
m	Empirical exponent
R	Lacey's regime scour depth
R^2	Coefficient of determination
R'	Rise of flood
R*	Particle Reynolds number
R_{*c}	Critical boundary Reynolds number
S	Horizontal settling distance
S_f	Safety factor
T	Thickness of slope stone
T_1	Thickness of stone on prospective slope below bottom of apron
U	Depth averaged horizontal velocity of element
u	Horizontal velocity of element
u_{oc}	Critical velocity near the bed
$\bar{u}_c$	Critical depth-averaged velocity
U_{*c}	Critical friction velocity
V	Depth averaged flow velocity
W	Weight of a particle
W'	Submerged weight of particle
w	Fall velocity
α, β	Empirical constants related with shape factor
γ	Unit weight of water
γ_s	Unit weight of particle
Δ	Relative submerged unit weight
ρ	Mass density of water
ρ_s	Mass density of particle
Ψ	Shape factor
τ_c	Critical shear stress
τ_{*c}	Critical Shields stress

ν	Kinematic viscosity of water
μ	Dynamic viscosity of water
$\forall$	Volume of original particle
ϕ	Slope of bed
θ	Angle of repose

ACKNOWLEDGEMENT

The author expresses his sincere gratitude and respect to Dr. Md. Abdul Matin, Professor, Department of Water Resources Engineering, BUET for his cordial and constant supervision, valuable suggestions and keen interest throughout the thesis work. His constructive comments and enormous expertise helped the author for better understanding of the study.

The author's sincere thanks go to Dr. Umme Kulsum Navera, Professor and Head, Department of Water Resources Engineering, BUET for her support throughout the study. The author is very much grateful to Dr. Md. Ataur Rahman, Associate Professor, Department of Water Resources Engineering, BUET for his valuable suggestions and cooperation. The author is grateful to Dr. M. R. Kabir, Professor and Pro-Vice-Chancellor, University of Asia Pacific, Dhaka, for his valuable criticism and constructive suggestions.

The author is profoundly obliged to his parents and wife without whose constant support, encouragement and pleasant cooperation, the study would not have been completed in due course. The author carries his immense thanks to them. The author also wishes to give thanks to his colleagues, friends and laboratory staff.

Above all, the author is grateful to the Almighty Allah who Has given him the opportunity to work hard with pleasure.

K. M. Ahtesham Hossain Raju
December, 2011.

ABSTRACT

River bank erosion has always been a challenging problem in Bangladesh. Conventional method of designing erosion protection structures are governed by the hydraulic loads resulting from currents and waves. The effectiveness of design of protection works mainly depends on its constructional aspects. The appropriate method of construction depends on mechanism of settling behavior of protection elements. In practice, toe protection elements are dumped into flowing water and settle somewhere on the river bed to form an apron. But the placement of elements at designated positions is difficult to ensure.

The present study has been undertaken to investigate experimentally two important aspect of underwater construction such as the settling behavior and threshold condition of toe protection elements. The experiments are conducted to determine the fall velocity in a square shaped settling column of 30 cm X 30 cm X 130 cm and in the large tilting flume of the Hydraulics and River Engineering Laboratory of Water Resources Engineering Department, BUET. Sixteen different sizes of elements ranging from 1.6 cm X 1.6 cm X 1.3 cm to 4.1 cm X 4.1 cm X 2.7 cm have been used to conduct 64 experimental runs with the discharges range from 0.033 m^3/s to 0.203 m^3/s. During experimentation various observations are made and the measured data are used to obtain various relationships for the settling behavior of the toe protection elements.

Experimental results are analyzed to develop relationships between the relative size and flow parameters. Developed empirical relationships can be used to predict the settling velocity, horizontal settling distance and incipient condition for selected types and sizes of toe protection elements. The proposed relationships are also compared with the equations available in previous studies. Comparisons show that the predictive capacity of the proposed relationships is found to be satisfactory i.e. for fall velocity prediction equation, the error is 3.91% for CC block and 2.38% for geobags. To estimate settling distance results show that the developed equation also performed better compared to Zhu et al. (2004). Also verification of the proposed equation has been done using the independent set of laboratory data and result shows satisfactory agreement with an error of 3.80%.

It is hoped that the outcome of the present study can be used as a tentative guideline for under water construction of toe protection elements in river bank protection works.

CHAPTER ONE

INTRODUCTION

1.1 Background of the Study

Rivers, especially large rivers of Bangladesh are unique in behavior because of its dimensions, discharge, sediment characteristics and morpho-dynamic activities. Bank erosion in these rivers has always been a difficult problem causing damage to valuable lands, settlements and infrastructures from year to year. Strong river currents erode the fine sand from the toe of the riverbank. To address this problem artificial covering of the riverbank and bed with erosion resistant material is constructed. Toe protection is required when water currents scour and undermine the toe of a bank resulting the sliding of slopes. Lack of suitable toe protection measures against undermining is vital for the stability of revetment works. Suitable methods for protecting toe of a revetment have to be explored. This is true not only for revetment, but also for a wide variety of protection techniques. Toe protection techniques such as (i) extension to maximum scour depth, and (ii) placing launchable stone are often provided in design of revetment works for large rivers.

A cover of stone known as an apron is laid on the toe of the bank of the river. An apron of toe protection is required to resist the undermining of bed resulting from scour in such a way that apron launches to cover the face with stone forming a continuous carpet below the permanent slope. Adequate quantity of stone for the apron has to be provided to ensure complete protection of the entire scoured face (Joglekar, 1971). This quantity should be placed in practice as accurately as possible.

The use of stone materials is often stipulated in revetment design procedures. However, such materials are not always available at many construction sites. Alternatively, cement concrete block (CC block) with geosynthetic products have increasingly been used in erosion control and bank protection projects. These protection elements can be more cost-effective if the readily available sand or slurry is used in a container like gabions, mattresses or geobags. In recent time, concrete blocks and geobags are commonly used as toe protection elements of revetment

works. The use of geosynthetic containers in marine structures is a relatively new approach, however the scope and limitations of their application are yet to be defined (Restall et al., 2002). Reliable procedures for design and construction based on good understanding of the processes involved are still needed (Recio and Omeraci, 2009). Among the various parameters in the processes, the settling and threshold behavior of toe protection elements are important.

Numerous investigators derive settling velocity of sediment particles. Notable works have been done by Cheng (1997), Chang and Liou (2001), Ahrens (2000, 2003), Jiménez and Madsen (2003), Smith and Cheung (2003), Göğüş et al. (2001) and Swamee and Ojha (1991). However, very few researches had been conducted for fall velocity of relatively large particles which can be used in other laboratory experiments.

Moreover, number of study had been conducted for incipient motion of sediment particle. Examples are, works of Neill and Yalin (1969), Van Rijn (1993), Ünal and Bayazit (1998), Lick et al. (2004), Smith and Cheung (2004), Ling (1995), Beheshti and Ashtiani (2008), Marsh et al. (2004), Göğüş and Defne (2005) and many others. Inglis (1949), Neill (1967), Maynord (1987), USACE (1991), NHC (2006) proposed relationship regarding incipient motion. Limited study had been done on incipient behavior of toe protection elements simulating the actual method of construction practiced in the field.

Most of the river bank and bed protection works in Bangladesh are to be constructed in under water condition. Therefore it is very important to know the settling behavior of protective elements. During construction and repair, geobags and concrete blocks are delivered directly from vessel with the intention to form a uniform coverage in the settling fashion. This process is simple but their dumping behavior plays a significant role. In under water condition, identification of placement of protective elements in under water flowing situation is found to be more difficult. This has been also reported by Stevens and Oberhagemann (2006). NHC (2006) recommended more drop test to be conducted for a better insight. Stevens and

Oberhagemann (2006) conducted research on rectangular shape and further recommended testing the behavior of square shaped geobag. Haque (2010) carried out an experimental investigation in a sand bed channel and observed the flow behavior around constructed apron for different flow conditions. The apron materials were singled sized geobags and concrete blocks of different sizes. RRI (2010) conducted physical model study to test the performance of geobags and concrete blocks as falling apron elements. But they did not carryout detail dumping tests for underwater condition.

In this study, an attempt has been made to conduct experimental investigation of two important aspects of under water construction as the settling and threshold behavior of toe protection elements for varying flow condition. Also experiment for fall velocity of toe protection elements has been conducted. The elements considered are rectangular and square shaped geobag and concrete blocks of different sizes.

1.2 Objectives of the Study

The main objectives of the study have been setup as follows:

1. To investigate the settling performance of different types of protective elements.
2. To compare the available drop velocity formula based on experimental data.
3. To investigate the threshold condition of protective elements after placement.
4. Finally, to develop correlation for the estimation of settling distance of the protective elements especially for the falling apron.

1.3 Organization of the Thesis

This thesis has been organized under six chapters. **Chapter one** describes the background and objectives of the study. In **Chapter two** the review of literature related to the subject matter of the study has been described. In **Chapter three,** theoretical background of experimentation is presented which is the basis of analysis of the experimental data. Analysis technique for fall velocity, settling distance and incipient condition are stated. **Chapter four** illustrates the experimentation set-up of the laboratory, size of protection elements used, test scenarios, test procedures

followed during measurements and the observations noted at that time. In **Chapter five,** the results of analyses and discussions are presented. The performances of these results are compared with relevant available formula in literature. Few nomographs are also presented in this chapter. Finally, the main conclusions of this study and recommendations for further study are presented in **Chapter six**.